VOL. 255 APRIL 1957 No. 4

American Journal of Science

Established in 1818 by Benjamin Silliman

EDITORS
JOHN RODGERS—JOSEPH T. GREGORY

ASSOCIATE EDITORS

REGINALD A. DALY, CAMBRIDGE, MASS.
A. F. BUDDINGTON, PRINCETON, N. J.
CARL O. DUNBAR
MATT WALTON
HENRY MARGENAU
RICHARD F. FLINT
HORACE WINCHELL
HAROLD G. CASSIDY
EDWARD S. DEEVEY, JR.
G. EVELYN HUTCHINSON
NEW HAVEN, CONN.
LEASON H. ADAMS
WILMOT H. BRADLEY
WASHINGTON, D. C.
GEORGE GAYLORD SIMPSON, NEW YORK, N. Y.
HOWEL WILLIAMS, BERKELEY, CALIF.
C. R. LONGWELL, PALO ALTO, CALIF.
ADOLPH KNOPF, STANFORD, CALIF.
FREDERICK J. ALCOCK, OTTAWA, CANADA
CECIL E. TILLEY, CAMBRIDGE, ENGLAND

STERLING TOWER
YALE UNIVERSITY
NEW HAVEN, CONNECTICUT

Published 10 times a year. Ten dollars a year. One dollar twenty-five cents a copy.
Foreign, ten dollars sixty cents Canada, ten dollars thirty-five cents.

AMERICAN JOURNAL OF SCIENCE

Established in 1818 by Benjamin Silliman

THE FIRST SCIENTIFIC JOURNAL IN THE UNITED STATES

DEVOTED TO THE GEOLOGICAL SCIENCES AND TO RELATED FIELDS

Editors: JOHN RODGERS—JOSEPH T. GREGORY

Managing Editor: BETH A. BROMBERT

Entered as second-class matter at the Post Office at New Haven, Conn., under the Act of March 3, 1879. Published monthly at Sterling Tower, Yale University, New Haven, Conn.

Subscription rate $10 per year ($1.25 a number). Student rate $5 per year (application blanks available on request). Postage prepaid to the United States; 35 cents per year to Canada; 60 cents per year elsewhere.

The JOURNAL completed its *first* series of 50 volumes in 1845, its *second* series of 50 volumes in 1870, its *third* series of 50 volumes in 1895, its *fourth* series of 50 volumes in 1920, its *fifth* series of 36 volumes in 1938. Since 1938 the numbering by series has been discontinued, and volumes are annual and bear the whole numbers as of 1818, that for 1939 being volume 237.

Back numbers and volumes, also cumulative indices of all series, may with few exceptions be obtained from the office of the AMERICAN JOURNAL OF SCIENCE, Sterling Tower, New Haven, Conn. Positive microfilm copies of each complete volume may be purchased by subscribers to the paper edition from *University Microfilms*, 313 N. First St., Ann Arbor, Michigan. Regular subscribers may purchase each past year in microcard form, from *The Microcard Foundation*, Wesleyan University, Middletown, Connecticut.

INSTRUCTIONS TO CONTRIBUTORS

Manuscripts of articles submitted should follow the recommendations in the pamphlet "Suggestions to Authors" (Lane, 1935) and should be preceded by brief abstracts. They should be checked with special care before being submitted, to avoid changes in proof other than printer's errors.

References to literature should be listed alphabetically by authors at the end of the article; all references should be complete. For articles in journals or other serial publications, the reference should give in order: Author's name, year of publication, full title: name of periodical or series, volume number, inclusive pages. For books or other unnumbered publications, it should give: Author's name, year of publication, full title: place of publication, publisher. This form follows the recommendations in the pamphlet "Abbreviations used in publications of the U. S. Geological Survey", which is also the standard used for abbreviating names of periodicals, etc. Citations within an article should be to author and year, with specific pages wherever appropriate.

Plates (photographs), *figures* (line drawings), and *footnotes* should each be numbered consecutively through each article, using arabic numerals. If two photographs form one plate, they are figures 1 and 2 of that plate.

Illustrations should be neat and legible and should include explanations of symbols used. Copy that cannot be reproduced cannot be accepted. Plates and figures should be capable of reduction to not more than 4 by 7 inches, all lettering being at least 1/16th inch high after reduction. When necessary, one large map or table can be accepted, if it will not exceed 7 inches in width after reduction. Line drawings should be in black India ink on white drawing board, tracing cloth, or coordinate paper printed in blue. Photographs should be positive glossy prints. Photostatic and typewritten material cannot be accepted as copy for illustrations.

Reprints. Thirty separate copies of each article will be furnished to the author free of cost and without previous notice from him; these will be without a cover. Additional copies will be furnished at cost, which will of course be greater if the article is accompanied by plates involving unusual expense. Copies will be furnished with a printed cover giving the title, author, volume, page, and year, when specially ordered.

REFERENCE

Lane, B. H., 1935, Suggestions to authors of papers submitted for publication by the United States Geological Survey: U. S. Geol. Survey, Washington, D. C. (For sale by Superintendent of Documents, Washington, D. C. 40c.)

[American Journal of Science, Vol. 255, April 1957, P. 241-253]

American Journal of Science

APRIL 1957

CONTRIBUTIONS TO THE PETROLOGY OF HAWAIIAN BASALTS
1. THE PICRITE-BASALTS OF KILAUEA

I. D. MUIR and C. E. TILLEY

with chemical analyses by J. H. SCOON

ABSTRACT. This is the first of two contributions devoted to the petrology of Hawaiian basalts. In this part the petrography of some Kilauean tholeiitic picrite basalts and their metamorphic representatives is described. A discussion of the genetic features of the rocks based on new chemical data, particularly of the composition of pyroxene phases, is provided.

INTRODUCTION

Among the desiderata in discussions on Hawaiian basalt petrogenesis has been adequate knowledge of the quantitative chemical composition of the commoner mineral phases of the lava types of Hawaiian volcanic centers.

Numerous first class analyses of the rocks themselves are available but chemical data on the constituent minerals have been few[1]—two olivines from the 1789 and 1840 flows from the Kilauean center were analyzed by Aurousseau and Merwin (1928), an olivine from the 1852 flow of Mauna Loa was analyzed by Steiger (Cross, 1915), and an analysis of an augite from an augite picrite-basalt at Haleakala crater on East Maui has been reported by Washington and Merwin (1922).

This is the first of two papers intended to help in filling this gap by the provision of precise data, particularly on the pyroxene phases of the basalts, and thus further to aid in the elucidation of genetic problems of these lavas in their oceanic setting.

The rocks of Kilauea now under study are of ultrabasic composition and include the well known picrite-basalt flow of 1840 (at Nanawale Bay) which together with the basalt erupted during the same period at the upper vents near Kilauea, has provided evidence of gravitative differentiation (Macdonald, 1944a); an intrusive in the wall of Kilauea caldera (Daly, 1911), and three picrite basalts, two of which were ejected in the explosion of 1924 at Halemaumau including an assemblage which presents a study in thermal metamorphism (Macdonald, 1944b). Altogether with the two analyses provided in this account there are now available six analyses of these ultrabasic rocks from the Kilauean center.

Four of these are set out in table 1, nos. 1-4. Washington (1923) analysed a picrite basalt west of the Kamakaia Hills, S.W. of Kilauea, and

[1] More information is available on the minerals of basic and ultrabasic inclusions in Hawaiian basalts, for Ross and his colleagues (1954) have supplied for these assemblages at various Hawaiian centers, analyses, including spectrographic data, of olivines, pyroxenes and spinels. Other chemical data on some vein minerals from the basalts of Moiliili Quarry, Honolulu, are recorded by Dunham (1933).

Shepherd (1938) a block of baked picrite basalt ejected during the 1924 explosion at Halemaumau. Unfortunately there is no petrographic description available of this interesting rock.

TABLE 1

	1	2	3	4	5	6		Norm of 6	
SiO_2	46.59	47.00	47.33	47.25	50.60	43.90			
Al_2O_3	7.69	9.17	9.85	9.07	14.63	3.51			
Fe_2O_3	2.20	1.47	4.58	1.45	2.38	0.52		Or	0.56
FeO	10.46	10.47	7.28	10.41	10.15	10.67		Ab	2.10
MnO	0.18	0.17	0.17	0.13	0.12	0.14		An	8.06
MgO	21.79	20.25	19.11	19.96	6.38	33.54		Wo	9.51
CaO	7.41	7.73	8.04	7.88	9.56	6.20	Di	En	7.10
Na_2O	1.33	1.56	1.62	1.38	2.51	0.25		Fs	1.45
K_2O	0.28	0.30	0.28	0.35	0.54	0.16		En	6.00
H_2O+	0.37	0.07	0.03	0.04	0.13		Hy	Fs	1.32
H_2O-	0.04	nil	nil	0.08	—			Fo	49.49
TiO_2	1.83	1.90	1.75	1.61	2.29	0.93	Ol	Fa	11.52
P_2O_5	0.11	0.15	0.12	0.21	0.43			Il	1.82
Cr_2O_3	0.13	0.12	0.18	0.12	0.09	0.15		Mt	0.93
NiO	0.12	0.11		0.09	0.07(SO_3)				99.86
	100.53	100.47	100.34	100.03	99.88	99.97			

1. "Porphyritic Gabbro", Uwekahuna 'laccolith', Kilauea (G. A. MacDonald 1949 (a) p. 73).
2. Picrite-basalt, ejected block 1924, Kilauea (Tilley 1950, p. 41).
3. Metamorphosed Picrite-basalt, ejected block 1924, Kilauea.
4. Picrite-basalt, flow of 1840, Nanawale Bay, Hawaii (G. A. MacDonald 1949 (b) p. 1572).
5. Basalt, lava of upper vents of 1840 eruption at Kilauea (G. A. MacDonald 1949 (b) p. 1572).
6. Composition of crystal extract (50%) from analysis 4 to produce analysis 5 = (removal of olivine 30.5%, clinopyroxene 12.7%, plagioclase 5.4% and ores 1.4%).

TABLE 2

Norms of Rocks of Table 1

	1	2	3	4	5
Qz					3.48
Or	1.67	1.67	1.67	2.22	2.78
Ab	11.53	13.10	13.62	11.53	20.96
An	13.90	17.24	18.90	17.51	27.24
Di	17.48	16.19	15.99	16.68	14.38
Hy	16.90	15.66	21.64	17.96	21.64
Ol	31.33	30.40	17.99	28.25	—
Il	3.50	3.65	3.34	3.04	4.41
Mt	3.47	2.27	6.96	2.31	3.48
Ap	0.34	0.34	0.34	0.34	1.01
Rest	0.41	0.07	0.03	0.12	0.29
	100.53	100.59	100.48	99.96	99.67

The position of these six analyses on a silica—magnesia variation diagram of Kilauean lavas is given in figure 1.

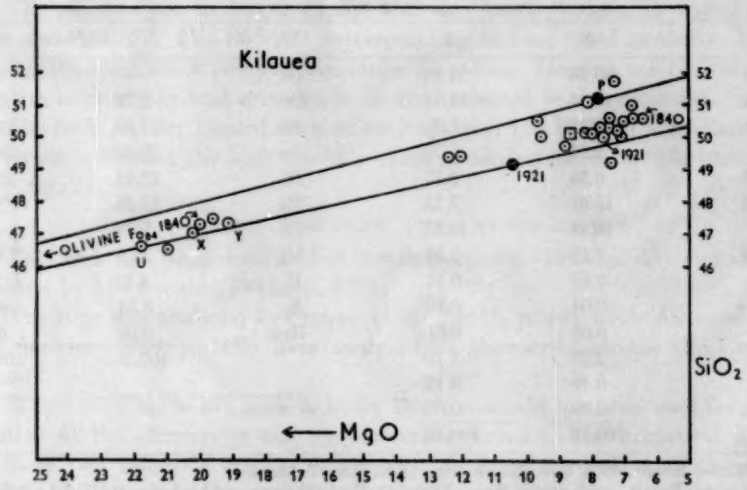

Fig. 1. Plot of variation of silica and magnesia in analyses of basaltic rocks of Kilauea. Control lines from olivine (Fo_{84}) through olivine basalt flow of 1921 (table 3, no. 1) and a prehistoric olivine basalt P (table 3, no. 2). The data for the picrite-basalts referred to in the text are indicated :-

U = Uwekahuna 'gabbro'; X and Y ejected blocks of picrite basalt (1924 explosion) (table 1, nos. 2 and 3); 1840 analysis of picrite-basalt of Nanawale Bay (table 1, no. 4) and corresponding basalt of upper vents (table 1, no. 5). A variant of the 1921 lava flow is shown in the figure by an open circle. Average composition of Kilauean historic magma (Powers, 1955, p. 85) shown by square around point.

On this have been placed olivine control lines from Fo_{84} (wt percent) through the composition points for the 1921 and prehistoric lava flows of Kilauea (table 3, nos. 1 and 2), a procedure which Powers (1955) has developed in his analysis of the nature of parental Kilauean magma.

Further reference to this diagram will be made in the sequel. We proceed to the new data now available on the rocks of table 1.

GABBRO MASS AT UWEKAHUNA BLUFF, KILAUEA CALDERA

This rock was originally described by Daly (1911, p. 291) who regarded it as a laccolithic intrusion. He noted it showed a distinctly chilled phase several decimetres thick, and Macdonald (1949a, p. 67) has supported this interpretation of it as an intrusive, recording also that a dike about two feet thick extends from it into the overlying lavas. The analysis given by Daly is by Steiger and is here reproduced (table 1, no. 1). Daly presented a mode as follows: olivine 40, augite 30, labradorite 27, iron ore and apatite 2 percent. The normative composition gives olivine 31.3 percent.

Pyroxene, however, is present both as augite and hypersthene, the latter hitherto not recognized in published accounts of the rock. Both these pyroxenes have been isolated from the rock and analysed (table 4, nos. 1a and 1b).

Both pyroxenes and olivine have a yellowish tint in thin section, the hypersthene feebly pleochroic with stronger absorption along α and β.

TABLE 3

	1	2		1	Norms	2
SiO_2	49.16	51.18	Qz	—		0.30
Al_2O_3	13.33	14.07	Or	2.78		2.22
Fe_2O_3	1.31	1.35	Ab	17.82		20.96
FeO	9.71	9.78	An	25.30		26.13
MnO	0.16	0.17	Di	22.93		22.04
MgO	10.41	7.78	Hy	15.35		22.44
CaO	10.93	10.83	Ol	9.14		—
Na_2O	2.15	2.39	Mt	2.09		1.86
K_2O	0.51	0.44	Il	4.41		3.95
H_2O+	0.04	0.10	Ap	0.34		0.34
H_2O-	0.05	0.01	Rest	0.09		0.16
TiO_2	2.29	2.10		100.25		100.40
P_2O_5	0.16	0.15				
Cr_2O_3	0.09	0.05				
	100.30	100.40				

1. Olivine Basalt, 1921 flow, South edge of Kilauea caldera.
2. Olivine Basalt, prehistoric flow, National Park Quarry on highway 0.75 mile NE of Volcano Observatory Kilauea (P(●) of figure 1).

Both are of similar grain size (1 mm) and their optical properties are set out below:-

Augite: α 1.684, β 1.689, γ 1.712. $2V_\gamma$ 52° - 50°.

Hypersthene: α 1.685, β 1.692, γ 1.696. $2V_\alpha$ 65°.

TABLE 4

Compositions of Pyroxenes of Rocks of Table 1

	1(a)	1(b)	4(a)	4(b)		Formula on basis of 6 oxygens 1(a)	1(b)	4(a)	4(b)
SiO_2	51.62	52.87	51.72	52.39	Si	1.894	1.907	1.890	1.924
Al_2O_3	3.14	2.14	3.82	4.00	Al	.106	.091	.110	.076
TiO_2	0.72	1.12	0.92	1.43	Al	.026	—	.052	.096
Cr_2O_3	0.49	0.11	0.52	0.54	Ti	.019	.031	.024	.040
Fe_2O_3	1.25	1.10	0.90	1.55	Cr	.013	.004	.013	.013
FeO	5.63	12.59	5.77	8.59	Fe‴	.035	.031	.026	.040
MnO	0.14	0.26	0.14	0.21	Fe″	.164	.379	.175	.262
MgO	17.42	26.70	16.80	15.25	Mn	.004	.006	.004	.007
CaO	19.45	2.72	19.13	15.17	Mg	.960	1.448	.921	.840
Na_2O	0.32	0.16	0.45	0.70	Ca	.763	.104	.750	.597
K_2O	0.01	0.04	0.05	0.21	Na	.022	.009	.030	.049
H_2O+	n.d.	n.d.	n.d.	n.d.	K	—	—	—	.009
H_2O-	n.d.	0.03	nil	nil	z	2.000	1.998	2.000	2.000
	100.19	99.84	100.22	100.04	x + y	2.006	2.012	1.995	1.953
					Ca	39.5	5.3	40.0	34.2
					Mg	49.8	73.4	49.0	48.0
					Fe	10.7	21.3	11.0	17.8

1 (a) and 1(b), clinopyroxene and hypersthene of "Porphyritic gabbro" (table 1, no. 1)
4 (a) and 4(b), clinopyroxenes-phenocryst (4(a)) and groundmass (4(b)) of picrite-basalt, flow of 1840 (table 1, no. 4).

The olivines are in larger grains and may reach 3 mms. in diameter. They show β1.673, $2V_\gamma$ 86°-90° corresponding to Fa_{11} (mol percent). The zoned plagioclase has a composition range An_{64}-An_{58}. There is a little brownish glass interstitially and cristobalite in small amount is also recorded.

The rock powder treated on a steam bath with 1:9 HCl left a residue of 37 percent indicating the high modal content of olivine in the sample studied (pl. I, fig. 2).

PICRITE-BASALT, 1840 FLOW, PUNA, NANAWALE BAY

This rock has been described at length by Cross (1915, p. 43) and subsequently by Macdonald (1944a, p. 177).

The rock was analyzed by Steiger (Cross, 1915, p. 44) while Aurousseau and Merwin (1928, p. 560) have analyzed its phenocryst olivine (Fa_{12} mol percent).

A specimen made available to us by Dr. Macdonald has been used for the isolation of the phenocryst and groundmass pyroxenes. The analytical data for these two minerals are set down in table 4, columns 4a and 4b; the analysis of the rock itself in table 1, No. 4.

The optical properties of the olivine and clinopyroxenes are as follows:

Olivine: β 1.687 (Fa_{17}); $2V_a$ 88° (Fa_{17}); Xray (Fa_{16})

Clinopyroxene α 1.686, β 1.692, γ 1.713, $2V_\gamma$ 56°-52° (phenocrysts)

Clinopyroxene α 1.688 (min.) to γ 1.717 (max.) $2V_\gamma$ 46°-32° (groundmass)

Microphenocrysts of plagioclase have the composition An_{60} while the groundmass plagioclase is zoned to An_{52}.

The rock powder treated on the steam bath with 1:9 HCl gave a residue of 44 percent.

A photomicrograph of this rock is presented in plate I, figure 1.

PICRITE BASALTS AS EJECTED BLOCKS FROM THE 1924 EXPLOSION AT HALEMAUMAU, KILAUEA

Macdonald (1944b, 1949a) has described the characters of blocks of basalt thrown out by the phreatic explosion of 1924. Attention is here directed to two such blocks of picrite-basalt composition. Both have been analyzed.

The first of these (analysis 2, table 1) corresponds to the description of hand specimens given by Macdonald (1944b, p. 323)—pale yellowish green of dense aspect and with numerous olivine phenocrysts, green-brown in color, with a brilliant lustre, almost submetallic and iridescent on the conchoidal fractures.

The second example (analysis 3, table 1) corresponds to the description by Macdonald of another variety (1944b, p. 324). The olivine in hand specimens is black and the color of the groundmass, dark gray—usually fine grained but showing coarser grained patches.

In the first type (X) as seen in thin section the olivine phenocrysts (β1.691, $2V_a$ 89° = Fa_{19}) are clear with occasional dendritic streaks of a platy brown translucent ore (chromite or chrome spinel) reminiscent of the

translucent dendrites seen in the olivines of the Rum allivalites. The plates are oriented in the plane (100).

PLATE I

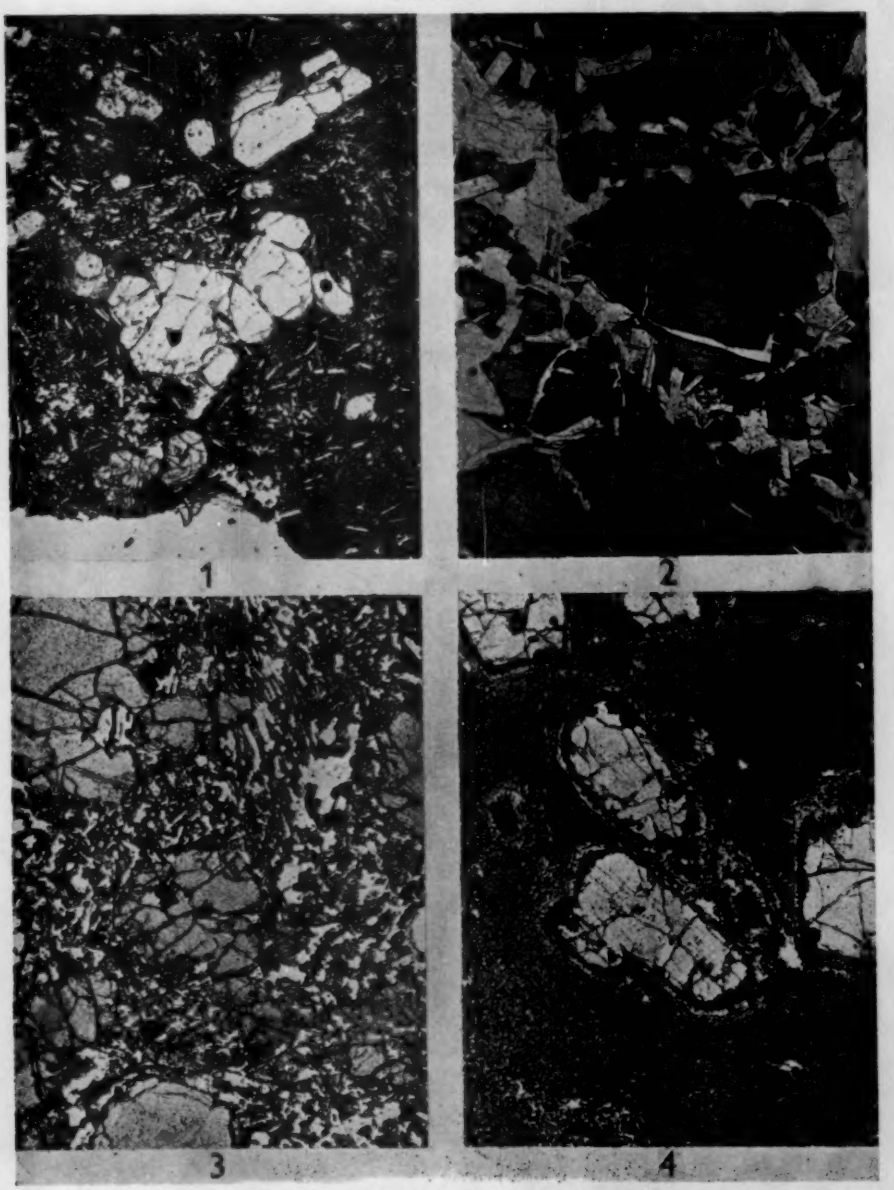

Ultrabasic rocks of Kilauea × 20 diameters

The groundmass is built of plagioclase augite and hypersthene (both yellowish to yellow green in section) and platy ilmenite. The texture in places shows a crude radial arrangement of the felspar laths (pl. I, fig. 3).

The optical properties of the two pyroxenes are:

Hypersthene: $2V_\alpha$ 63°; β 1.694, γ 1.699 (Fs_{27})

Augite: $2V_\gamma$ 45½°; α 1.690, β 1.695, γ 1.718 ($Ca_{38}Mg_{41}Fe_{21}$)

A colorless glass (n = 1.502) is sparingly developed, wedged between the feldspar laths (composition An_{52-42}, average An_{46}).

The second picrite-basalt (Y) is a thoroughly metamorphosed rock with a hornfelsic texture in the groundmass as described and figured by Macdonald (1944b, fig. 1a).

This texture merges into one similar to that met with in the first example, and this is associated with still coarser textured patches.

The constituents of this variable textured groundmass are augite, hypersthene—both notably colored in thin section, yellow to greenish yellow—plagioclase (An_{62}) together with brown translucent laths of a mineral identified as pseudobrookite. Some tridymite plates appear among the felspar laths of the coarse textured patches.

The olivine phenocrysts (β1.693, $2V_\alpha$ 88½°, Fa_{20}) unlike those of picrite-basalt X are in process of dissolution with separation of magnetite (strongly magnetic, cell size 8.40 Å) on their peripheries. This release of iron oxide is in part accompanied by the formation of hypersthene which appears as a wreath around the olivines as well as intergrown with the magnetite. The same process has been at work at scattered centres in the interior of the olivines. The olivines are otherwise clouded with opaque clots of magnetite strung together in curved lines.

The smaller olivine phenocrysts may be completely replaced by magnetite and granular hypersthene. These features are revealed in the photomicrograph of plate I, figure 4, which presents a clear picture of the hornfelsic groudmass of this picrite-basalt. The optical data of the two pyroxenes in their varying environment are indicated below.

Fig. 1. Picrite-basalt, 1840 flow of Nanawale Bay, E. of Kilauea. Phenocrysts of olivine and clinopyroxene (lower edge) in a fine grained base of plagioclase, clinopyroxene and iron ores. The phenocryst and groundmass pyroxenes have been analyzed (table 4, nos. 4(a) and 4(b)).

Fig. 2. Gabbro of Uwekahuna Bluff, Kilauea caldera wall. Large olivines, clinopyroxene, hypersthene and plagioclase. The pyroxenes have been analyzed. (table 4, nos. 1(a) and 1 (b)).

Fig. 3. Picrite-basalt ejected block from the 1924 explosion of Halemaumau. Phenocryst olivine in a groundmass of hypersthene, clinopyroxene, plagioclase and iron ore. The rude radiate arrangement of the plagioclase laths is visible. Rock analyzed (table 1, no. 2).

Fig. 4. Metamorphosed picrite-basalt, ejected block from the 1924 explosion of Halemaumau. Phenocryst olivine in a dense hornfelsic aggregate of hypersthene, augite, plagioclase and laths of pseudobrookite. The larger olivines mantled by magnetite and surrounded by a sheath of new hypersthene. Smaller grains of olivine are almost completely replaced by an aggregate of magnetite and hypersthene. Rock analyzed (table 1, no. 3).

Coarse textured patches.
hypersthene: $2V_\alpha$ 68°, (Fs_{27})
augite: $2V_\gamma$ 51°, α 1.692, β 1.698, γ 1.720, ($Ca_{40}Mg_{37}Fe_{23}$)

Hornfelsic textured patches
hypersthene: $2V_\alpha$ 71°, (Fs_{24})
augite: $2V_\gamma$ 52°, α 1.691, β 1.695 γ 1.718, ($Ca_{39}Mg_{40}Fe_{21}$)

Coronas around olivine
hypersthene: $2V_\alpha$ 76°, (Fs_{21}); in coarse patches near olivine
$2V_\alpha$ 71°, (Fs_{24}); α 1.684, β 1.690, γ 1.695.

Enclosures in olivine
hypersthene: $2V_\alpha$ 78°, α 1.678, β 1.683, γ 1.688 (Fs_{19})

The rock powder treated on the steam bath with 1:9 HCl gave a residue of 63.3 percent.

TABLE 5

	Olivine	Hypersthene	Clinopyroxene
Picrite-basalt (CD) 1840 flow	Fa_{17}	—	‡$Wo_{40.0}$ $En_{49.0}$ $Fs_{11.0}$ ‡$Wo_{34.2}$ $En_{48.0}$ $Fs_{17.8}$
Picritic basalt (W) (pre-1924 explosion)	Fa_{14} ↓ $Fa_{10(rims)}$	—	Wo_{37} En_{47} Fs_{16} ↓ Wo_{29} En_{47} Fs_{24} Wo_{15} En_{53} Fs_{32}
"Olivine gabbro Porphyry (AB)	Fa_{11}	‡$Wo_{5.2}$ $En_{73.4}$ $Fs_{21.3}$	‡$Wo_{39.5}$ $En_{49.8}$ $Fs_{10.7}$
Picrite-basalt (X) 1924 explosion	Fa_{19}	Fs_{27}	Wo_{38} En_{41} Fs_{21}
Picrite-basalt (Y) 1924 explosion.	Fa_{20}	Fs_{27} (coarse patches) Fs_{24} (hornfelsic patches) Fs_{21} (olivine coronas) Fs_{19} (olivine enclosures)	Wo_{40} En_{37} Fs_{23} (coarse patches) Wo_{39} En_{40} Fs_{21} (hornfelsic patches) — —

‡ data from chemical analysis

PICRITIC BASALT (W), PRE-1924 EXPLOSION KILAUEA

An olivine-rich basalt with a distinctive igneous texture and mineralogy found as a bomb at Kilauea remains to be noted.

The hand specimen shows conspicuous olivine as green phenocrysts in a grey groundmass.

These olivines are colorless in thin section ($2V_\alpha$ 88°, β1.681, Fa_{14}) and range in size from four millimetres to less than one millimetre. They are frequently sharply zoned by a narrow rim, light yellow in color ranging in composition to Fa_{27} ($2V_\alpha$ 82°) indicating regrowth during the later stages of crystallization.

Octahedra of chromespinel occur as enclosures.

There are a few scattered microphenocrysts of augite ($2V_\gamma$ 49°-38° average 44°, β 1.691 corresponding to $Ca_{37}Mg_{47}Fe_{16}$). The groundmass is fine grained built of two clinopyroxenes, augite and pigeonite, less than 1/10 mm. in length, plagioclase (An_{60}) and ilmenite. Cristobalite of late development is present in interstitial patches.

The augite of the groundmass has a composition of $Ca_{29}Mg_{47}Fe_{24}$ with a limiting 2V of 30°, range 38°-30°, while the pigeonite, the dominant groundmass pyroxene in subidiomorphic stumpy prisms has the properties $2V_\gamma$ 0°-15°, optic plane (010), β 1.693 with a mean composition $Ca_{15}Mg_{53}Fe_{32}$. The compositions of the phenocryst and groundmass augite and pigeonite (W^1, W^{11} and W^{111}) are plotted in figure 3.

TABLE 6

Comparison of Iron Enrichment in Associated Olivines and Pyroxenes (atom percent)

	Picrite-basalt 1840 flow	Olivine gabbro Porphyry	Olivine Basalt 1921 flow	Picritic basalt pre-1924 (W)	Picrite-basalt (X)	Picrite-basalt (Y)
Olivine	17	11	18	14-16	19	20
Hypersthene	—	22.3*	—	—	27	27 (coarse patches) 24 (horn-felsic areas)
Clinopyroxenes	18.2 ↓ 26.9	17.4	17.5 ↓ 28.6 ↓ 30.9	25 ↓ 34 38	34	38 (coarse patches) 34 (horn-felsic areas)

* In the case of the hypersthene ($Fs_{22.3}$) from the olivine gabbro porphyry, the agreement between the chemical composition and the optical properties is not very close, for the refractive indices correspond with Fs_{26} and the optical axial angle (mean value 65°, limits 67°-63°) corresponds with Fs_{25} using Hess's chart. (AM. JOUR. SCI., 1952, Bowen volume p. 180). The discrepancies can probably be attributed to the notably high ferric iron and titanium content of this pyroxene which would certainly influence its refractive indices. Dr. P. Gay kindly determined the parameters of this hypersthene using a Geiger counter spectrometer. The dimensions a = 18.31 Å ± .03, b = 8.867 Å ± .014, c = 5.201 Å ± .001 agree fairly well with Hess and Kuno's curves (Hess, 1952) for volcanic pyroxenes of this composition high in alumina.

The hypersthene from picrite-basalt X is similar in colour to that from the olivine gabbro porphyry; its refractive indices and optic axial angle indicate Fs_{37} and Fs_{39}, very iron-rich compositions for Hawaiian orthopyroxenes.

It is probable that this hypersthene is closely similar to that discussed above, and is more magnesian than the composition indicated in the table from its optical properties. The orthopyroxenes of the picrite-basalt Y appear to be completely normal.

DISCUSSION

The chemical composition and optical data on the olivines and pyroxenes of the five rocks just described are set down together in table 5, and a comparison of the relative iron enrichment of these associated mineral phases summarized in table 6.

The composition of the chemically analysed pyroxenes is graphically depicted in figure 2, which also includes the three fractions of the clinopyroxene (E, F, G) analyzed from the 1921 lava of Kilauea (table 3, no. 1).

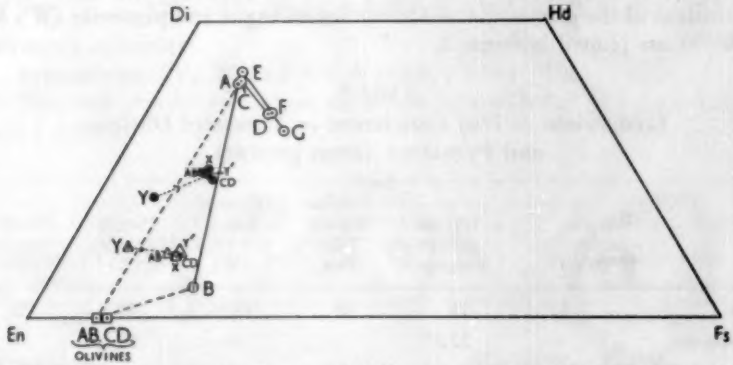

Fig. 2. Plot of compositions of analysed pyroxenes from picrite basalts and a related ultrabasic rock from Kilauea:

A-B from the 'porphyritic gabbro' (AB) of Uwekahuna (table 1, no. 1);

C-D from the picrite-basalt (CD) 1840 flow at Nanawale Bay (table 1, no. 4);

Also plotted are the three fractions (E-F-G) of pyroxenes isolated from the 1921 olivine basalt flow of Kilauea. (table 3, no. 1). The solid circles and open triangles give the compositions respectively of mol normative pyroxenes and mol normative pyroxenes + olivines of the rocks AB, CD and two ejected blocks of picrite-basalt (1924 explosion) from Kilauea—X and Y (table 1, nos. 2 and 3);

Y′ the corresponding compositions for rock Y in which the Fe_2O_3 content has been adjusted (table 7, no. 2).

The compositions of the olivines of rocks AB and CD are projected on to the plane of the diagram.

In this diagram the compositions of normative pyroxenes, normative pyroxenes + olivines, mol percent, are also indicated, together with other data noted in the legend of this figure.

In the artificial system MgO—FeO—SiO_2, olivine in equilibrium with a magnesia-iron pyroxene is less magnesian than that pyroxene (Bowen and Schairer, 1935) and this relationship has been confirmed by Ramberg and De Vore (1951) in their study of natural olivine-orthopyroxene pairs, though they note that in highly magnesian parageneses the natural olivine may in some cases be richer in magnesium than the coexisting hypersthene. In the present assemblages however, olivine is uniformly more magnesian than the associated hypersthene, or the bulk composition of the associated clinopyroxenes—a relation corresponding to non-equilibrium conditions associated with the early separation of olivine in these assemblages (fig. 2). This statement applies not only to the rocks with a straight igneous crystallization but also to

the metamorphic representatives where olivine is in effect a residual of igneous crystallization.

The relations of the ortho- and clino-pyroxenes are not so uniform. In the 'olivine gabbro porphyry' the greater relative enrichment in iron of the hypersthene is in accord with the findings of Hess (1941) for the two pyroxenes of some mafic intrusions.

The enrichment of iron in the later fractions of a series of clinopyroxenes is also well shown in the data for the phenocryst and groundmass clinopyroxenes of the 1840 picrite-basalt flow and the 1921 Kilauean lava (table 6).

In the picrite basalt Y the metamorphic texture indicates the simultaneous crystallization of hypersthene and augite in the hornfelsic groundmass and this would apply to the coarser textured patches, where it may be suspected recrystallization took place in the presence of interstitial liquid. We may interpret the textures seen in picrite-basalt X which has also been reheated as indicating recrystallization in the presence of some liquid to give the rude radiate arrangement of the felspar laths seen in plate I, figure 3.

Optical data on the associated groundmass pyroxenes of both these rocks reveal now that the clinopyroxene is the one relatively enriched in iron (table 6).

In picrite basalt Y however, we have a second hypersthene which has been produced partly at the expense of olivine seen in the magnetite-hypersthene coronas which surround this phenocryst mineral.

As seen from the table these hypersthenes are somewhat more magnesian than those associated with the main groundmass.

The strong development of magnetite associated with the olivine is a result of oxidation processes probably in the presence of water vapor and as

TABLE 7

	1	2		Norms 1	2
SiO_2	47.33	47.33	Or	1.67	1.67
Al_2O_3	9.85	9.85	Ab	13.62	13.62
Fe_2O_3	4.58	1.50	An	18.90	18.90
FeO	7.28	10.05	Di	15.99	16.22
MnO	0.17	0.17	Hy	21.64	15.90
MgO	19.11	19.11	Ol	17.99	27.83
CaO	8.04	8.04	Il	3.34	3.34
Na_2O	1.62	1.62	Mt	6.96	2.32
K_2O	0.28	0.28	Ap	0.34	0.34
H_2O+	0.03	0.03	Rest	0.03	0.03
H_2O-	nil	nil			
TiO_2	1.75	1.75		100.48	100.17
			normative pyroxene (atom %)		
P_2O_5	0.12	0.12	Ca	20.5	24.5
Cr_2O_3	0.18	0.18	Mg	71.6	61.6
	100.34	100.03	Fe	7.9	13.9

1. Metamorphosed Picrite-basalt, ejected block 1924, Kilauea.
2. The same rock with Fe_2O_3 adjusted to 1.50, FeO 10.05 (total iron as in 1).

we have noted smaller olivines may be completely replaced by magnetite-hypersthene aggregates.

We are justified in recalculating the analysis of this picrite basalt by reducing its high Fe_2O_3 content to one comparable with that of picrite basalt X. When this is done (table 7, no. 2) the normative olivine rises from 18 to 27.8 percent, a figure comparable with that for olivine of rocks of table 1 nos. 1, 2, 4).

In the production of orthopyroxene and magnetite from olivine by an oxidation reaction, for every mol of fayalite converted to magnetite sufficient silica is released to convert one mol of forsterite to enstatite thus:

$$3\ Fe_2SiO_4 + 3\ Mg_2\ SiO_4 + O_2 \rightarrow 2\ Fe_3O_4 + 6\ MgSiO_3$$

This reaction however does not suffice to explain the replacement of an olivine Fa_{20} by the visible aggregates of magnetite and hypersthene ($Fs_{18\text{-}24}$) and it is clear that the mechanism involves introduction of iron from the environment of the phenocryst olivine, magnesia moving out, and silica likewise if the content of magnetite in the aggregate is high.

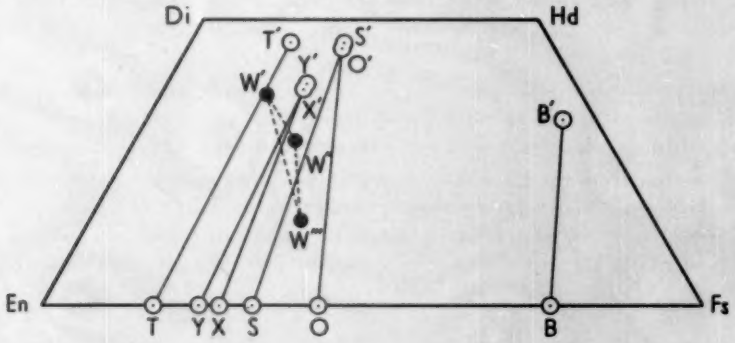

Fig. 3. Plot of compositions (optically determined) of pyroxenes of the picritic basalt W (W^1, W^{11}, W^{111}) and the two metamorphosed picrite-basalts X ($X\ X^1$) and Y (YY^1). In addition the tie lines of coexisting orthorhombic and monoclinic pyroxenes from four metamorphic assemblages have also been plotted in the figure—$0\text{-}0^1$ from a hypersthene diopside plagioclase hornfels (Class VI), Aarvold, Norway; $S\text{-}S^1$ from a hypersthene augite plagioclase gneiss from the Lewisian of Scourie, Sutherland; $T\text{-}T^1$ from an olivine hypersthene pyroxenite from the same rock group at Scourie.

$B\text{-}B^1$ gives the tie line for coexisting pyroxenes in an almanditic ultramafic pyroxenite gneiss from the Adirondacks (Buddington, 1952, p. 54).

The compositions of the pyroxenes of the picritic basalt and the metamorphosed picrite-basalts X and Y are plotted in figure 3. The metamorphic assemblages show a tie line trend which is in contrast to that revealed in many mafic intrusive bodies; the same feature is brought out by the tie line trend of the two pyroxenes of some other metamorphic assemblages which have been examined, and indicated in figure 3. The significance attached to this contrasting trend will be better appreciated when more examples of metamorphic assemblages, hitherto little studied, have been closely investigated.

PICRITE-BASALTS AS GRAVITATIVE DIFFERENTIATES

Powers (1955) in his analysis of the composition of Kilauean lavas concludes that movement of olivine phenocrysts from a silica saturated magma suffices to explain the main chemical variation of the suite of lavas emanating

from this center. This conception is illustrated in the diagram of figure 1 already referred to which is based on diagrams due to Powers. The same conclusion had already been reached for a specific pair of lavas by Macdonald (1944a, 1949b) in his investigation of the 1840 picrite basalt of Nanawale Bay and the 1840 basalt of the upper vents at Kilauea.

He attempted to show that subtraction of 29 percent of olivine of the appropriate composition from the picrite-basalt of 1840 gives a figure of composition of the residue comparable with the lava of the upper vents (columns 1, 2 and 3 of table 6, Macdonald, 1949b, p. 1572).

The match however is not very close as the product contains more lime and magnesia than the upper vent lava. It is unlikely that olivine is the only mineral to be extracted, for the picrite-basalt also contains phenocrysts of pyroxene and plagioclase.

A preferable solution is the extraction of olivine in bulk together with subordinate pyroxene and plagioclase, and the result shown in table 1 is on a basis of extraction of 50 percent of material of the composition shown in column 6.

Extraction of zero soda falls at a silica percentage of 43.1 (extract 45 percent) and the preferred solution extracts a small content of soda.

As we know crystallization of olivine from Kilauean basaltic liquid is followed closely in time by that of pyroxene and plagioclase. Choice must here be made between extracting too large an amount of crystallate and the limit presented by the relative soda contents of the two lavas.

CAMBRIDGE, ENGLAND

REFERENCES

Aurousseau, M., and Merwin, H. E., 1928, Olivine; I. From the Hawaiian Islands; II. Pure Forsterite: Amer. Mineralogist, v. 13, p. 559-564.

Bowen, N. L., and Schairer, J. F., 1935, The system MgO—FeO—SiO_2: AM. JOUR. SCI., v. 29, p. 151-217.

Buddington, A. F., 1952, Chemical Petrology of some metamorphosed Adirondack gabbroic, syenitic and quartz syenitic rocks: AM. JOUR. SCI., Bowen volume, p. 37-84.

Cross, W., 1915, Lavas of Hawaii and their relations: U. S. Geol. Survey, Prof. Paper 88, 97 p.

Daly, R. A., 1911, Magmatic differentiation in Hawaii: Jour. Geol., v. 19, p. 289-316.

Dunham, K. C., 1933, Crystal cavities in lavas from the Hawaiian Islands: Amer. Mineralogist, v. 18, p. 369-385.

Hess, H. H., 1941, Pyroxenes of common mafic magmas, Part 2: Amer. Mineralogist, v. 26, p. 573-594.

Macdonald, G. A., 1944 (a), The 1840 eruption and crystal differentiation in the Kilauean magma column: AM. JOUR. SCI., v. 242, p. 177-189.

————, 1944 (b), Unusual features in ejected blocks at Kilauea Volcano: AM. JOUR. SCI., v. 242, p. 232-326.

————, 1949 (a), Petrography of the Island of Hawaii: U. S. Geol. Survey, Prof. Paper 214-D, 96 p.

————, 1949 (b), Hawaiaan Petrographic Province: Geol. Soc. America, Bull., v. 60, p. 1541-1596.

Powers, H. A., 1955, Composition and origin of basaltic magma of the Hawaiian Islands: Geochim. et Cosmochim. Acta, v. 7, p. 77-107.

Ramberg, H. and De Vore, G., 1951, The distribution of Fe^{++} and Mg^{++} in coexisting olivines and pyroxenes: Jour. Geol. v. 59, p. 193-210.

Ross, C. S., *et al.*, 1954, Origin of dunites and of olivine-rich inclusions in basaltic rocks: Amer. Mineralogist, v. 39, p. 693-737.

Shepherd, E. S., 1938, The gases in rocks and some related problems: AM. JOUR. SCI., v. 35-A, p. 311-351.

Tilley, C. E., 1950, Some aspects of magmatic evolution: Quart. Jour. Geol. Soc. London, v. 106, p. 37-61.

Washington, H. S., 1923, Petrology of the Hawaiian Islands: III Kilauea and general petrology of Hawaii: AM. JOUR. SCI., v. 6, p. 338-367.

[American Journal of Science, Vol. 255, April 1957, P. 254-260]

POLLEN ANALYSIS OF A VALLEY FILL NEAR UMIAT, ALASKA

D. A. LIVINGSTONE

ABSTRACT. Microfossil analysis of a valley fill near Umiat, Alaska, has yielded a pollen chronology, consisting of an herbaceous pollen zone, a birch pollen zone and an alder zone, that can be correlated with the established chronology of the central Brooks Range. The boundary between the lower two zones has a radiocarbon age of between about 7,500 and 8,000 years, and the boundary between the upper two zones an age of about 6,000 years.

The bottom ten feet of the valley fill consists of clay, silt, sand and gravel without primary fossils or organic matter. The upper 25 feet consists of silt and peat and apparently began to accumulate under cold climatic conditions. Deposition of silt and peat continued for about 2,000 years, while the climate warmed to approximately its present temperature, and then ceased.

Correlation with pollen profiles of the central Brooks Range indicates that the postglacial thermal maximum occurred at about the same time in arctic Alaska as it did in the rest of the world. Correlation with pollen profiles of the central Brooks Range indicates that glacier retreat from the Eight Lake (Eschooka) position occurred about 8,000 years ago.

INTRODUCTION

In an earlier paper (Livingstone, 1955) a three-zone pollen stratigraphy was established for the central Brooks Range in glaciated northern Alaska. This contribution extends the same stratigraphy to the unglaciated foothills north of the Brooks Range. The new pollen profile comes from a deposit sufficiently rich in organic matter for radiocarbon dating, and the age of three levels has been estimated. The earlier profiles were from inorganic silts which could not be dated in this way.

Samples were collected by field workers of the Physical Research Laboratories of Boston University at the suggestion of Dr. John Cantlon. The author is very much obliged to Dr. Charles M. Matthews and Dr. Ralph Fellows of Boston University for an opportunity to examine the material for pollen.

Analysis of the core was carried out during tenure of a National Research Council of Canada post-doctorate fellowship at Dalhousie University, Halifax, Nova Scotia.

METHODS

Cores eight to ten inches long were taken with a light rotary drill rig having a four-inch barrel, and were shaved in the field to a thickness of two inches while still frozen solid. They were wrapped in aluminum foil, tied up in cotton bags and then placed in wooden boxes to melt and drain. By the time samples were picked out for pollen analysis the material was air-dry.

Quantities weighing about five grams were boiled briefly in a small beaker with a little five percent KOH. After boiling the material was strained through a seive with 200 meshes to the inch and washed with water into a large beaker. After standing for at least twenty-four hours the samples were decanted and transferred to a 40 ml. tapered centrifuge tube. They were then rinsed in acetone and suspended in an acetone-bromoform mixture of specific gravity 2.0. A pinch of anhydrous $CuSO_4$ was added to most samples to prevent the formation of coacervates. The material was run through the bromo-

form method of Frey (1951) in the usual way, after which it was transferred to a 15 ml. tapered centrifuge tube, acetolyzed, and run through the method of Frey one more. Finally it was boiled briefly in KOH and washed repeatedly in water until all the dispersable colloidal material was removed.

Following this treatment the small amount of material remaining was sucked up in a drop of water and mounted in safranin-stained glycerine jelly on a micro-slide. Examination was carried out at a magnification of 430 times, except for a few almost empty slides, which were searched for pollen at a magnification of 100 times. Identification of difficult grains was carried out with an oil-immersion apochromatic objective.

DESCRIPTION OF THE SAMPLING LOCALITY

The core was taken from a fill in the valley of Bearpaw Creek, about three miles north of Umiat, at 69° 24′ 35″ N., 152° 6′ 15″ W. Bearpaw Creek appears to have been recently rejuvenated and is actively eroding headward, with a nick-point just below the sampling locality. Above the nick-point the bed of the creek is choked with 35 feet of fibrous peat, silt and sand, grading into silt with bits of shale and siltstone near the bedrock. The material composing this deposit can be seen in section at the nick-point and consists of coarsely bedded horizontal layers of peat and silt.

Several cores were taken at this locality. The one analyzed for pollen was Boston University number 33U, taken at a spot a little to the east of the aggraded stream bed, where the valley floor is a few feet above stream level. From the core samples it was evident that the material in this place was of the same sort as that exposed at the nick-point, but the topographic relations suggested that it was an older deposit which had been subjected to less reworking.

The vegetation of the Umiat region has been described in detail by Churchill (1955). Briefly, it is low-arctic tundra with alder bushes and willows approaching tree size in favored localities. The climate is cool in summer and cold in winter, with light precipitation. There is perennial frost under all of the land surface and only the upper foot or so of the ground thaws out in summer.

Valley fills accumulate by the deposition of a creeping mantle of peat and vegetation from the surrounding slopes. This material probably creeps slowly down the valleys and it is occasionally thawed out and removed very rapidly by stream down-cutting. It is such a phase of active erosion that is currently in progress in Bearpaw Creek below the coring station.

Presumably both the process of creep which deposits the valley fills and the process of stream down-cutting which removes them are favored by warm and wet summers, but there is no reason to believe that they are both influenced to the same extent. The balance between deposition and erosion of the valley deposit is likely to depend on a rather complex and delicate interplay of climatic forces.

STRATIGRAPHY

Gross and microscopic stratigraphy are summarized in figure 1. The lowest pollen spectrum was obtained by dissolving a few silt-stone pebbles in

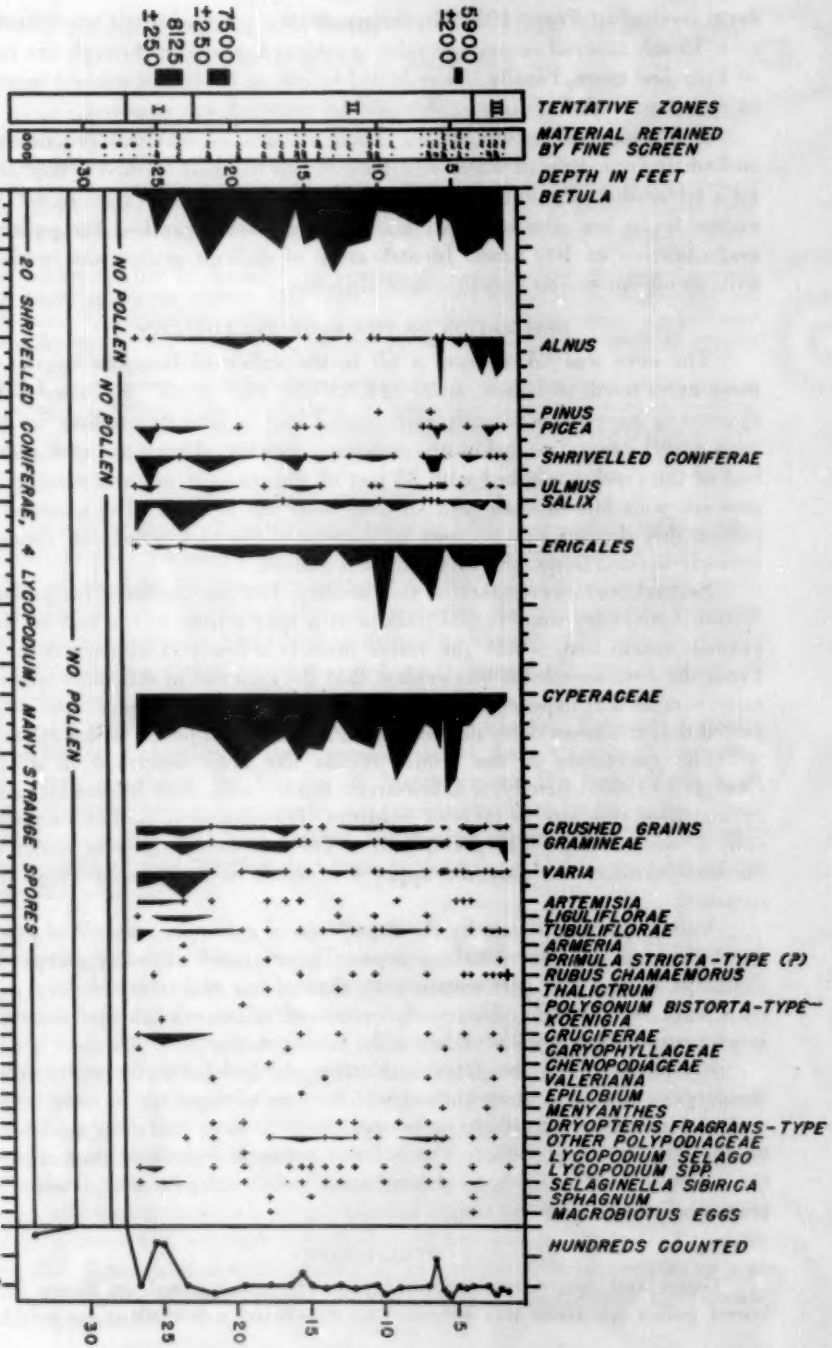

CORE 33U BEARPAW CREEK, UMIAT, ALASKA

Fig. 1. Core 33U Bearpaw Creek, Umiat, Alaska.

hydrofluoric acid, so it is representative of the fossil flora in the silt-stone bed from which the pebbles came, and does not properly belong with the rest of the diagram.

From the bottom of the core to the 26.5 foot level no pollen was present. The material here consisted mostly of expanding clays. One sample swelled to about twenty times its dry volume when it was boiled in KOH. The complete absence of pollen suggests that this material, if derived from polliniferous sedimentary deposits, has been subjected to prolonged oxidative weathering. If the clay were mechanically broken siltstone which had not been oxidized it would have contained some of the microfossils abundant in the bottom sample of the core.

Above the 26.5 foot level pollen is uniformly present, although the amount in four samples below 20 feet was too low to permit the calculation of reliable percentages. These samples have been omitted from the diagram.

The most striking features above 26 feet, 6 inches are general uniformity combined with short sharp flucuations of no apparent significance. *Betula* (birch) pollen is abundant at all levels, except near the bottom and *Cyperaceae* (sedge) pollen is abundant at all levels except near the top. *Alnus* (alder) is present in trace amounts except in the upper six feet, where it is rather abundant. *Picea* (spruce) is intermittently present throughout the diagram. Ericales show some tendency to be less abundant at the bottom of the diagram than they are generally.

Most of the minor constituents are so scarce that it is not possible to see any trend in their abundance. Only a few follow a consistent pattern. *Rubus chamaemorus* (bake-apple) is more abundant in the upper part of the diagram than the lower. A number of types—*Salix* (willow), Compositae (*Artemisia*, other Tubuliflorae, Liguliflorae), Cruciferae and Varia—are all significantly more abundant in the bottom of the diagram than elsewhere. The category Varia consists of a number of grains which could not be identified with certainty and were tentatively referred to the families Rosaceae, Leguminosae, Saxifragaceae and Umbelliferae.

VEGETATIONAL INTERPRETATION

The bottom level of the pollen diagram, based on grains and spores dissolved out of the siltstone, appears to represent a vegetation in which coniferous trees were very important. The proportion of unfamiliar spores is so high that it would be unsafe to say more about it. Many of the spores are very bizarre and so different from anything that occurs in Pleistocene deposits of the arctic and north temperate zones that the siltstone must be very old. Possibly it comes from the Cretaceous strata in the immediate vicinity, or it may originate in the early Tertiary beds which occur in nearby parts of northern Alaska. The latter possibility is suggested by the fact that Payne, et al. (1951) gave siltstone as a common facies of the Tertiary beds, but did not mention it in their discussion of the Cretaceous. In either case it is evident that the siltstone flora is at least a complete order of magnitude older than the bulk of the valley fill.

Above 26.5 feet only tundra vegetation appears to be represented in the pollen diagram. *Pinus, Picea* and *Ulmus* are the only genera present which are reliable indicators of forest. The slides were made up at the beginning of the spring flowering season, when a good deal of *Ulmus* pollen was in the air, and it was evident from the freshness and the excellent state of preservation of the *Ulmus* grains that they were atmospheric contaminants. The same is true of the two pine grains that were encountered.

The spruce grains were fossil ones but small amounts of wind-blown spruce are characteristic of the pollen rain all over the north slope of Alaska at the present time. A trace of spruce is usual through most of the postglacial section in the Brooks Range, due apparently to long-distance transport by the wind.

Disregarding the three above mentioned genera, the core seems to indicate the same three-fold vegetational history as is exhibited in the Brooks Range. At the bottom there is evidence of tundra vegetation with many indicators of open ground. In the middle there is strong evidence of tundra with fewer open ground species but with more dwarf birch shrubs. At the top alder becomes important.

The major pollen curves fluctuate considerably. Such fluctuation is more pronounced in the arctic than elsewhere, but it is not usually this strong. Perhaps some of the irregularities are due to the nature of the deposit. Unlike a lake, which integrates the pollen rain from a wide area, an accumulating deposit of terrestrial peat and silt will reflect minor fluctuations in the local vegetation. The sedge maximum at 5 feet, for example, may be due to the inclusion of a few sedge flowers in the sample analyzed.

It is quite evident that some secondary deposition of old microfossils has occurred during the accumulation of this deposit. There are spores throughout the polliniferous section that have been derived from pre-Pleistocene sedimentary deposits and there is also a considerable amount of shrivelled coniferous pollen of the types abundant in the siltstone sample. The proportion of this coniferous pollen is plotted on the diagram to give an indication of the amount of contamination from one kind of old deposit.

The thinness and weak development of the alder zone is worthy of note. In the Brooks Range the birch and alder zones were of approximately equal thickness. Here the alder zone is much the thinner and shows no sign of the internal differentiation which suggested a thermal maximum at Chandler Lake. This indicates that deposition has been very slow or absent during most of alder time at Bearpaw Creek.

The pollen diagram has been divided into zones I, II and III, in accordance with the Brooks Range sequence, but there are a few rather disquieting differences in the stratigraphy of the two localities. In particular, zone I is not well developed here. It includes a good deal of birch and shows no trace of internal differentiation into high-sedge and low-sedge sub-zones. Despite these reservations, however, it appears that the vegetational sequence covered by this profile is roughly the same as that covered by the long profile from Chandler Lake: first, tundra with many indicators of open ground;

next, tundra in which dwarf birch shrubs were more important; finally, tundra with enough alder bushes to influence the pollen rain.

STRATIGRAPHIC CORRELATION

If we assume that the vegetational changes reflected in this pollen diagram were synchronous over the entire North Slope of Alaska, then the easiest and most direct correlation which can be established is between this core and the ones from the Chandler Lake region. The two sampling localities are separated by only about ninety miles and are both in the same low-arctic vegetational province, so pollen correlation between them is fairly safe. In assuming synchrony of zone boundaries, however, it must be remembered that the herbaceous-birch transition at Bearpaw Creek is not sharply defined, nor is the herbaceous zone well developed. This makes correlations depending on the lower transition less reliable than ones depending on the upper.

The Chandler Lake zones have previously (Livingstone, 1955) been correlated with the drift stratigraphy of Detterman (Péwé et al., 1953). By this correlation the herbaceous-birch transition marks the time of retreat of the Brooks Range glaciers from the Eight Lake (Eschooka) position. Detterman has correlated the Eschooka glaciation with the Kenai Peninsula Naptowne glaciation which has a radiocarbon age of less than 14,000 years and greater than 8,000 years.

By this rather tenuous thread of argument the lowermost polleniferous deposits at Bearpaw Creek ought to be at least 8,000 years old. It is very reassuring to have the information (personal letter from J. L. Kulp to C. M. Matthews, 1955) that the peat just above the 25 foot level, in zone I, has a radiocarbon age of 8,125 $\pm$ 250 years. A layer just above the transition between zones I and II gives a date of 7,500 $\pm$ 250 years.

A third determination, a sample taken in the neighborhood of the birch-alder transition, gave a radiocarbon age of 5900 $\pm$ 250 years. Accepting the correlation with Chandler Lake, this sample lies somewhat below the post-glacial alder maximum, which the author interprets as the local manifestation of the world-wide thermal maximum. The thermal maximum has been radiocarbon dated in Europe (Flint and Deevey, 1951) at 3,000-6,000 years ago. Apparently the alder maximum was not only climatically equivalent to the thermal maximum, but was contemporaneous with it.

DISCUSSION

In addition to extending the Brooks Range pollen chronology to the foothills and providing three radiocarbon dates for it, the Bearpaw Creek core has some geomorphic interest.

It appears from the pollen record that deposition of silt and peat in the valley began under a climate a good deal colder than the present and that it ceased with the onset of climatic conditions approximately like those now prevailing. During thermal maximum time there may have been a certain amount of erosion, though not necessarily at the location of this core: the stream may have cut into the valley fill elsewhere during thermal maximum time and later aggraded to its present level. Under present conditions the deposit which occupies the stream bed is being degraded.

The relation between temperature and deposition of the valley fill can hardly be a simple one. If it were only a matter of deposition during cold times and erosion during warm ones, then one would expect to find in the valley the deposits which accumulated during the cool time at the end of the last interglacial or major interstadial. There is no trace of them. One is forced to conclude that active erosion goes on not only under unusually warm conditions but under periglacial conditions as well. Precipitation is probably involved but present knowledge of paleoclimate in northern Alaska does not include the information on precipitation necessary for complete understanding of the aggradation-degradation balance in the valley.

References

Churchill, Ethan D., 1955, Phytosociological and environmental characteristics of some plant communities in the Umiat region of Alaska: Ecology, v. 36, no. 4, p. 606-626.

Flint, R. F. and E. S. Deevey, Jr., 1951, Radiocarbon dating of late-Pleistocene events: Am. Jour. Sci., v. 249, p. 257-300.

Frey, D. G., 1951, Pollen succession in the sediments of Singletary Lake, North Carolina: Ecology, v. 32, no. 3, p. 518-533.

Livingstone, D. A., 1955, Some pollen profiles from arctic Alaska: Ecology, v. 36, no. 4, p. 587-600.

Payne, T. G., et al., 1951, Geology of the arctic slope of Alaska: U. S. Geol. Survey Oil and Gas Inv. Map OM 126.

Péwé, Troy L., et al., 1953, Multiple glaciation in Alaska: U. S. Geol. Survey Circ. 289, 13 p.

Dept. of Zoology
Duke University
Durham, N. C.

[AMERICAN JOURNAL OF SCIENCE, VOL. 255, APRIL 1957, P. 261-265]

EVALUATION OF THE CHEMICAL POTENTIAL IN TERMS OF INTENSIVE QUANTITIES

GEORGE TUNELL

ABSTRACT. The chemical potential was defined by J. Willard Gibbs in terms of extensive quantities. That it is nevertheless an intensive quantity therefore requires proof. In this paper an elementary proof is given that results in an explicit evaluation of the chemical potential in terms of intensive quantities:

$$\mu_k = E - TS + pV - m_1\left(\frac{\partial E}{\partial m_1}\right)_{SVm_2 \ldots m_{n-1}} - \ldots$$

$$+ (1-m_k)\left(\frac{\partial E}{\partial m_k}\right)_{SVm_1 \ldots m_{k-1}m_{k+1} \ldots m_{n-1}}$$

$$- \ldots - m_{n-1}\left(\frac{\partial E}{\partial m_{n-1}}\right)_{SVm_1 \ldots m_{n-2}},$$

where μ_k denotes the chemical potential, E denotes the specific energy, T denotes the absolute temperature, S denotes the specific entropy, p denotes the pressure, V denotes the specific volume, and m_k denotes the mass fraction of component k.

Since the chemical potential is thus shown to be equal to a function of intensive quantities only it is itself an intensive quantity.

The chemical potential, which was introduced by J. Willard Gibbs (1876, p. 116, 144) is the cornerstone of chemical thermodynamics, and the phase rule, which has come to play such an important role in studies of mineral and rock formation as well as in chemical and metallurgical researches, is a corollary of the quantitative relations of the chemical potentials in phases at equilibrium established by him.

The chemical potential μ_k of a phase made up of n components with respect to the kth component was defined by Gibbs (1876, p. 116, 144) by the equation

$$\mu_k = \left(\frac{\partial \mathbf{E}}{\partial \mathbf{m}_k}\right)_{\mathbf{SVm}_1 \ldots \mathbf{m}_{k-1}\mathbf{m}_{k+1} \ldots \mathbf{m}_n}, \qquad (1)$$

where $\mathbf{E}$ denotes the total energy of the phase, $\mathbf{S}$ denotes its total entropy, $\mathbf{V}$ denotes its total volume, $\mathbf{m}_1$ denotes the mass of component 1 in the phase, $\mathbf{m}_2$ the mass of component 2, $\mathbf{m}_k$ the mass of component k and $\mathbf{m}_n$ the mass of component n. Gibbs (1876, p. 144) stated that the chemical potential is "independent of the quantity of the mass considered" and proofs that a partial quantity such as the chemical potential depends only on the temperature, pressure, and composition have been given by Butler (1936, p. 89, 90), by Keenan (1941, p. 231), and by Glasstone (1947, p. 215).[1] An elementary proof that the chemical potential depends only on intensive quantities is pre-

[1] The derivation given by Butler (1936) and by Glasstone (1947) was carried out by the application of Euler's theorem on homogeneous functions and is elegant and brief. Euler's theorem was itself proved by means of the chain rule for differentiation of a function of a function. The proof given in this paper, which makes use only of the chain rule for differentiation of a function of a function, is thus more elementary. Almost all petrologists and physical chemists have studied the chain rule for differentiation of a function of a function, but not all have studied Euler's theorem on homogeneous functions and the more elementary proof is of value particularly to the latter.

sented in this paper. This proof is accomplished by the use of the standard equation for change of variables in partial differentiation and it results in an explicit evaluation of the chemical potential in terms of functions involving only quantities that are intensive by definition. The resulting equation may or may not be found of direct practical use. It is presented chiefly for its value in showing clearly that the chemical potential depends only on intensive quantities and is therefore itself an intensive quantity.

The evaluation of the chemical potential in terms of intensive quantities is carried out by the following method. The specific energy E of the phase is defined as the total energy $\mathbf{E}$ divided by the total mass $\mathbf{M}$,

$$E = \frac{\mathbf{E}}{\mathbf{M}}, \tag{2}$$

and the total mass $\mathbf{M}$ is of course equal to the sum of the masses of the n components

$$\mathbf{M} = \mathbf{m}_1 + \ldots + \mathbf{m}_n . \tag{3}$$

Thus

$$\mu_k = \left(\frac{\partial \mathbf{M}E}{\partial \mathbf{m}_k}\right)_{\mathbf{SVm}_1 \ldots \mathbf{m}_{k-1}\mathbf{m}_{k+1} \ldots \mathbf{m}_n}$$
$$= \mathbf{M}\left(\frac{\partial E}{\partial \mathbf{m}_k}\right)_{\mathbf{SVm}_1 \ldots \mathbf{m}_{k-1}\mathbf{m}_{k+1} \ldots \mathbf{m}_n} + E . \tag{4}$$

The specific energy E is a function of the specific entropy S, the specific volume V, and the mass fractions $m_1, m_2, \ldots m_{n-1}$, which are defined by the equations $S = \mathbf{S/M}$, $V = \mathbf{V/M}$, $m_1 = \mathbf{m}_1/\mathbf{M}$, $m_2 = \mathbf{m}_2/\mathbf{M}$, $\ldots$, $m_{n-1} = \mathbf{m}_{n-1}/\mathbf{M}$ respectively. Application of the theorem for change of variables in partial differentiation therefore gives the equation

$$\left(\frac{\partial E}{\partial \mathbf{m}_k}\right)_{\mathbf{SVm}_1 \ldots \mathbf{m}_{k-1}\mathbf{m}_{k+1} \ldots \mathbf{m}_n} =$$
$$\left(\frac{\partial E}{\partial S}\right)_{Vm_1 \ldots m_{n-1}} \left(\frac{\partial S}{\partial \mathbf{m}_k}\right)_{\mathbf{SVm}_1 \ldots \mathbf{m}_{k-1}\mathbf{m}_{k+1} \ldots \mathbf{m}_n}$$
$$+ \left(\frac{\partial E}{\partial V}\right)_{Sm_1 \ldots m_{n-1}} \left(\frac{\partial V}{\partial \mathbf{m}_k}\right)_{\mathbf{SVm}_1 \ldots \mathbf{m}_{k-1}\mathbf{m}_{k+1} \ldots \mathbf{m}_n}$$
$$+ \left(\frac{\partial E}{\partial m_1}\right)_{SVm_2 \ldots m_{n-1}} \left(\frac{\partial m_1}{\partial \mathbf{m}_k}\right)_{\mathbf{SVm}_1 \ldots \mathbf{m}_{k-1}\mathbf{m}_{k+1} \ldots \mathbf{m}_n} + \ldots +$$
$$\left(\frac{\partial E}{\partial m_k}\right)_{SVm_1 \ldots m_{k-1}m_{k+1} \ldots m_{n-1}} \left(\frac{\partial m_k}{\partial \mathbf{m}_k}\right)_{\mathbf{SVm}_1 \ldots \mathbf{m}_{k-1}\mathbf{m}_{k+1} \ldots \mathbf{m}_n}$$
$$+ \ldots + \left(\frac{\partial E}{\partial m_{n-1}}\right)_{SVm_1 \ldots m_{n-2}} \left(\frac{\partial m_{n-1}}{\partial \mathbf{m}_k}\right)_{\mathbf{SVm}_1 \ldots \mathbf{m}_{k-1}\mathbf{m}_{k+1} \ldots \mathbf{m}_n} . \tag{5}$$

The partial derivative $\left(\frac{\partial S}{\partial \mathbf{m}_k}\right)_{\mathbf{SVm}_1 \ldots \mathbf{m}_{k-1}\mathbf{m}_{k+1} \ldots \mathbf{m}_n}$ can also be evaluated by application of the theorem for change of variables. Thus one has

$$\left(\frac{\partial S}{\partial \mathbf{m}_k}\right)_{\mathbf{SVm}_1 \ldots \mathbf{m}_{k-1}\mathbf{m}_{k+1} \ldots \mathbf{m}_n}$$
$$= \mathbf{S}\left(\frac{\partial \mathbf{M}^{-1}}{\partial \mathbf{m}_k}\right)_{\mathbf{SVm}_1 \ldots \mathbf{m}_{k-1}\mathbf{m}_{k+1} \ldots \mathbf{m}_n}$$
$$= -\frac{\mathbf{S}}{\mathbf{M}^2} = -\frac{S}{\mathbf{M}} \,. \tag{6}$$

Likewise one has

$$\left(\frac{\partial V}{\partial \mathbf{m}_k}\right)_{\mathbf{SVm}_1 \ldots \mathbf{m}_{k-1}\mathbf{m}_{k+1} \ldots \mathbf{m}_n}$$
$$= \mathbf{V}\left(\frac{\partial \mathbf{M}^{-1}}{\partial \mathbf{m}_k}\right)_{\mathbf{SVm}_1 \ldots \mathbf{m}_{k-1}\mathbf{m}_{k+1} \ldots \mathbf{m}_n}$$
$$= -\frac{\mathbf{V}}{\mathbf{M}^2} = -\frac{V}{\mathbf{M}} \,, \tag{7}$$

also

$$\left(\frac{\partial m_1}{\partial \mathbf{m}_k}\right)_{\mathbf{SVm}_1 \ldots \mathbf{m}_{k-1}\mathbf{m}_{k+1} \ldots \mathbf{m}_n}$$
$$= \mathbf{m}_1\left(\frac{\partial \mathbf{M}^{-1}}{\partial \mathbf{m}_k}\right)_{\mathbf{SVm}_1 \ldots \mathbf{m}_{k-1}\mathbf{m}_{k+1} \ldots \mathbf{m}_n}$$
$$= -\frac{\mathbf{m}_1}{\mathbf{M}^2}$$
$$= -\frac{m_1}{\mathbf{M}} \,, \tag{8}$$

and

$$\left(\frac{\partial m_k}{\partial \mathbf{m}_k}\right)_{\mathbf{SVm}_1 \ldots \mathbf{m}_{k-1}\mathbf{m}_{k+1} \ldots \mathbf{m}_n}$$
$$= \mathbf{m}_k\left(\frac{\partial \mathbf{M}^{-1}}{\partial \mathbf{m}_k}\right)_{\mathbf{SVm}_1 \ldots \mathbf{m}_{k-1}\mathbf{m}_{k+1} \ldots \mathbf{m}_n} + \frac{\mathbf{1}}{\mathbf{M}}$$
$$= -\frac{\mathbf{m}_k}{\mathbf{M}^2} + \frac{1}{\mathbf{M}}$$
$$= \frac{\mathbf{1} - m_k}{\mathbf{M}} \,, \tag{9}$$

and

$$\left(\frac{\partial m_{n-1}}{\partial \mathbf{m}_k}\right)_{\mathbf{SVm}_1 \ldots \mathbf{m}_{k-1}\mathbf{m}_{k+1} \ldots \mathbf{m}_n}$$
$$= \mathbf{m}_{n-1}\left(\frac{\partial \mathbf{M}^{-1}}{\partial \mathbf{m}_k}\right)_{\mathbf{SVm}_1 \ldots \mathbf{m}_{k-1}\mathbf{m}_{k+1} \ldots \mathbf{m}_n}$$
$$= -\frac{\mathbf{m}_{n-1}}{\mathbf{M}^2}$$
$$= -\frac{m_{n-1}}{\mathbf{M}} \,. \tag{10}$$

Substituting in equation (4) the values of the partial derivatives in equations (5), (6), (7), (8), (9), and (10) one obtains the result

$$\mu_k = E - S\left(\frac{\partial E}{\partial S}\right)_{Vm_1 \ldots m_{n-1}} - V\left(\frac{\partial E}{\partial V}\right)_{Sm_1 \ldots m_{n-1}}$$
$$- m_1\left(\frac{\partial E}{\partial m_1}\right)_{SVm_2 \ldots m_{n-1}} - \ldots$$
$$+ (1-m_k)\left(\frac{\partial E}{\partial m_k}\right)_{SVm_1 \ldots m_{k-1}m_{k+1} \ldots m_{n-1}}$$
$$- \ldots - m_{n-1}\left(\frac{\partial E}{\partial m_{n-1}}\right)_{SVm_1 \ldots m_{n-2}} . \qquad (11)$$

The values of the partial derivatives $\left(\frac{\partial E}{\partial S}\right)_{Vm_1 \ldots m_{n-1}}$ and $\left(\frac{\partial E}{\partial V}\right)_{Sm_1 \ldots m_{n-1}}$ are the same as the values of the partial derivatives of the energy of a one-component one-phase system of constant mass with respect to the entropy and with respect to the volume,[2] that is,

$$\left(\frac{\partial E}{\partial S}\right)_{Vm_1 \ldots m_{n-1}} = T \quad , \qquad (12)$$

and

$$\left(\frac{\partial E}{\partial V}\right)_{Sm_1 \ldots m_{n-1}} = -p . \qquad (13)$$

Hence one has finally

$$\mu_k = E - TS + pV - m_1\left(\frac{\partial E}{\partial m_1}\right)_{SVm_2 \ldots m_{n-1}} - \ldots$$
$$+ (1-m_k)\left(\frac{\partial E}{\partial m_k}\right)_{SVm_1 \ldots m_{k-1}m_{k+1} \ldots m_{n-1}} - \ldots$$
$$- m_{n-1}\left(\frac{\partial E}{\partial m_{n-1}}\right)_{SVm_1 \ldots m_{n-2}} .[3] \qquad (14)$$

This equation expresses the chemical potential explicitly in terms of intensive quantities.

$$\mu_k = \left(\frac{\partial G}{\partial m_k}\right)_{Tpm_1 \cdots m_{k-1}m_{k+1} \cdots m_n} ,$$

but for the purposes of this paper it seemed best to start with Gibbs' original definition.

In the special case of a phase made up of two components, the two chemical potentials can thus be expressed by the equations

[2] The values of the partial derivatives of the energy of a one-component one-phase system of constant mass with respect to the entropy and with respect to the volume are given by Bridgman (1925, p. 11, 12).

[3] The chemical potential can be evaluated in terms of intensive quantities more briefly by starting with the equation

$$\mu_1 = E - TS + pV + m_2\left(\frac{\partial E}{\partial m_1}\right)_{SV} \tag{15}$$

and

$$\mu_2 = E - TS + pV - m_1\left(\frac{\partial E}{\partial m_1}\right)_{SV}. \tag{16}$$

References

Bridgman, P. W., 1925, A condensed collection of thermodynamic formulas: Cambridge, Harvard University Press.

Butler, J. A. V., 1936, *in* A commentary on the scientific writings of J. Willard Gibbs, Ph.D, LL.D., formerly professor of mathematical physics in Yale University: New Haven, Yale University Press.

Gibbs, J. W., 1876 and 1878, On the equilibrium of heterogeneous substances: Trans. Conn. Acad., v. 3, p. 108-248; 343-524.

Glasstone, S., 1947, Thermodynamics for chemists: New York, D. Van Nostrand Co., Inc.

Keenan, J. H., 1941, Thermodynamics: New York, John Wiley & Sons, Inc.

University of California
Los Angeles, California

[American Journal of Science, Vol. 255, April 1957, P. 266-281]

THERMODYNAMICS OF SOLIDS UNDER NON-HYDROSTATIC STRESS WITH GEOLOGIC APPLICATIONS

GORDON J. F. MacDONALD

ABSTRACT. Using the methods of Gibbs, the general thermodynamics of elastic solids is developed. A phase under a non-hydrostatic stress defined by three principal pressures is unstable relative to the same phase under an equal hydrostatic pressure. The equation for the surface of equilibrium between two polymorphs in a one-component system in a general stress field is shown to contain terms involving the differences in the principal pressures acting on the solid. These terms will be small relative to the change in entropy and volume for first order transitions, such as andalusite to kyanite, and for stress differences of a few thousand bars.

It is shown that the anisotropic elastic properties of minerals *may* be important in the formation of an oriented fabric provided that the mechanism of deformation is one of solution and redeposition. If the mineral deforms by some mechanism of mechanical flow (twin gliding, etc.) then the orientation of the mineral results from the detailed mechanism of the mechanical deformation. In general, the driving potential in plastic flow is the difference in chemical potential between that part of the crystal at high pressure and that part at low pressure.

INTRODUCTION

The physical appearance of rocks from areas of regional metamorphism indicates that such rocks have in many cases undergone deformation beyond the elastic limit, and this deformation has taken the form of a plastic flow of the rock. A necessary condition for plastic flow to take place is that the rock be under a non-hydrostatic stress. The question then arises as to what is the influence of the non-hydrostatic pressure on the recrystallization of the rock; in particular, what will be the effect of non-hydrostatic pressure on the equilibrium mineral assemblage and how will the non-hydrostatic pressure influence the orientation of the crystallizing minerals. In discussing the role of non-hydrostatic stress in metamorphism, two aspects of the problem should be kept clearly separate. Non-hydrostatic stress may be expected to influence the equilibrium assemblage and also the rate at which equilibrium is attained. In the following we will investigate the time-independent effects of non-hydrostatic stress, omitting the much more difficult problem of the influence of stress on the rate of reaction.

The possible effect of a non-hydrostatic stress on the stability of various minerals has given rise to much controversy. Harker (1939) clearly states the geologic evidence for the effect of non-hydrostatic stress on mineral assemblages. Harker asserts that certain minerals are commonly found in rocks that have structures indicating non-hydrostatic conditions of crystallization, and are not found in rocks not showing such structures. Harker labels these minerals "stress minerals", while minerals not found in rocks showing structures attributed to non-hydrostatic stress are termed "anti-stress" minerals. Kyanite, staurolite and almandine are examples of "stress minerals", while andalusite, leucite and nepheline are considered to be "anti-stress minerals". In recent years various specific examples have been cited as exceptions to the association of "stress minerals" with flow structure (Miyashiro, 1949).

The geologic evidence on the existence of "stress minerals" is somewhat uncertain, and current theoretical treatments leave much to be desired. Bridgman (1936) states that there is no thermodynamic reason why transitions should not occur under non-hydrostatic stress which would never occur under any combination of temperature and hydrostatic stress. Verhoogen (1951) in a treatment of the chemical potential of a stressed solid, states that the effect of shear on chemical equilibrium appears to be small. However, there are inconsistencies in Verhoogen's treatment. Indeed, various attempts to interpret or extend Gibbs' (1906) analysis of the thermodynamics of elastic bodies are not completely correct. Verhoogen points out such inconsistencies in Goranson (1930) and Rice (1936).

The present paper deals with the thermodynamics of elastic bodies and in doing so, follows Gibbs' treatment closely. Gibbs gives a masterful treatment of elasticity, a treatment that has been uniformly neglected by workers in elastic theory. An example of this neglect is that Gibbs is not mentioned once in Love's (1945) classic treatise on elasticity. On the basis of the present analysis of the thermodynamics of elastic bodies, the effect of non-hydrostatic stress on mineral equilibrium is considered and an attempt is made to state the problem of the orientation of anisotropic minerals in a stress field.

THERMODYNAMICS OF ELASTIC BODIES

In treating the thermodynamics of elastic bodies we will consider a special case that illustrates the main features of the thermodynamics of solids under a non-hydrostatic stress. By considering this special case we find the mathematics is simplified and the physics of the problem is emphasized. The generalization of the results will be indicated but not treated in detail.

Consider one mole of a solid in the form of a rectangular parallelepiped. The edge lengths of the parallelepiped in the state of initial strain are X_1^0, X_2^0, X_3^0. Due to forces f_1, f_2, f_3 acting perpendicular to the pairs of faces 1, 2 and 3, the parellelepiped is deformed to another parallelepiped with edges X_1, X_2, X_3, as is illustrated in figure 1. The deformation in each direction is assumed to be uniform, so that the position of a fixed point (x_1, x_2, x_3) in the strained solid is related to a point (x_1^0, x_2^0, x_3^0) in the stage of initial strain by the relations

$$x_i = \frac{x_i^0 X_i}{X_i^0} \qquad (i = 1, 2, 3)$$

We are thus assuming that the solid is undergoing a pure homogeneous strain with lines parallel to one of the three principal directions in the solid remaining unchanged in the strained state.

The first and second laws of thermodynamics can be combined in the form

$$dU = TdS + dW$$

where U is the internal energy per mole, S is the entropy per mole, and dW is the work done on the system. The system we are considering is the solid in the form of a parallelepiped. The work done on the system by the external forces f_1, f_2, f_3 will be the sum of the products of the various forces and the distance over which they act.

$$dW = f_1 dX_1 + f_2 dX_2 + f_3 dX_3$$

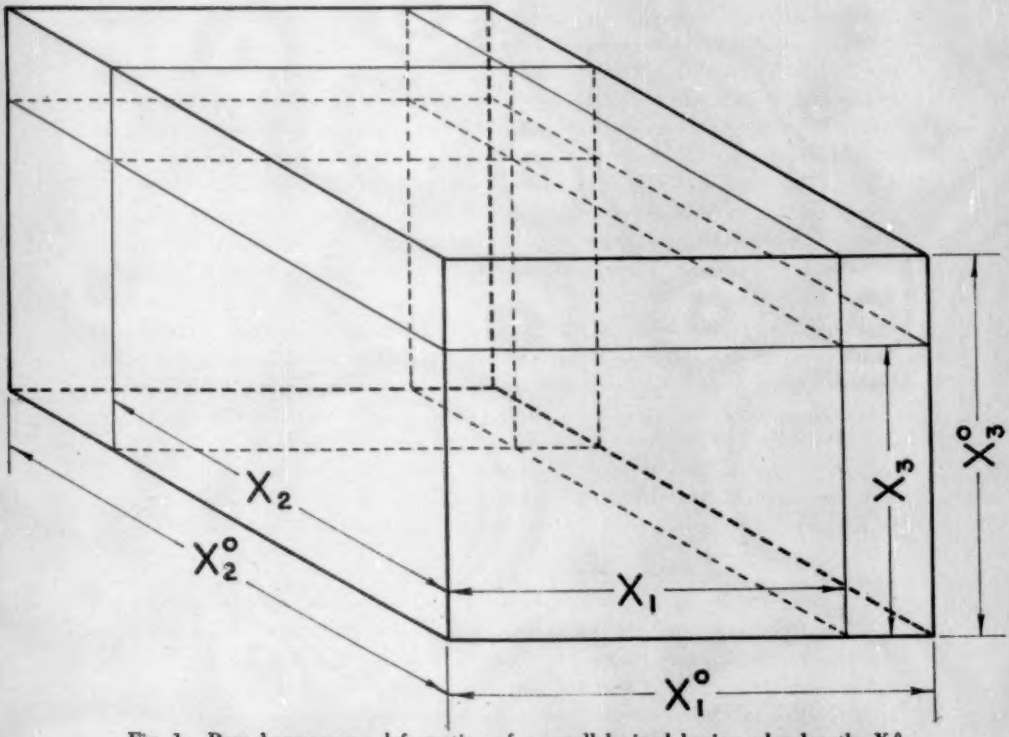

Fig. 1. Pure homogenous deformation of a parallelepiped having edge lengths X_1°, X_2° and X_3° in state of initial strain.

By changing variables in the expression for internal energy from entropy to temperature we obtain the expression for the Helmholtz free energy of the strained solid.

$$dF = \sum_{i=1}^{3} f_i dX_i - SdT$$

This expression reduces to the more familiar form

$$dF = -SdT - PdV$$

where V is the molar volume, when the solid is under a uniform hydrostatic pressure P. In this case the forces acting on any face will be equal to the negative product of the pressure and the area of the face,

$$f_1 = -PX_2X_3 \qquad f_2 = -PX_1X_3 \qquad f_3 = -PX_1X_2$$

$$V = X_1X_2X_3$$

$$dV = X_2X_3dX_1 + X_1X_3dX_2 + X_1X_2dX_3$$

$$\sum_{i=1}^{3} f_i dX_i = -PdV$$

where X_1, X_2 and X_3 are the edge lengths at any stage of the deformation.

We now consider the condition for equilibrium of a strained solid. The condition for thermal equilibrium requires that the temperature be uniform throughout the solid. The condition of mechanical equilibrium requires that the surfaces bounding the solid be stationary; that is, that the forces acting on each of the six faces be exactly balanced by the internal forces of the solid. In general the forces acting on the solid can be specified by indicating the three principal pressures acting on the pairs of opposing faces of the solid.

We can denote these three principal pressures by P_1, P_2 and P_3 where

$$P_1 = -f_1/X_2X_3 \qquad P_2 = -f_2/X_1X_3 \qquad P_3 = -f_3/X_1X_2$$

The condition for equilibrium with respect to diffusion may not be so obvious, and to demonstrate these conditions we follow Gibbs and imagine the solid to be bounded by a fluid, where the fluid acting on the faces perpendicular to the edge X_1, is at a pressure P_1, the fluid acting on the faces perpendicular to edge X_2 is at a pressure P_2, and the fluid acting on the faces perpendicular to X_3 is at a pressure P_3. Since the fluids are at different pressures, this requires that the fluids acting on the various faces be separated by rigid impermeable membranes. Now we need the conditions for equilibrium of the solid with respect to solution of the solid in the fluid with which it is in contact. For simplicity we assume that the solid can be treated as a one-component system. The Helmholtz free energy of the solid is simply

$$dF = \sum_{i=1}^{3} \mu_i dn_i$$

Now consider the system composed of the solid under a non-hydrostatic stress system and the fluid in contact with the solid across the faces perpendicular to edge X_1. The fluid is at a pressure P_1. The Helmholtz free energy of the system solid plus fluid is given by

$$dF = dF^s + dF^f$$

where dF^f for the fluid at constant volume and temperature is given by

$$dF^f = \sum_{i=1}^{n} \bar{\mu}_1{}^i d\bar{n}_1{}^i$$

where $\bar{\mu}_1{}^i$ is the chemical potential of the ith component of the fluid at pressure P_1

$$dF = \mu_1{}^s dn_1{}^s + \Sigma \bar{\mu}^i d\bar{n}^i \qquad dn_2 = dn_3 = 0$$

The system fluid plus solid is at equilibrium when the Helmholtz free energy is at a minimum. The subsidiary condition on this minimum is that the total mass of each component be a constant. The system of fluid plus solid is a closed system since the membranes between the fluids are impermeable. Since the solid is a one-component system, the conditions for a closed system can be written as

$$dn_1{}^s + d\bar{n} = 0$$

where $dn_1{}^s$ is the number of moles of the component of the solid going into solution across faces perpendicular to X_1. Using the method of Lagrange multipliers, the condition for the Helmholtz free energy to be a minimum is then that

$$\mu_1{}^s = \bar{\mu} = \mu$$

The condition for equilibrium with respect to solution of the solid in the fluid acting on the face perpendicular to X_1, is that the chemical potential of the component of the solid in the fluid be equal to the chemical potential of the component along the surface of the solid.

Similarly, the condition for equilibrium across surfaces in contact with fluid is that the chemical potential of the component be equal in the two phases in contact. In general the three pairs of faces will be at different pressures, so the chemical potentials of the component of the solid will be different in the three fluids. This means that the chemical potential of the component of the solid will in general have three different values corresponding to the three pairs of faces under the three principal pressures. This important result was obtained by Gibbs (1906, p. 196) and emphasized by him in his subsequent discussion. Verhoogen (1951) quotes this result but proceeds to consider the chemical potential as uniform throughout the solid.

Perhaps the best experimental evidence that Gibbs is correct in his deduction that the chemical potential varies from face to face of a stressed solid, can be found in the behavior of stressed ice. Pressure tends to decrease the melting point of ice, since the volume of the water at low pressures is less than the volume of ice. If two cubes of ice at 0° C. are pressed together, the ice will melt along the surface of contact between the cubes. If the chemical potential of the ice were uniform over the entire surface, the cubes should melt uniformly over their surface and not just at the surface where the pressure is greatest.

In deriving the conditions for diffusion equilibrium we assumed the solid to be in equilibrium with a fluid. The chemical potential of the component of the solid, of course, does not depend on the presence of the fluid. The chemical potential is still defined regardless of whether a fluid or another solid is acting upon the system and producing the non-hydrostatic pressure.

We now examine how we might express a quantity analogous to the Gibbs free energy of the solid. If we subtract

$$d(f_1X_1 + f_2X_2 + f_3X_3)$$

from both sides of

$$dF = -SdT + \sum_{i=1}^{3} f_i dX_i$$

we obtain

$$dG = -SdT - \sum_{i=1}^{3} X_i df_i$$

where G is given by

$$G = F - \sum_{i=1}^{3} f_i X_i$$

and F is the Helmholtz free energy per mole of the solid. The function G defined in this way reduces to the familiar form of the Gibbs free energy for a hydrostatic pressure, provided we set

$$dP = \frac{dP_1 + dP_2 + dP_3}{3}$$

and

$$df_1 = -X_2X_3dP_1$$
$$df_2 = -X_1X_3dP_2$$
$$df_3 = -X_1X_2dP_3$$

as we then have

$$dG = -SdT + VdP$$

We thus have to introduce a factor of 1/3 in our expression for G in order to have it reduced to the ordinary Gibbs free energy. The factor of 1/3 enters since we are defining an average Gibbs free energy for the solid as a whole, the chemical potential of the solid having three principal values. The average Gibbs free energy for the solid with three principal pressures can be written as

$$dG = -SdT - 1/3 \sum_{i=1}^{3} X_i df_i$$

In the case of a solid under a general non-hydrostatic stress, the average Gibbs free energy can be written as

$$dG = -SdT - V_o \sum_i \sum_j \left(\frac{\delta ij}{3} + \varepsilon_{ij} d\sigma_{ij} \right)$$

where V_o is the initial volume of the solid, ε_{ij} the strain tensor, σ_{ij} the stress tensor, and δ_{ij}, Kronecker delta. It should be emphasized that this is the average Gibbs free energy for the solid. In considering phase equilibrium we will have to examine how the chemical potential varies over the surface of a solid.

GEOLOGIC PROBLEMS

We now consider how the above formulation of thermodynamics of elastic solids can be used to solve specific geologic problems. We first examine the stability of a solid under a non-hydrostatic stress with reference to a solid under hydrostatic stress. This problem was originally treated by Gibbs and as it forms the basis for our discussion of various other problems, we will treat it in detail. Consider a solid in the form of a rectangular parallelepiped under a hydrostatic pressure P_x. The chemical potential, μ_x, of the component of the solid will then be given by

$$\mu_x^* = PV^* + U^* - TS^*$$

where V^*, U^* and S^* are the volume, internal energy and entropy per mole of the solid. Now, keeping the pressure constant on the faces perpendicular to the edge X_1, and keeping the temperature constant, change the pressures acting on the faces perpendicular to X_2 and X_3 to P_2 and P_3, where in general $P_2 \neq P_3$, $P_3 \neq P_1$. This situation is illustrated diagrammatically in figure 2. Solid A^0 with edge lengths X_1^0, X_2^0 and X_3^0 represents the solid in the initial state of strain at a hydrostatic pressure P_1. Solid A represents the solid with the pressures P_2 and P_3 acting on the faces normal to X_2 and X_3, where in general P_2 and P_3 are not equal to P_1. In changing the pressures we will do work on the solid and will in general alter the internal energy, volume and

entropy of the solid. The chemical potential of the component of the solid along the faces acted on by the constant pressure P_1 will be given by

$$\mu_1 = P_1V + U - TS$$

where in general V, U and S are not the same as for the solid under a hydrostatic pressure. The chemical potential along the face at pressure P_1 in the non-hydrostatically stressed solid differs from that of the hydrostatically stressed solid by

$$\mu_1 - \mu_1^* = P_1(V - V^*) + (U - U^*) - T(S - S^*)$$

The last two terms represent the work done on the solid in straining it, since by the first and second law we have that

$$W = \Delta U - T\Delta S$$

The term $P_1(V - V^*)$ represents the work done by the solid in displacing the fluid. The work done on the solid will always be positive and by the second law will always be greater than or equal to the work done by the solid on the fluid. The work done on the fluid by the solid will equal the work done on the solid only in the case of a hydrostatic pressure. Since for non-hydrostatic stress, the work W done on the solid is greater than $P_1\Delta V$, the work done by the solid on the fluid, the chemical potential of the 1 face of the solid under a non-hydrostatic stress is greater than the chemical potential of the solid under a hydrostatic pressure P_1. As Gibbs emphasizes, if the face of the strained solid is in contact with a fluid in which is immersed a piece of the solid, material will tend to dissolve from the face of the strained solid and deposit on the solid under a hydrostatic pressure. Figure 2 shows diagrammatically the direction in which material would move for the given stress distribution, provided both solids A and A^0 were in contact with a fluid.

In general, if a solid is in a state of strain fixed by three principal pressures P_1, P_2 and P_3 acting on three pairs of faces, then the chemical potential of the component of the solid along these faces will be greater than the chemical potential for the component in a solid under an equal hydrostatic pressure. These considerations thus answer the general question as to whether there exist *stable* phases under non-hydrostatic stress that would not be stable under hydrostatic stress. The non-hydrostatically stressed phase will *always* be unstable relative to a phase under a hydrostatic pressure equal to the least of the principal pressures acting on the non-hydrostatically stressed solid. It is thus theoretically impossible for a phase to be stable only under conditions of non-hydrostatic stress. This does not rule out the theoretical possibility mentioned by Bridgman (1936) of transitions under shearing stress which would never occur under any combination of temperature and hydrostatic pressure. In order to examine the probability of such transitions actually taking place, we need to consider the effect of shearing stress on the position of equilibrium surface. Polymorphic transitions in stressed solids are considered in the following sections.

In order to illustrate the numerical magnitude of the effects of non-hydrostatic stress, we consider a cube of quartzite originally at one bar hydrostatic pressure, then subjected to compression of 1000 bars normal to the X_3 edge, the faces parallel to the X_3 edge being kept at atmospheric pressure.

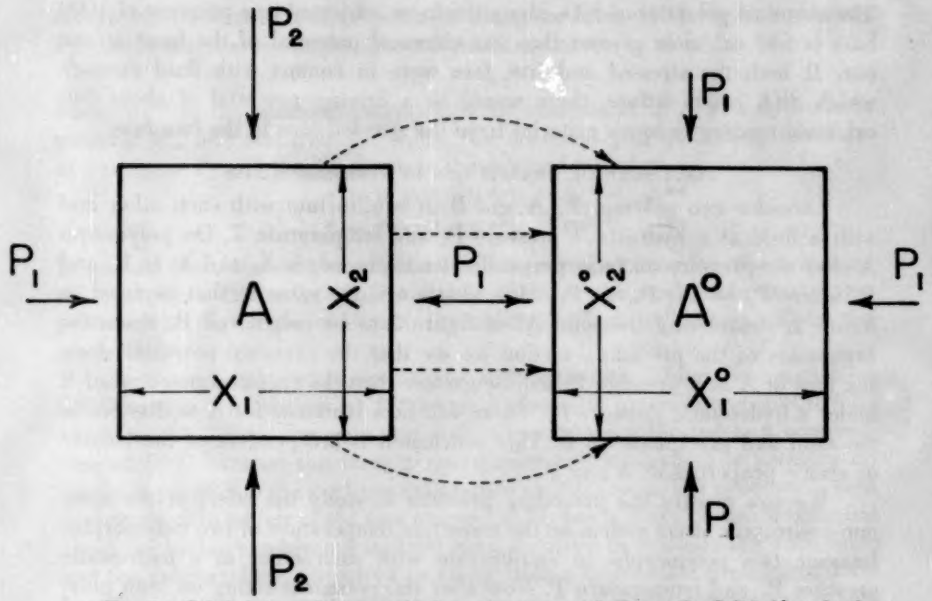

Fig. 2. Solid A is under a non-hydrostatic stress with $P_2 \neq P_1$. Solid A° under hydrostatic pressure P_1.

In order to calculate the difference in chemical potential of SiO_2 at one bar in the stressed and unstressed state, we have to assume a mechanical equation of state for the solid, and in addition we need to know the elastic constants of the material. We assume that the solid obeys Hooke's law, that the strain is a linear function of the stress. The work done on the solid in raising the pressure to 1000 bars on the face perpendicular to X_3 will be given by

$$\int dW = X_1^\circ X_2^\circ X_3^\circ \int_0^{1000} \frac{P_3}{E}\, dP_3$$

since

$$dX_3 = X_3^\circ \frac{dP_3}{E}$$

at a constant temperature, where E is Young's modulus for the material and is equal to about 7×10^5 bars for quartzite (Birch, Schairer and Spicer, 1942). The work done on the solid is then given by $W = 1/1.4\ V_0$ bar cc/mole $= 0.29$ cal./mole, where V_0 is the volume per mole in the unstrained state. The chemical potential of SiO_2 along the faces at one bar in the sample subjected to a unidirectional compression of 1000 bars is 0.3 cal/mole greater than the chemical potential of SiO_2 in the sample at a hydrostatic pressure of one bar. The variation of the chemical potential along the stressed face is given to a first order approximation by

$$\left(\frac{\partial \mu_1}{\partial P_1}\right) = V$$

The chemical potential of SiO_2 along the faces subjected to a pressure of 1000 bars is 540 cal/mole greater than the chemical potential of the faces at one bar. If both the stressed and free face were in contact with fluid through which SiO_2 could diffuse, there would be a driving potential of about 540 cal/mole tending to move material from the stressed face to the free face.

POLYMORPHIC TRANSITIONS IN STRESSED SOLIDS

Consider two polymorphs A and B in equilibrium with each other and with a fluid at a hydrostatic pressure P_1 and temperature T. On polymorph A alter the pressure on faces perpendicular to the edges X_2 and X_3 to P_2 and P_3 where $P_2 \neq P_3$, $P_3 \neq P_1$. This situation is the same as that depicted in figure 2, considering the solid A^0 of figure 2 to be polymorph B. From the arguments of the preceding section we see that the chemical potential along the face of A at a pressure P_1 will be greater than the chemical potential of B under a hydrostatic pressure P_1. There will be a tendency for A to dissolve in the fluid and precipitate on B. This conclusion is independent of the volume or elastic properties of A and B.

We can modify the preceding problem to study the effect of the same non-hydrostatic stress system on the transition temperature of two polymorphs. Imagine two polymorphs in equilibrium with each other at a hydrostatic pressure P_1 and temperature T. Now alter the pressures acting on both polymorphs such that $P_2 \neq P_1$, $P_3 \neq P_1$, so that both polymorphs are in identical stress fields as shown in figure 3. The problem is then to determine which poly-

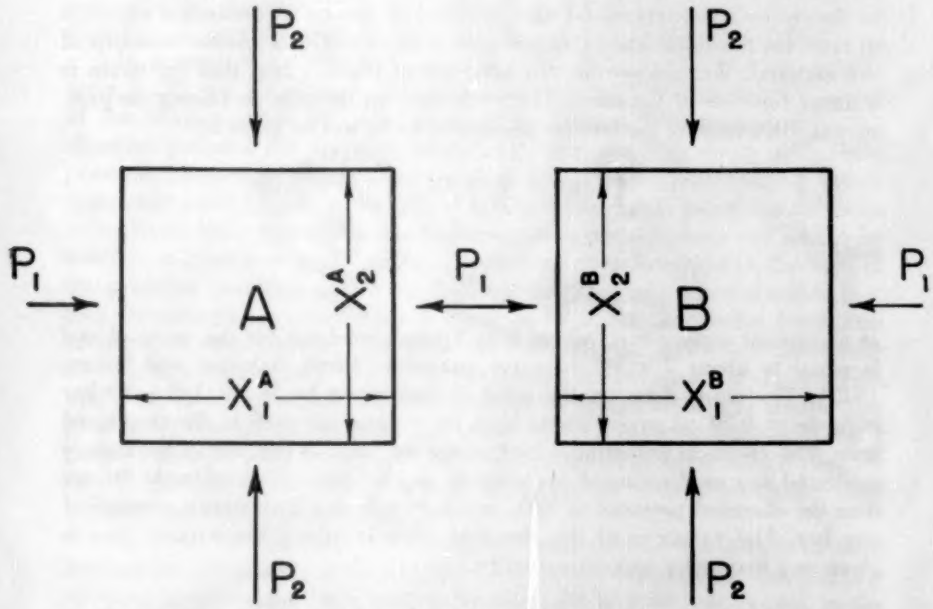

Fig. 3. Polymorphs A and B under identical conditions of non-hydrostatic stress.

morph has the lower chemical potential along the faces which are at a pressure P_1. At the original condition of equilibrium we have

$$\mu_1^{*A} = \mu_1^{*B}$$

where μ_1^{*A} is the chemical potential of the component in A at a hydrostatic pressure P_1, and similarly for μ_1^{*B}. The chemical potential along the faces at a pressure P_1 will then be given in the strained state by

$$\mu_1^A = P_1(V^A - V^{*A}) + W^A + \mu_1^{*A}$$
$$\mu_1^B = P_1(V^B - V^{*B}) + W^B + \mu_1^{*B}$$

In general the chemical potential will be lower in the phase on which is done the least work. Since for perfect elastic behavior the work is inversely proportional to the elastic constants, the elastically "harder" phase will be the more stable.

As an example, consider calcite and aragonite. These two phases of $CaCO_3$ are in equilibrium at 2500 bars hydrostatic pressure and 298.16° K. (MacDonald, 1956). Suppose that both minerals are subjected to a compression of 5000 bars on the faces perpendicular to the c-axis. The pressure on the faces parallel to the c-axis is maintained at 2500 bars. The problem is then to determine in which of the two phases $CaCO_3$ has a lower chemical potential along the surfaces subjected to 2500 bars. In order to evaluate the work done and the volume change involved in going from a hydrostatic pressure of 2500 bars to a state of non-hydrostatic stress, we need the elastic constants of calcite and aragonite. The values listed by Birch, Schairer and Spicer (1942) show that aragonite is "stiffer" along the c-axis than calcite and consequently less work will be done on aragonite and thus less strain energy is stored in aragonite. Using numerical values for the elastic constant, it turns out that the chemical potential of $CaCO_3$ in calcite is 3.7 cal/mole greater than the chemical potential in aragonite along the surfaces kept at 2500 bars.

We now obtain the expression for the variation of temperature of transition of two polymorphs with change of non-hydrostatic pressure. We assume two polymorphs in the form of rectangular parallelepipeds with pressures P_1, P_2 and P_3 acting in the three principal directions. We assume that the chemical potentials of the common component in the two phases are equal along the surfaces acted on by the pressure P_1. We next alter the pressure P_1, keeping P_2 and P_3 constant, and determine the change in temperature required to maintain the equality of chemical potential along surfaces at pressure P_1. From the definition of chemical potential we have for phases A and B

$$\mu_1^A = P_1V^A + U^A - TS^A$$
$$\mu_1^B = P_1V^B + U^B - TS^B$$

Using the following relations:

$$d\mu = PdV + VdP + dU - TdS - SdT$$

$$dU = TdS + \sum_{i=1}^{3} f_i dX_i$$

$$dV = X_2X_3dX_1 + X_1X_3dX_2 + X_1X_2dX_3$$

we obtain that the variation of chemical potential with P_1 and T is given by

$$d\mu = (P_1 - P_2)X_1X_3dX_2 + (P_1 - P_3)X_1X_2dX_3 + VdP_2 - SdT$$

The condition for equilibrium between phases A and B is then that

$$d\mu_1^A = d\mu_1^B$$

which leads to

$$\left(\frac{\partial T}{\partial P_1}\right)_{X_2^A, X_2^B, X_3^A, X_3^B, P_2, P_3} = \frac{V^A - V^B}{S^A - S^B} = \frac{\Delta V}{\Delta S}$$

That is, if both polymorphs are constrained so that the edges X_2 and X_3 remain constant during the change of pressure P_1, we obtain a formula that is analogous to the more familiar relation of change of melting point with hydrostatic pressure. In general, however, the ΔV and ΔS in the equation will be almost but not equal to the change of volume and entropy in the case of hydrostatic pressure.

The constraints on the X_2 and X_3 can be removed by assuming isotropic solids having a linear dependence of the edge lengths on temperature and pressure such that

$$dX = \left(\frac{\partial X}{\partial P_1}\right) dP_1 + \left(\frac{\partial X}{\partial T}\right) dT$$

$$dX = \frac{\sigma X^0}{E} dP_1 + X^0 \alpha dT$$

where α is the linear thermal expansion defined by

$$\alpha = \frac{1}{X^0}\left(\frac{\partial X}{\partial T}\right)_P$$

σ is Poisson's ratio, and E is Young's modulus. Substituting these relations for dX_2 and dX_3 in our expression for the variation of chemical potential, we obtain

$$\left(\frac{\partial T}{\partial P_1}\right)_{P_2P_3} = \frac{V^{0A}\left[(P_1-P_2)\frac{\sigma^A}{E^A} + (P_1-P_3)\frac{\sigma^A}{E^A}\right] - V^{0B}\left[(P_1-P_2)\frac{\sigma^B}{E^B} + (P_1-P_3)\frac{\sigma^B}{E^B}\right] + \Delta V}{\Delta S - [V^{0A}(P_1-P_2)\alpha^A - V^{0B}(P_1-P_3)\alpha^B]}$$

This equation gives the variation of the equilibrium temperature of two nonhydrostatically stressed phases with variation of the pressure P_1, keeping P_2 and P_3 constant. The important feature of this equation is that the ΔV term is the dominant term in the numerator and ΔS the dominant term in the denominator. The terms in the numerator involving the stress differences $P_1 - P_2$ and $P_1 - P_3$ are small in comparison with ΔV for stress differences on the order of 10^3 bars, since these terms depend on the elastic constant σ/E, which for most materials is on the order of 10^{-5} bars. Similarly, the terms involving the thermal expansion in the denominator will be small, since α is on the order of 10^{-5} deg^{-1}. Thus to a good approximation the variation of transition temperature with pressure P_1 along the surface acted on by pressure P_1 will be given by

$$\left(\frac{\partial T}{\partial P_1}\right)_{P_2P_3} = \frac{\Delta V}{\Delta S}$$

where ΔV and ΔS will be approximately equal to the differences of volume and entropy between the two phases under a hydrostatic pressure.

A non-hydrostatic stress should have a very large effect on the equilibrium curve in a second order transition. In a second order transition the difference in entropy and volume between the two phases approaches zero and thus the terms involving the elastic constants will be important. If the transition from low to high quartz is a true second order transition, then this is an example of a transition that would be influenced greatly by non-hydrostatic stress.

Changing the pressure on the surface of two polymorphs in equilibrium across this surface has to a first order approximation the same effect on a non-hydrostatically stressed solid as on solids under a hydrostatic pressure. We now show that the effect of changing the pressure on the surfaces not in equilibrium is much less. Consider two polymorphs in equilibrium at a hydrostatic pressure P_1. Change the pressure P_3 such that $P_3 \neq P_1$ on both polymorphs. How will the temperature have to be altered to maintain equilibrium along the surfaces at a pressure P_1? Using our general expression for the variation of chemical potential, and assuming that the polymorphs can be treated as isotropic solids obeying Hooke's law, we have that

$$\left(\frac{\partial T}{\partial P_3}\right)_{P_1} = \frac{V^{0A}(P_1-P_2)\frac{\sigma^A}{E^A} - V^{0B}(P_1-P_3)\frac{\sigma^B}{E^B}}{S^A - S^B - [V^{0A}(P_1-P_2)\alpha^A - V^{0B}(P_1-P_3)\alpha^B]}$$

Since the numerator involves only terms multiplied by an elastic constant, we should expect the change of equilibrium temperature along the surfaces at P_1 with a change of P_3 to be small for $P_1 - P_3$ on the order of a few thousand bars. As a numerical example of this effect we consider again calcite and aragonite in equilibrium at 2500 bars and room temperature. We increase the pressure on the surface perpendicular to the c-axis of both crystals to 5000 bars, maintaining the pressure of 2500 bars on the surfaces parallel to the c-axis. To maintain equilibrium along the surfaces at 2500 bars, the temperature would have to be lowered by about 3 degrees; while in order to maintain equilibrium across the surfaces at 5000 bars, the temperature would have to be increased about 150°. The effect of the non-hydrostatic pressure is therefore far greater on the surfaces subjected to a change in pressure than on the surfaces kept at a constant pressure.

As an illustration of the application of thermodynamics to the concept of stress minerals, we examine the equilibrium between andalusite and kyanite. Since andalusite is less dense than kyanite, andalusite should be stable at a lower pressure than kyanite. If equilibrium could be maintained at some temperature, an increase of pressure acting on the andalusite should result in the conversion of andalusite to kyanite, provided temperature—pressure conditions were such that there were no other phases more stable than either kyanite or andalusite. If the stress mineral concept were valid, the transition of andalusite, an anti-stress mineral, to kyanite, a stress mineral, should take place at a lower pressure if andalusite were under a non-hydrostatic stress than if andalusite were under a hydrostatic pressure.

Let us assume that for a given temperature T, the equilibrium hydrostatic pressure between andalusite and kyanite is P_1. Consider a cube of andalusite in simple uniaxial compression as illustrated diagrammatically in figure 3, with a pressure P_2 acting on the faces normal to X_2, and $P_1 = P_3$ acting on the other faces. The pressure on the free faces, P_1, is less than the equilibrium pressure P_1. If equilibrium is maintained as the pressure P_2 is raised, kyanite will begin to form along the stressed face at some pressure P_J. The theory we have developed shows that

$$P_J \cong P_1$$

for $P_1 - P_2 \cong 10^3$ bars. This result follows from the expression for the variation of chemical potential with pressure P_2 in a stressed solid at constant temperature.

$$\left(\frac{\partial \mu}{\partial P_2}\right)_T = 2(P_1 - P_2)\, V^0 \frac{\sigma}{E} + V$$

and since for $P_1 - P_2 \cong 10^3 - 10^4$ bars, we have that

$$\left(\frac{\partial \mu}{\partial P_2}\right)_T \cong V$$

The variation of chemical potential in the stressed solid is to a good approximation equal to the variation of chemical potential in a body under hydrostatic stress. Similarly we have shown that the slope of the curve relating the equilibrium temperature T to the equilibrium pressure P_J in the stressed solid will be very nearly the same as the slope of the equilibrium curve in the hydrostatic case for transitions in which the change of entropy and volume are large compared with the terms involving the stress differences and elastic constants. Transitions such as andalusite to kyanite involving large volume and entropy changes should not be affected by shearing stress. The difference in volume and entropy between andalusite and sillimanite is much smaller and stress might have an effect on the slope of the equilibrium curve. A transition between two phases as alike as α and β quartz would be affected by shearing stress. We can summarize the effect of stress on a polymorphic transition A→B by the following condition. The slope of the transition curve between polymorphs A and B will be unaffected by a maximum stress difference $P_1 - P_2$ acting on the system, provided the following inequalities hold:

$$\Delta V >> (P_1 - P_2)\left[V^{0A}\frac{\sigma^A}{E^A} - V^{0B}\frac{\sigma^B}{E^B}\right]$$

$$\Delta S >> (P_1 - P_2)\,[V^{0A}\alpha^A - V^{0B}\alpha^B]$$

These inequalities follow directly from our expression for the slope of an equilibrium curve in a general stress field.

ORIENTATION OF MINERALS IN A NON-HYDROSTATIC STRESS FIELD

The problem of the orientation of minerals in a given stress field can be divided into two parts: determination of the most stable orientation of a mineral in a given stress field and the process by which the mineral attains this orientation. The first problem is a problem of thermodynamics, the second a problem of the kinetics and mechanics of such processes as plastic flow and

solution and recrystallization. We will consider only the thermodynamic problem.

If a crystal is loaded in simple compression, the stressed faces have a higher chemical potential than the unstressed faces. If a fluid is in contact with both faces, there will be a tendency for material to move through the fluid from the stressed face to the free face, the crystal thus growing in a direction perpendicular to the axis of compression. The crystal in so growing would tend to increase the area under the load, thus reducing the pressure acting on the stressed face. The orientation of a given grain would not change in such a process. Only the shape of the original grain would be altered. If the mineral were anistropic there would be at least one orientation in which the elastic work done on the crystal would be a minimum, and thus the strain energy stored within the grain would be minimized. The grains having an orientation with a minimum strain energy might be expected to grow at the expense of grains in which the strain energy was greater. For a given stress field, and provided the elastic constants of the material are known, the orientation in which the strain energy is minimized can be easily calculated. For calcite the strain energy is a minimum when the c-axis of a grain of calcite is parallel to the axis of minimum stress. Quartz has a minimum strain energy when the c-axis of the grain is parallel to the axis of maximum stress. Thus if solution and redeposition were the major mechanism of recrystallization in a marble, the c-axis of the calcite should be parallel to the axis of minimum stress. In a quartzite the c-axis of the quartz should represent the axis of maximum stress, provided solution and redeposition were the mechanism of recrystallization. It should be emphasized that the difference in strain energies between various orientations is small, on the order of calories per mole for stress differences of thousands of bars. If the grains deform by a mechanism other than that of solution and redeposition, then the influence of strain energy on the orientation of the grains might be expected to be negligible.

If a crystal is put in simple compression in the absence of a fluid, there is still the potential difference between the stressed and unstressed faces. Removing the fluid removes a mechanism of solution and redeposition by which the potential difference can be ironed out. Other mechanisms by which a difference in chemical potential can be reduced include a mechanical flow of the crystal. These mechanisms are probably characterized by an "activation energy" which must be exceeded before flow can take place. We should expect that this activation energy would be determined by the maximum stress difference times the volume of the crystal, since this quantity gives the potential difference between the stressed and unstressed faces. We should also expect that the activation energy would be greater for mechanical flow in a dry system than for deformation in the presence of a fluid. The rate of strain $\frac{d\varepsilon}{dt}$ should be given by an expression of the form

$$\frac{d\varepsilon}{dt} = A\varepsilon - \frac{V(P_3 - P_1)}{RT}$$

where $P_3 - P_1$ is the maximum stress difference and A is a constant.

The importance of the mechanism of deformation in producing an oriented fabric is illustrated by the detailed studies of Griggs, Turner, Borg and Sosoka (1951, 1953) on the Yule marble. Cylinders of marble were subjected to uniaxial compression at various conditions of temperature and pressure. The resulting fabric showed a strong orientation of the c-axis of calcite parallel to the axis of compression. If solution and redeposition had been the mechanism of recrystallization, the c-axis should be oriented perpendicular to the axis of compression, since such an orientation would minimize the strain energy stored in the crystals. In the experiments the crystals deformed by a mechanical flow in which "twin gliding" was the most important mechanism.

The actual mechanism of twin gliding results in an oriented fabric with the c-axis parallel to the axis of compression. In terms of the thermodynamic theory this fabric is explained by the fact that the potential difference tending to flatten the crystals perpendicular to the axis of compression is much greater than the potential difference between crystals having differing orientation. Since the twin glide mechanism of flow results in both the crystal flattening out and in the orientation of the c-axis parallel to the axis of compresssion, the increase of area perpendicular to the axis of compression reduces the chemical potential much more than the orientation of the c-axis parallel to the axis of compression increases the chemical potential. The potential difference tending to flatten the grains for stress differences of a thousand bars is on the order of hundreds of calories per mole, while the potential difference tending to orient the c-axis perpendicular to the axis of compression is only on the order of a calorie per mole. The biggest reduction in chemical potential results from flattening of the crystal, even though the mechanism of flattening results in an orientation of maximum strain energy in the crystals.

CONCLUSIONS

In the detailed application of theory it must be remembered that any single mineral grain in a rock undergoing metamorphism is seldom if ever under a homogeneous strain. The non-homogeneity of strain means that the chemical potential will in general vary over the grain in a much more complicated way than in the case of a rectangular parallelepiped subjected to three principal pressures. This complication, however, will not alter the major conclusions of this paper. A portion of the non-homogeneously stressed mineral is unstable relative to the same mineral under equal hydrostatic stress. The difference of chemical potentials between hydrostatically and non-hydrostatically stressed minerals will be on the order of a few calories per mole for a maximum stress difference on the order of 10^4 bars, since this difference depends on the elastic constants of the material. The slope of equilibrium curves in a general stress field will be, to a good approximation, equal to the slope of the curve in the hydrostatic case for transitions satisfying the conditions

$$\Delta V >> (P_1 - P_2)\left[V^{0A}\frac{\sigma^A}{E^A} - V^{0B}\frac{\sigma^B}{E^B}\right]$$

$$\Delta S >> (P_1 - P_2)[V^{0A}\alpha^A - V^{0B}\alpha^B]$$

where ΔV and ΔS are the changes in volume and entropy for the transition; $(P_1 - P_2)$ is the maximum stress difference acting on the system; V^{0A} and

V^{α} are the volumes of polymorphs A and B; σ, E and α are the Poisson's ratio, Young's modulus, and thermal expansion.

ACKNOWLEDGMENTS

Professors Harold Fairbairn, William Brace, and James B. Thompson, Jr., critically reviewed the manuscript, and their suggestions have been most welcome. This paper was originally presented at a symposium on metamorphic facies sponsored by the Geophysical Laboratory of the Carnegie Institution. The author is grateful to Dr. Phillip Abelson and Dr. Hatten S. Yoder for arranging the symposium and providing the opportunity of presenting this paper to a constructively critical audience.

REFERENCES

Birch, F., Schairer, J., Spicer, H. C., 1942, Handbook of physical constants: Geol. Soc. America Special Paper 36.

Bridgman, P. W., 1936, Shearing phenomena at high pressure of possible importance for geology: Jour. Geology, v. 44, p. 653-669.

Gibbs, J. W., 1906, Scientific papers: New York, Longmans, Green Co., 434 p.

Goranson, R. W., 1930, Thermodynamic relations in multi-component systems: Carnegie Inst. Wash. Pub. 408, 329 p.

Griggs, D., Turner, F. J., Borg, I., and Soska, J., 1951, Deformation of Yule Marble: Part IV—Effects at 150° C: Geol. Soc. America, Bull. 62, p. 1385-1406.

Griggs, D., Turner, F. J., Borg, I., and Sosoka, J., 1953, Deformation of Yule Marble: Part V—Effects at 300° C: Geol. Soc. America, Bull. 64, p. 1327-1342.

Harker, A., 1939, Metamorphism, 2nd. rev. ed.: New York, E. P. Dutton, 362 p.

Love, A. E. H., 1945, The mathematical theory of elasticity, 4th rev. ed.: Cambridge University Press.

MacDonald, G. J. F., 1956, Experimental determination of calcite-aragonite equilibrium relations at elevated temperatures and pressures: Am. Mineralogist, in press.

Miyashiro, A., 1949, A note on "stress minerals": Geol. Soc. Japan, Jour. 55, p. 211-217.

Rice, J., 1936, The thermodynamics of strained elastic solids in a commentary on the scientific writings of J. W. Gibbs (edited by Donnan and Haas): New Haven, Yale University Press, 742 p.

Verhoogen, J., 1951, The chemical potential of a stressed solid: Am. Geophys. Union, Trans., v. 32, p. 251-258.

MASSACHUSETTS INSTITUTE OF TECHNOLOGY
CAMBRIDGE, MASSACHUSETTS

[American Journal of Science, Vol. 255, April 1957, P. 282-305]

THE NEPHELINE-KALSILITE SYSTEM: I. X-RAY DATA FOR THE CRYSTALLINE PHASES

J. V. SMITH* and O. F. TUTTLE*

ABSTRACT. X-ray data are given for the following phases: high- and low-carnegieite, high- and low-nepheline, kalsilite, orthorhombic $KAlSiO_4$, synthetic kaliophilite, natural kaliophilite, anomalous natural kaliophilite, tetrakalsilite, and O2. Comparison of the cell dimensions indicates that the structures of all the phases except carnegieite are based on a tridymite-type framework. Synthetic natural and anomalous natural kaliophilite are not identical but comparison of their x-ray properties indicates that they are structurally related. The variation of the cell dimensions of nepheline and kalsilite solid solutions has been determined. Discontinuities in the curves of composition vs. cell dimensions are discussed in terms of the known crystal structure.

INTRODUCTION

The nepheline-kalsilite system forms one side of the ternary system $NaAlSiO_4$-$KAlSiO_4$-SiO_2 in which a number of important rock types are represented. The liquidus relations in the ternary system have been determined by Schairer and Bowen (1935) and Schairer (1950) but the sub-solidus relations have so far not been investigated in detail. The phase relations in the subsystem $NaAlSi_3O_8$-$KAlSi_3O_8$-SiO_2 have been extensively studied in the past decade by Tuttle and Bowen and considerable light has been thrown on the origin of granites and other rocks. Elucidation of the relations in the remainder of the ternary system is of importance in the understanding of the crystallization history of the alkaline rocks. Recent investigation of the mineralogy and petrology of a wide range of alkaline rocks by Tilley (see, for example, Tilley, 1954) has revealed the existence of important sub-solidus reactions between the phases existing in the feldspar-feldspathoid quadrilateral and has emphasized the pressing need for a study of the sub-solidus region by laboratory synthesis under controlled conditions. The present investigation of the sub-solidus region of the nepheline-kalsilite system is a necessary step towards the investigation of the ternary system.

This two-component system has been previously studied by Bowen (1917), who established the positions of the phase boundaries in the higher temperature range by synthesizing the phases in the dry way. Use of hydrothermal methods in the present study has led to an extension of the temperature range down to 400°C. The phases have been identified by x-ray powder methods and the composition of the nepheline and kalsilite phases has been estimated from the change of x-ray spacing. Two new phases have been identified by x-ray methods.

Considerable difficulty has been caused by changes in composition during crystallization of the charges. Many of the crystalline charges in the potash-rich end of the system contain small amounts of leucite, indicating that some potash was lost during preparation of the mixtures. These mixtures were made with customary care by Bowen and Schairer, and the loss of potash results from the high temperature needed for the solution of Al_2O_3. A further loss of potash has occurred during the runs made in the present study. It is believed that the

* Present address:
Division of Earth Sciences, The Pennsylvania State University.

change of composition has been especially serious for potash-rich compositions run at temperatures over 1000°C and it has so far not been possible to elucidate completely the phase relations in this region. For lower temperatures and for the whole of the soda-rich portion of the system, consistent results have been obtained (see preliminary reports by Tuttle and Smith, 1953, and Smith and Tuttle, 1954).

This paper is concerned with the x-ray properties of the crystalline phases. A subsequent paper will describe the high-low inversion in nepheline, the miscibility gap between nepheline and kalsilite and the polymorphism of $KAlSiO_4$.

THE X-RAY TECHNIQUES

Because of the fine-grained character of the synthetic crystals most of the measurements reported here were made by the powder diffractometer method. The specimens were made by smearing the powdered crystals onto a glass slide and the records were calibrated by mixing quartz or silicon with the charge. Details of the method are given by Smith and Sahama (1954), who claim an accuracy of about 0.01° in 2θ. X-ray powder records at high temperatures were obtained by the use of a furnace mounted on the diffractometer (see MacKenzie, 1952, for description). The powder records were calibrated by mixing quartz with the powdered charge and using the data obtained by Jay (1933) for the thermal expansion of quartz.

It should be noted that the determination of symmetry and lattice parameters from powder records may be unreliable if pseudo-symmetry is present. The possible error cannot be large for the Norelco diffractometer used in the present work has excellent sensitivity and resolution.

SUMMARY OF THE PHASE RELATIONS

In order to clarify the interpretation of the x-ray data, a brief description of the phase relations is given here.

Four polymorphs of $NaAlSiO_4$ are known. *High-carnegieite* (cubic) is stable from the liquidus down to 1250°C, where it transforms to *high-nepheline* (orthorhombic). At a temperature near 900°C, high-nepheline inverts to *low-nepheline* (hexagonal) which is stable down to room temperature. The transformation of high-carnegieite to high-nepheline is sluggish and, by quenching, high-carnegeite may be obtained in the stability field of nepheline but at 690°C it undergoes a displacive inversion into *low-carnegeite* (low symmetry).

Five polymorphs of $KAlSiO_4$ are known. Below 850°C., *kalsilite* (hexagonal) is the stable phase. Near 1000°C, *synthetic kaliophilite* (hexagonal) has been obtained but the remainder of the laboratory syntheses from 900°C. to the liquidus have yielded *orthorhombic* $KAlSiO_4$ (denoted Ol). The synthetic kaliophilite is not identical with *natural kaliophilite* (hexagonal) but there is a remarkable similarity between their powder patterns. A second form of natural kaliophilite—*anomalous natural kaliophilite*—is also known.

Below 1100°C there is a solvus (miscibility gap) between kalsilite of composition Ne_0 (weight per cent of $NaAlSiO_4$) and (low)-nepheline of com-

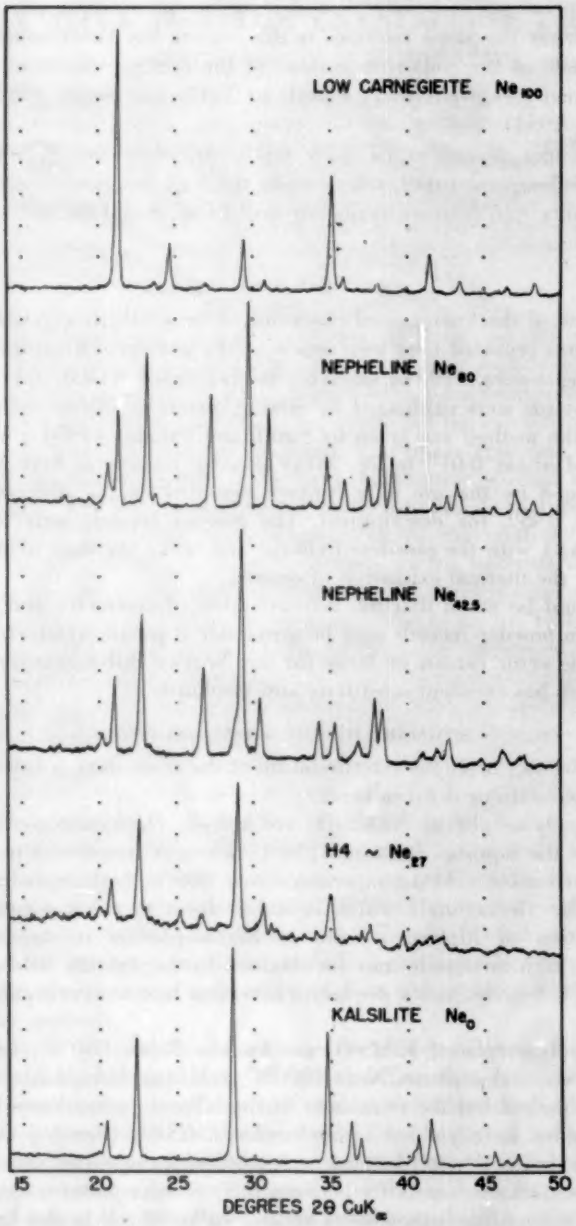

Fig. 1. Tracings of powder records of low-carnegieite, nepheline, tetrakalsilite (H4) and kalsilite. CuK_α radiation.

position Ne_{71}. Above the solvus kalsilite has been obtained from Ne_0 to Ne_{20} and nepheline is the stable phase above the solvus for compositions containing

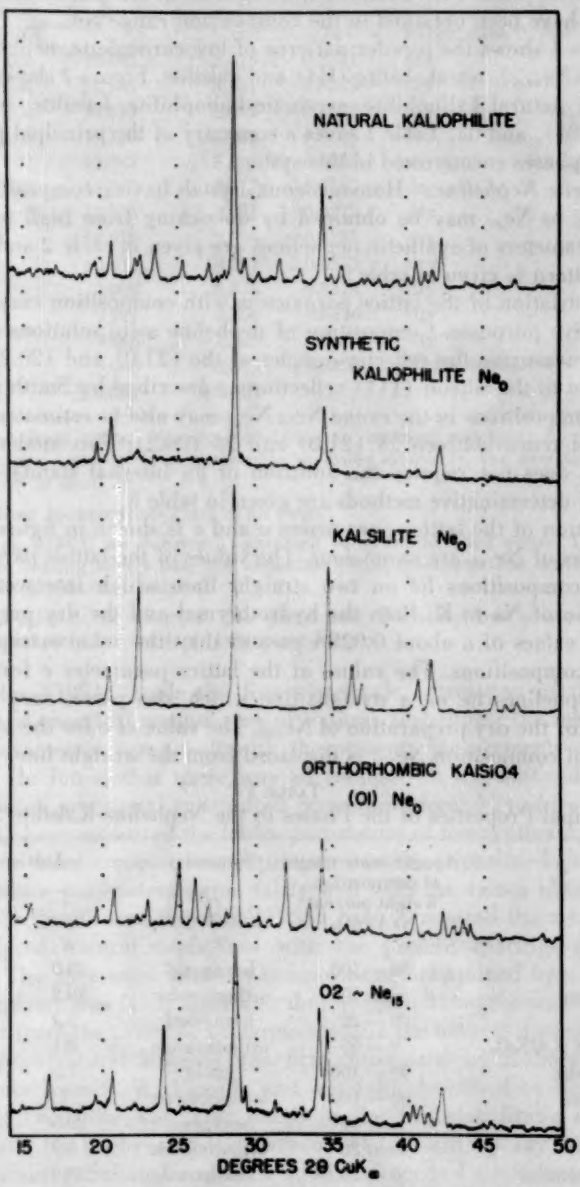

Fig. 2. Tracings of powder records of natural kaliophilite, synthetic kaliophilite, kalsilite, orthorhombic $KAlSiO_4$(01) and 02. CuK_α radiation.

more soda than Ne_{30}. Both nepheline and kalsilite solid solutions may be quenched to room temperature without unmixing.

Two new phases, *tetrakalsilite* (hexagonal, denoted H4) and O2 (orthorhombic), have been obtained in the composition range $Ne_{20\text{-}30}$.

Figure 1 shows the powder patterns of low-carnegieite, nepheline (Ne_{80}), nepheline ($Ne_{42.5}$), tetrakalsilite (H4) and kalsilite. Figure 2 shows the powder patterns of natural kaliophilite, synthetic kaliophilite, kalsilite, orthorhombic $KAlSiO_4$ (01), and 02. Table 1 gives a summary of the principal properties of the eleven phases encountered in this system.

Synthetic Nepheline.—Homogeneous crystals having compositions ranging from Ne_{100} to Ne_{30} may be obtained by quenching from high temperatures. Lattice parameters of synthetic nephelines are given in table 2 and an indexed powder pattern is given in table 3.

The variation of the lattice parameters with composition may be used for determinative purposes. Composition of nepheline solid solutions may be estimated by measuring the reflection angles of the (21.0) and (20.2) reflections with respect to the silicon (111) reflection as described by Smith and Sahama (1954). Compositions in the range Ne_{30}-Ne_{71} may also be estimated by measuring the difference between 2θ (21.0) and 2θ (00.2). This method is less accurate but does not require the addition of an internal standard. The data for the two determinative methods are given in table 4.

Variation of the lattice parameters a and c is shown in figure 3. The two preparations of Ne_{100} are anomalous. The values of the lattice parameter a for the other compositions lie on two straight lines which intersect at the 3:1 atomic ratio of Na to K. Both the hydrothermal and the dry preparations of Ne_{100} give values of a about 0.025Å greater than the value extrapolated from the other compositions. The values of the lattice parameter c for the potash-bearing nephelines lie on a straight line which also passes very close to the value of c for the dry preparation of Ne_{100}. The value of c for the hydrothermal nepheline of composition Ne_{100} is displaced from the straight line.

TABLE 1

Principal Properties of the Phases in the Nepheline-Kalsilite System

Name	Approximate range of composition. Weight percent $NaAlSiO_4$	Symmetry	Lattice parameters Å		
			a	b	c
nepheline	30 — 100	hexagonal	10.0	—	8.4
high-nepheline	near 100	orthorhombic	10.2	17.6	8.5
kalsilite	0 — 20	hexagonal	5.2	—	8.7
orthorhombic $KAlSiO_4$	0 — 10	orthorhombic	9.1	15.7	8.6
high-carnegieite	90 — 100	cubic	7.3	—	—
low-carnegieite	90 — 100	low-symmetry	?	?	?
tetrakalsilite	near 30	hexagonal	20.5	—	8.5
02	near 20	orthorhombic	8.9	10.5	8.5
natural kaliophilite	0 — 10	hexagonal	26.9	—	8.5
anomalous natural kaliophilite	0 — 10	hexagonal	26.9	—	8.5
synthetic kaliophilite	0 — 10	hexagonal	5.2	—	8.6

TABLE 2
Lattice Parameters* of Synthetic Nephelines

Composition $NaAlSiO_4$	Composition $KAlSiO_4$	a	c	c/a	Preparation**	a^2c
37 1/2	62 1/2	10.183 Å	8.473 Å	0.8321	dry	878.6 Å^3
42 1/2	57 1/2	10.163	8.461	0.8325	dry	873.9
47 1/2	52 1/2	10.133	8.449	0.8338	dry	867.5
52 1/2	47 1/2	10.110	8.440	0.8348	dry	862.7
57 1/2	42 1/2	10.087	8.428	0.8355	dry	857.5
62 1/2	37 1/2	10.060	8.417	0.8367	dry	851.8
67 1/2	32 1/2	10.035	8.401	0.8372	dry	846.0
71	29	10.018	8.396	0.8381	dry	842.6
75	25	10.011	8.387	0.8378	dry	840.5
80	20	9.998	8.376	0.8378	dry	837.3
90	10	9.981	8.360	0.8376	dry	832.8
100	0	9.986	8.333	0.8345	dry***	831.0
100	0	9.983	8.319	0.8333	hydrothermal****	829.1
		±0.005	±0.004			

* Measured from smear mounts containing an internal standard. All crystals give hexagonal powder patterns. If orthorhombic or lower symmetry, the deviation from hexagonal geometry is small.

** Grown from homogeneous glass in all cases.

*** Grown at 1050°C by Schairer. Contained some unidentified phase. Upon heating to 1100°C and cooling slowly only the nepheline phase remained. The lattice parameters were measured on this final material.

**** 800°C., 34 hours, at 4000 psi. One phase only. No other heat treatment. Material grown for 3 hours only has the same lattice parameters.

Bannister (1931) made the first systematic correlation of the physical properties and chemical composition of natural nephelines. His measurements of lattice parameters agree well with the present measurements of synthetic nephelines. He found that there was an increase in the unit-cell volume of 13.6Å^3 for each additional substituted potassium atom. Miyashiro and Miyashiro (1954) have measured the lattice parameters of five synthetic nephelines; three of them have compositions represented in the nepheline-kalsilite system and their lattice parameters agree fairly well with the values obtained in the present study. Smith and Sahama (1954) have compared the x-ray spacings of 24 analyzed natural nephelines with the present spacings of synthetic nephelines. The agreement between compositions determined by x-ray and by chemical analyses was fairly close and they suggested that the small differences might result from the presence of excess silica in the natural nephelines.

Kalsilite.—Natural kalsilite was first recognized by Holmes (1942) in volcanic rocks from S. W. Uganda and was fully described by Bannister and Hey (1942). Kalsilite was later found in the firebrick lining of worn-out blast furnaces by Rigby and Richardson (1947) and by Jay and Andrews (1947). Bannister, Sahama and Wiik (1952) described a specimen of natural kalsilite from San Venanzo, Italy, and Sahama (1953 a, b) has described both kalsilite phenocrysts and nepheline-kalsilite microperthites from the Belgian

TABLE 3

Indexed Powder Pattern of a Synthetic Nepheline

Material: $Ne_{99-1/2}Ks_{97-1/2}$, grown dry from glass at 1300°C.
Method: Smear mount with internal standard. CuKα.
Lattice parameters: hexagonal, $a = 10.060$ Å, $c = 8.417$ Å.

I	d obs.	2θ obs.	2θ calc.	Indices
3	5.030	17.63	17.63	11.0
10	4.354	20.395	20.385	20.0
10	4.319	20.555	20.57	11.1
35	4.211	21.095	21.11	00.2
60	3.870	22.98	22.985	20.1
5	3.789	23.48	23.47	10.2
40	3.294	27.07	27.075	21.0
10	3.065	29.13	29.12	21.1
100	3.027	29.505	29.51	20.2
35	2.905	30.78	30.785	30.0
1	2.670	33.56	33.55	10.3
20	2.593	34.585	34.585	21.2
15	2.515	35.695	35.70	22.0
10	2.415	37.225	37.21	31.0
3	2.390	37.64	37.625	30.2
30	2.359	38.15	38.15	20.3
20	2.322	38.78	38.77	31.1
α_1 —				
5	2.1773	41.445	41.425	40.0
1	2.1582	41.82	41.80	22.2
7	2.1350	42.295	42.285	21.3
15	2.1046	42.935	42.945	00.4
5	2.092	43.2	43.125	31.2
2	1.9990	45.35	45.335	32.0
7	1.945	46.65	46.665	32.1
5	1.939	46.8	46.755	11.4
5	1.900	47.82	47.80	41.0
5	1.895	47.96	47.97	20.4
1	1.8527	49.13	49.085	41.1
5	1.8047	50.53	50.51	32.2
1	1.7200	53.205	53.19	40.3
5	1.7051	53.71	53.67 53.75	50.1 30.4
3	1.6458	55.81	55.785 55.865	42.0 33.1
7	1.6276	56.49	56.48	32.3
4	1.6094	57.19	57.17	50.2
5	1.574	58.6	58.60	41.3
15	1.5705	58.74	58.75	20.5
		etc.		

Congo and S. W. Uganda. Sahama, Neuvonen and Hytönen (1956) described two additional specimens of kalsilite.

Synthetic kalsilites have been prepared hydrothermally from mixes of composition Ne_0 and Ne_{10}. Both preparations contain small amounts of leucite which arose, presumably, from a loss of alkali during preparation. The lattice

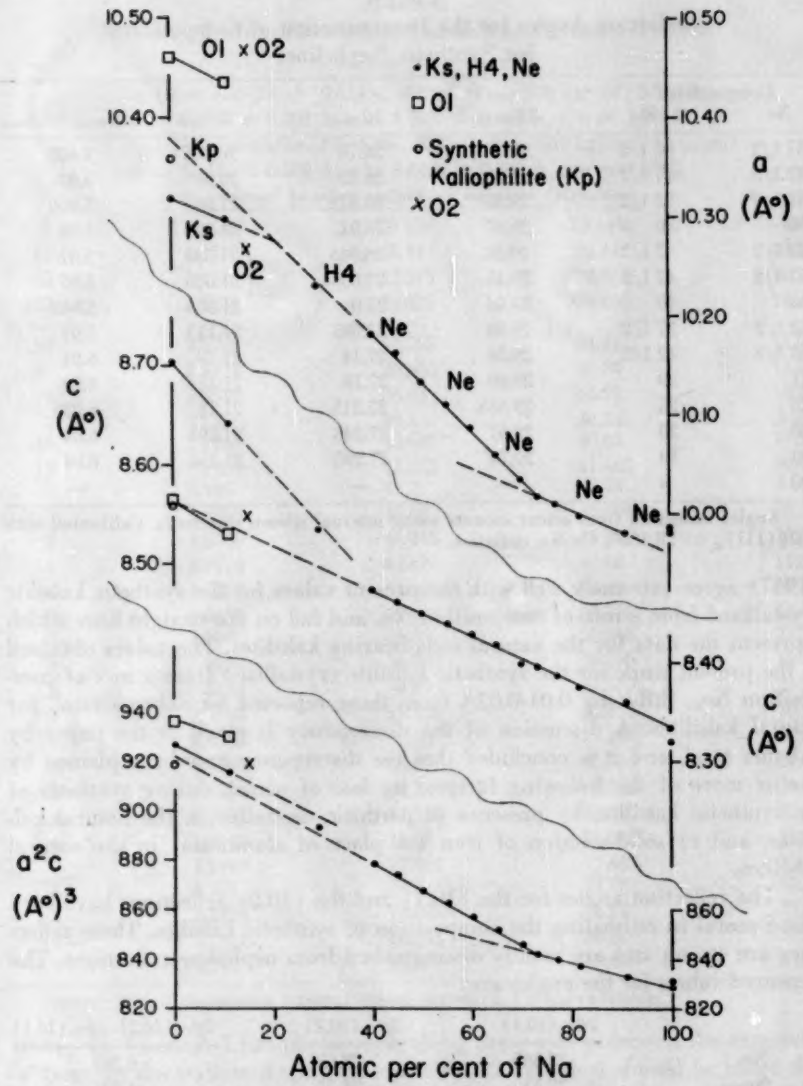

Fig. 3. The relations between the lattice functions *a*, *c*, a^2c and the atomic percent of Na for the phases in the nepheline-kalsilite system.

parameters are listed in table 5 and are plotted on figure 3. An indexed powder pattern is also set out in table 5.

Sahama, Neuvonen and Hytönen (1956) have measured the lattice parameters of four analyzed natural kalsilites and compared them with the lattice parameters obtained in the present work and by Jay and Andrews (table 5). The values for the synthetic kalsilite (Ne_0) measured by Jay and Andrews

TABLE 4
Reflection Angles for the Determination of Composition for Synthetic Nephelines

Composition Ne	Ks	$2\theta_{(20.1)}$	$2\theta_{(21.0)}$	$2\theta_{(00.2)}$	$2\theta_{(21.0)} - 2\theta_{(00.2)}$
37 1/2	62 1/2	29.235	26.76	20.955	5.805
42 1/2	57 1/2	29.28	26.82	20.99	5.83
47 1/2	52 1/2	29.35	26.875	21.01	5.865
50	50	29.37	26.91	21.02	5.89
52 1/2	47 1/2	29.38	26.945	21.035	5.91
57 1/2	42 1/2	29.45	27.005	21.075	5.95
60	40	29.48	27.04	21.095	5.945
62 1/2	37 1/2	29.53	27.085	21.115	5.97
67 1/2	32 1/2	29.56	27.14	21.13	6.01
71	29	29.60	27.18	21.16	6.02
75	25	29.635	27.215	21.18	6.035
80	20	29.67	27.245	21.205	6.04
90	10	29.73	27.295	21.255	6.04
100	0	—	—	—	—

Angles measured from smear mounts using internal silicon standards. Calibrated with Si,$2\theta(111)_\alpha = 28.466°$, Cu-K$\alpha$ radiation.

(1947) agree extremely well with the present values for the synthetic kalsilite crystallized from a mix of composition Ne_0 and fall on the straight lines which represent the data for the natural soda-bearing kalsilites. The values obtained in the present work for the synthetic kalsilite crystallized from a mix of composition Ne_{10} differ by 0.01-0.02Å from those reported by Sahama et al. for natural kalsilites. A discussion of the discrepancy is given in the paper by Sahama et al. and it is concluded that the discrepancy may be explained by one or more of the following factors: a) loss of potash during synthesis of the synthetic kalsilite, b) presence of perthitic nepheline in the natural kalsilites, and c) solid-solution of iron (in place of aluminum) in the natural kalsilites.

The reflection angles for the (10.1) and the (10.2) reflections have been found useful in estimating the composition of synthetic kalsilite. These reflections are strong and are readily distinguished from nepheline reflections. The measured values for the angles are:

	$2\theta_{Cu}(10.1)$	$2\theta_{Cu}(10.2)$	$2\theta_{Cu}(10.2)-2\theta_{Cu}(10.1)$
Ne_0	22.365	28.63	6.265
Ne_{10}	22.435	28.77	6.335

The Tetrakalsilite Phase.—Crystals of the tetrakalsilite (H4) phase large enough for single-crystal x-ray methods were obtained by heating a glass of composition Ne_{30} dry at 1520°C for six hours. There is some uncertainty in the composition of these crystals because the quenched product contains some glass; nevertheless it is likely that the composition is near Ne_{27}.

Precession photographs revealed that the H4 phase is hexagonal with $a \sim 20.4$Å and $c \sim 8.7$Å. The only systematic absences were for (00.l) reflec-

TABLE 5

Kalsilite. Lattice Parameters and Indexed Powder Pattern

a. Lattice parameters

Ne_9 (from $K_2Si_2O_5 + \beta Al_2O_3$, 800° C, P_{H_2O} 500 kg/cm², 3-3/4 hours)
$a = 5.159_7 \pm 0.002$ Å, $c = 8.703_2 \pm 0.002$ Å, $c/a = 1.6868$.
Ne_{10} (from orthorhombic form, 800° C, P_{H_2O} 500 kg/cm², 16 hours)
$a = 5.148_5 \pm 0.002$ Å, $c = 8.642_9 \pm 0.002$ Å, $c/a = 1.6787$.

b. Indexed powder pattern of kalsilite ($Ks_{100}Ne_9$)

I	d obs. (Å)	2θ obs.	2θ calc.	Indices
12	4.3512	20.41	20.41	00.2
45	3.9733	22.375	22.365	10.1
100	3.1184	28.625	28.635	10.2
α_1 —				
50	2.5789	34.755	34.74	11.0
15	2.4724	36.305	36.29	11.1
10	2.4319	36.93	36.91	10.3
3	2.236	40.3	40.335	20.0
10	2.2183	40.635	40.62	11.2
17	2.1753	41.475	41.465	00.4
5	2.164	41.7	41.70	20.1
5	1.9868	45.62	45.605	20.2
3	1.9546	46.415	46.375	10.4
4	1.9270	47.12	47.10	11.3
3	1.7703	51.585	51.59	20.3
4	1.6621	55.205	55.175	11.4
4	1.6580	55.365	55.365	21.1
6	1.6220	56.705	56.705	10.5
9	1.5742	58.59	58.575	21.2
3	1.5588	59.225	59.225	20.4
10	1.4895	62.28	62.28	30.0
3	1.4598	63.69	63.705	21.3
3	1.3734	68.23	68.245	20.5
3	1.2902	73.315	73.33	22.0
4	1.2645	75.05	75.065	11.6
2	1.2293	77.595	77.605	30.4
1	1.227	77.8	77.78	31.1
2	1.2124	78.885	78.91	21.5
4	1.1921	80.495	80.51	31.2
1	1.140	85.0	85.04	31.3

Smear mount containing internal silicon standard. Cu-Kα radiation.

tions with l odd. A Laue photograph along the c-axis possessed the symmetry of 6mm so the indicated space-group is $P6_322$ though it should be noted that twinning could produce this space-group from a true space-group $P6_3$ as for nepheline (Buerger, 1954). The data from the powder pattern are given in table 6: The lattice parameters are $a = 20.463 \pm 0.01$Å, $c = 8.534 \pm 0.004$Å.

The c-axis of the H4 phase has the same length as the c-axes of nepheline and kalsilite and its a-axis is twice as large as that of nepheline and four times as large as that of kalsilite. Study of the geometry and the x-ray patterns made it virtually certain that, like nepheline and kalsilite, its structure is based on the tridymite scaffolding. The name tetrakalsilite was assigned from the hexa-

TABLE 6

Indexed Powder Pattern of the H4 Phase

Source: Ne_{50} glass, grown dry for 6 hours at 1520°C. Composition is probably $Ne_{27}Ks_{73}$ ± 3%.

Method: Smear mount with internal standard. CuKα.

Lattice parameters: hexagonal, $a = 20.46_3 \pm 0.01$ Å, $c = 8.534 \pm 0.004$ Å.

I	d obs.	2θ obs.	2θ calc.	Indices
5	4.4361	20.015	20.04	40.0
25	4.2715	20.795	20.815	00.2
60	3.9316	22.615	22.61	40.1
5	3.8667	23.00	23.00	41.0
15	3.5229	25.28	25.28	41.1
5	3.3485	26.62	26.615	42.0
5	3.2249	27.66	27.68	31.2
100	3.0716	29.07	29.05	40.2
5	2.9469	30.33	30.365	32.2
30	2.9130	30.69	30.685	43.0
10	2.8661	31.205	31.21	41.2
7	2.8379	31.525	31.525	52.0
3	2.6329	34.05	34.03	42.2
30	2.5583	35.075	35.08	44.0
7	2.5307	35.47	35.455	70.0
			35.455	53.0
1	2.462	36.5	36.49	31.3
10	2.4273	37.035	37.04	53.1
			37.04	70.1
			37.015	60.2
20	2.3933	37.58	37.57	40.3
3	2.3589	38.15	38.105	62.1
			39.72	54.0
20	2.2664	39.77	39.83	71.1
α_1 —				
5	2.2128	40.74	40.695	80.0
10	2.1776	41.43	41.435	70.2
			41.435	53.2
15	2.1379	42.335	42.325	00.4
3	1.967	46.1	Not indexed.	
1	1.614	57.0		
3	1.594	57.8 –		
	1.586	58.1		

gonal symmetry and the length of the *a*-axis and was suggested by Professor Th. G. Sahama.

Orthorhombic $KAlSiO_4$.—The phase equilibrium studies suggest that orthorhombic $KAlSiO_4$ is the stable form of $KAlSiO_4$ at high temperatures and that only 10-20% of $NaAlSiO_4$ may be taken into solid solution. The symmetry of this phase (denoted Ol for simplicity) has been shown to be orthorhombic by the optical studies of Duboin (1892) who first prepared it, and by Bowen (1917). Its lattice parameters have been given as $a = 9.00$, $b = 15.68$, and $c = 8.53$ KX by Bannister and Hey (1942). Dr. A.M.B. Douglas (private communication, 1953) kindly informed the authors that she had obtained the following lattice parameters for a synthetic preparation: $a = 9.00$, $b = 15.68$,

TABLE 7

X-ray Data for Orthorhombic $KAlSiO_4$

Source: Ne_0 grown at 1100°C, P_{H_2O} 500 kg/cm², 1 hour, from Bowen's preparation.
Method: Smear mount with internal standard. CuKα.

I	d obs.	2θ obs.	2θ calc.	(*hkl*) orthorhombic	(*hk.l*) hexagonal
1?	6.2195	14.24	14.23	101	11.1
7	5.7910	15.30	15.315	021, 111	20.1
2*	5.505	16.1			
7	4.5337	19.58	19.595	200, 130	22.0
2*	4.484	19.8			
15	4.2868	20.72	20.745	002	00.2
1*	4.171	21.3			
2	4.0042	22.20	22.20	201, 131	22.1
1?	3.9257	22.65	22.66	040, 220	40.0
10	3.8826	22.905	22.92	211	31.1
25	3.5659	24.97	24.965	221, 041	40.1
7*	3.4890	25.53			
20	3.4257	26.01	26.02	230	41.0
7	3.3167	26.88	26.86	141	32.1
			26.91	032	30.2
5*	3.267	27.30			
4	3.1777	28.08	28.06	231	41.1
100	3.1114	28.69	28.69	132, 202	22.2
3	2.969	30.1	30.13	240, 310	42.0
2	2.950	30.3	30.33	051	50.1
4*	2.9011	30.82			
30	2.8015	31.945	31.935	241, 311	42.1
15	2.6789	33.45	33.405	023, 113	20.3
			33.47	321	51.1
			33.51	232	41.2
35	2.6209	34.275	34.28	330, 060	60.0
3	2.4378	36.87	36.865	242, 312	42.2
2	2.4138	37.25	37.23	133, 203	22.3
			37.29	161	52.1
2	2.2675	39.75	39.79	260, 400	44.0
7	2.2334	40.385	40.41	332, 062	60.2
α_1 —					
10	2.1406	42.18	42.18	004	00.4
3	2.1091	42.84	42.835	421, 351	62.1
5	2.0777	43.52	43.50	430	71.0
3	2.0586	43.945	43.99	243, 313	42.3
1?	1.975	45.9			
1?	1.868	48.7			
2	1.7615	51.86	Not indexed.		
3	1.7302	52.87			
2	1.5888	58.0			

* See text.

and $c = 8.56$Å (accuracy ± 1%). Kunze (1954) has obtained the values $a = 9.013$, $b = 15.673$, and $c = 8.574$Å from a synthetic preparation. He assigned the space-group P222, and published an indexed powder pattern.

Powder patterns (see table 7) of Ol prepared in this study at temperatures of around 1500°C contain weak reflections additional to those found in the powder patterns of Ol synthesized at lower temperatures around 1000°C. An optical study kindly made by Dr. W. S. MacKenzie, Geophysical Laboratory, showed that the high-temperature material contains two types of crystals. About 95 percent of the crystals have hexagonal or rectangular outlines with a suggestion of 60° sector growth; the mean index of refraction is 1.530 ± 0.002 and the birefringence about 0.005, in agreement with previous optical measurements on Ol. The remainder are isotropic with refractive index 1.535 ± 0.002 and of irregular shape. The observations agree fairly closely with those of Bowen (the refractive indices differ a little and Bowen found that the isotropic phase had octahedral outlines), who presented evidence that the less abundant phase was $K_2Al_2SiO_6$. It seems probable that the extra reflections (starred in table 7) arise from this extraneous phase. The remainder of the reflections agree closely with data obtained by Dr. Douglas (personal communication) but differ in detail from the data given by Kunze (1954). This difference probably arises from variation of composition. It is unlikely that any sample of Ol so far prepared is stoichiometric $KAlSiO_4$, especially those made in the presence of a large amount of flux.

Although the symmetry is orthorhombic the powder pattern may be indexed on the basis of hexagonal geometry thus demonstrating the marked pseudo-hexagonal nature of the Ol phase. The lattice parameters of Ol prepared from a mix of composition Ne_0 are $a = 18.122 \pm 0.01$, and $c = 8.562 \pm 0.04$Å for the pseudo-hexagonal cell. These values correspond to $a = 9.06$, $b = 15.69$, and $c = 8.562$Å for the orthorhombic cell. The lattice parameters for Ol prepared from a mix of composition Ne_{10} are somewhat smaller, as would be expected from the substitution of the smaller sodium ions: $a = 18.07_3 \pm 0.01$, and $c = 8.528 \pm 0.004$ for the pseudo-hexagonal cell. Assuming that the compositions of the two samples of the Ol phase closely aproach the values of Ne_0 and Ne_{10}, the composition of Ol may be estimated from the reflection angles of the (42.1) and (60.0) reflections. The values calculated from the powder patterns are:

	$2\theta_{Cu}$(42.1)	$2\theta_{Cu}$(60.0)
Ne_0	31.935	34.28
Ne_{10}	32.03	34.39

The 02 Phase.—This phase was found in association with glass when charges of composition Ne_{20} were heated above 1520°C and then quenched. The composition of the crystals is not known but is probably near Ne_{15}. The crystals were not large enough for single-crystal study and the symmetry and lattice parameters were determined from the powder data. Table 8 contains the powder data which were indexed on the basis of an orthorhombic cell with $a = 8.892 \pm 0.004$, $b = 10.468 \pm 0.005$, and $c = 8.547 \pm 0.004$Å.

The powder pattern was indexed by comparison with the pattern of orthorhombic high-nepheline. In high-nepheline the peaks which most clearly indicated the orthorhombic symmetry were (400) and (260) at $2\theta_{Cu} = 35.2°$ and 35.4° respectively. For a potash-rich material these peaks would be ex-

TABLE 8

Indexed Powder Pattern of the 02 Phase

Material: Ne_{30} (Bowen's preparation), held 3 hours dry at 1540°C.
Method: Smear mount containing internal standard. Cu-Kα.

I	d obs.	2θ obs.	2θ calc.	Indices
20	5.3074	16.705	16.695	111
8	4.5120	19.675	19.68	120
6	4.4471	19.965	19.97	200
20	4.2755	20.775	20.785	002
45	3.3919	24.105	24.11	211
100	3.1014	28.785	28.775	122
50	3.0821	28.97	28.97	202
15	3.0374	29.405	29.41	131
8	2.8520	31.365	31.365	310
			31.40	003
6	2.7047	33.12	33.115	311
			33.145	032
55	2.6169	34.265	34.265	040
50	2.5790	34.785	34.785	320
4	2.4069	37.36	37.33	141
			37.33	123
6	2.2556	39.97	39.975	240
α_1 —				
4	2.2317	40.38	40.38	042
10	2.2058	40.875	40.83	322
			40.855	033
4	2.1806	41.37	41.37	241
			41.37	223
8?	2.1410	42.17	42.155	133
20	2.1367	42.26	42.26	004
6d*	1.6978	52.96		
4d	1.713	53.45		
6d	1.656	55.435		
4d	1.589	58.0	Not indexed.	
10	1.574	58.6		
6d	1.564	59.0		
2d	1.550	59.6		

Lattice parameters: orthorhombic, $a = 8.892 \pm 0.004$ Å
$b = 10.468 \pm 0.005$ Å
$c = 8.547 \pm 0.004$ Å

* d denotes broad reflection.

pected at about 34.5°. In the pattern of 02 there were two peaks at 34.265° and 34.785° and these were provisionally indexed as (400) and (260). All the phases in the nepheline-kalsilite system (except carnegieite which is a derivative of cristobalite) give a strong reflection near $2\theta_{Cu} = 42°$, as a result of the tridymite-type framework in these structures. By analogy with these structures the strong reflection at $2\theta = 42°$ in the 02 powder pattern was indexed as (004). It was found possible to index the other reflections on the basis of the values of a, b, and c deduced from the (400), (260), and (004) reflections.

TABLE 9

Indexed Powder Pattern of Natural Kaliophilite

Material: Specimen X, Bannister (1931).
Method: Smear mount containing internal silicon standard. Cu-Kα.
Lattice parameters: $a = 26.930 \pm 0.01$, $c = 8.522 \pm 0.004$ Å.

I	d obs.	2θ obs.	2θ calc.	Indices
2	6.1149	14.485	14.455	21.1
4	5.1523	17.21	17.21	31.1
2	4.529	19.6	19.59	32.1
7	4.4883	19.78	19.78	33.0
15	4.2624	20.84	20.845	00.2
5	3.9706	22.39	22.39	33.1
10	3.9145	22.715	22.71	42.1
12	3.7596	23.665	23.665	51.1
7	3.7323	23.84	23.825	52.0
10	3.4964	25.475	25.475	43.1
1	3.4257	26.01	26.05	52.1
2	3.3659	26.48	26.475	44.0
8	3.2826	27.165	27.17	61.2
100	3.0909	28.885	28.89	33.2
			28.90	71.0
12	3.0248	29.53	29.54	62.1
4	2.9393	30.41	30.42	63.0
1	2.871	31.15 to	31.145	60.2
	2.853	31.35	31.385	43.2
			31.395	72.0
11d	2.8139	31.80	31.73	11.3
			31.75	54.1
			31.86	52.2
1	2.7280	32.83	32.80	61.2
			32.81	81.0
7	2.7043	33.125	33.13	21.3
			33.15	72.1
30	2.5931	34.59	34.615	90.0
4	2.5516	35.17	35.14	40.3
			35.16	64.1
7d	2.506	35.835	35.785	32.3
			35.805	73.1
			35.905	71.2
1	2.4430	36.79	36.75	54.2
			36.76	65.0
				91.0
2	2.4203	37.145	37.165	63.2
			37.175	74.0
2d	2.404	37.4 to	37.37	80.2
	2.386	37.7	37.465	33.3
			37.67	42.3
2	2.3521	38.265	38.28	51.3
			38.30	91.1
2d	2.284	39.46	39.475	43.3
			39.495	83.1
α_1 —				
3	2.2440	40.15	40.145	66.0
9	2.2134	40.73	40.715	101.0
			40.725	90.2

TABLE 9 (Continued)

7	2.1849	41.285	41.285	82.2
5	2.1621	41.74	41.75	70.3
			41.765	75.1
5	2.1564	41.855	41.86	93.0
25	2.1307	42.385	42.385	00.4
		etc.		etc.

The k index was found to be even for all reflections and b was halved and interchanged with a to maintain the conventional relation b greater than a.

Kaliophilite.—Two types of natural kaliophilite have been described. Bannister (1931) described the first type and found that it was hexagonal with $a = 26.75$, and $c = 8.50$Å (converted from KX). These values compare well with $a = 26.94$, $c = 8.55$Å (Lukesh and Buerger, 1942) and with $a = 26.93 \pm 0.01$, $c = 8.522 \pm 0.004$Å (table 9, this paper). The space-group is $P6_322$ (Lukesh and Buerger) though Buerger (1954) envisaged the possibility that the true symmetry is orthorhombic and that the observed hexagonal symmetry is caused by twinning. Tilley and Henry (1953) mentioned the association of kaliophilite with the new mineral, latiumite, and Dr. A.M.B. Douglas (personal communication) found that it gave anomalous x-ray reflections. She kindly informed the authors that reflections with $k = 3n$ are sharp and identical with the corresponding reflections of the normal kaliophilite. Reflections with $k = 3n$ are diffuse in the anomalous kaliophilite and sharp in the normal kaliophilite. The anomalous kaliophilite must therefore contain some type of lattice disorder.

So far as is known, crystals identical with natural kaliophilite have not yet been synthesized and positively identified. Examination of crystals prepared by Bowen (1917) from a charge of composition Ne_0 showed that they consist of a phase which is not kaliophilite but which gives a powder pattern showing a striking relation to the pattern of natural kaliophilite. The peaks of the synthetic material correspond to the strong reflections of the natural kaliophilite but careful examination of the pattern revealed no trace of the weaker reflections of natural kaliophilite. Rigby and Richardson (1947) crystallized several samples of composition near Ne_0 at various temperatures from 900°C. to 1300°C. At the higher temperatures 01 was formed and at the lower temperatures a phase was produced which was not kalsilite or 01. Its x-ray powder photograph could be indexed on the unit-cell of natural kaliophilite. They suggested that it was probably identical with the form produced by Bowen. The powder data given by Rigby and Richardson are identical with the data obtained in the present work, thus confirming the suspected identity of the synthetic preparations. Thugutt (1937) claims to have prepared at 210°C material with the x-ray and optical properties of natural kaliophilite but it is not possible to test whether the product is natural kaliophilite or the new phase because x-ray data were not published. Kunze (1954) also synthesized a material with the optical and x-ray properties of kaliophilite but again no x-ray data were listed.

TABLE 10

X-ray Data for Synthetic Kaliophilite Compared with Natural Kaliophilite and Kalsilite

Synthetic kaliophilite*					Natural kaliophilite**			Kalsilite***		
I	d obs.	2θ obs.	2θ calc.	Indices	I	2θ obs.	Indices	I	2θ obs.	Indices
			10.335	00.1			00.1			00.1
10	4.488	19.78	19.79	10.0	7	19.78	33.0			10.0
15	4.283	20.74	20.755	00.2	15	20.84	00.2	10	20.41	00.2
3	3.972	22.38	22.375	10.1	5	22.39	33.1	35	22.375	10.1
100	3.098	28.82	28.835	10.2	100	28.885	33.2	100	28.625	10.2
			31.35	00.3			00.3			00.3
30	2.589	34.64	34.635	11.0	30	34.59	90.0	35	34.755	11.0
			36.24	11.1			90.1	10	36.305	11.1
			37.35	10.3	2?	37.4	33.3	7	36.93	10.3
3	2.243	40.21	40.205	20.0	3	40.15	66.0	2	40.3	20.0
5	2.214	40.75	40.72	11.2	9	40.73	90.2	7	40.635	11.2
			41.62	20.1			66.1	3	41.7	20.1
12	2.139	42.24	42.23	00.4	25	42.385	00.4	10	41.475	00.4
α_1 —										
			45.625	20.2				3	45.62	20.2
			47.01	10.4		Further indexing		2	46.415	10.4
			47.365	11.3		too difficult		3	47.12	11.3
			51.805	20.3				2	51.585	20.3
			53.48	00.5						00.5
			54.04	21.0						21.0
			55.18	21.1				3	55.365	21.1
			55.67	11.4				3	55.205	11.4
			57.58	10.5				5	56.705	10.5
3	1.5749	58.56	58.505	21.2				7	58.59	21.2
2	1.5477	59.69	59.67	20.4				2	59.225	20.4
2	1.4944	62.05	62.015	30.0				8	62.28	30.0
			63.06	30.1						30.1
			63.805	21.3				2	63.69	21.3
			65.28	11.5						11.5
3	1.4257	65.40	65.36	00.6						00.6

* Ne_6 crystallized dry at 1075°C. Smear mount with internal standard. CuKα radiation. $a = 5.180 \pm 0.002$, $c = 8.559 \pm 0.004$ Å.

** Specimen X, Bannister (1931). See table 9.

*** Ne_6, hydrothermal, 800°C.

The x-ray pattern of the synthetic material (table 10) may be indexed on a hexagonal cell with $a = 5.180 \pm 0.002$, and $c = 8.559 \pm 0.004$Å. Bowen also deduced hexagonal symmetry from an optical examination and in addition found that the material was optically negative with $o = 1.532$, and $e = 1.527$. The new phase probably has a pseudo-cell with $a = 5.180$, and $c = 4.279$Å for only one out of the twelve observed reflections has l odd. The only observed systematic absences are for l odd in (00.l) giving two possible space groups $P6_3$ and $P6_322$.

The lattice geometry of the new phase is close to that of kalsilite but the intensities of equivalent reflections are quite different (table 10). The intensi-

ties and positions of the reflections are very similar to those reflections of natural kaliophilite which arise from a sub-cell obtained by reducing the *a*-axis of natural kaliophilite by 3 $\sqrt{3}$ (multiplication by $\sqrt{3}$ is equivalent to choosing a new cell at 30° to the original cell). As the intensities for the sub-cell of natural kaliophilite are greater than the intensities of the other reflections, natural kaliophilite must have a pseudo-structure. The correspondence between the intensities and position of the reflections from the new phase and from the kaliophilite sub-cell suggests strongly that the structure of the new phase is very similar to the pseudo-structure of natural kaliophilite. It is therefore suggested that the new phase is a disordered form of natural kaliophilite and that by appropriate heat treatment ("annealing" at moderate temperatures, for example), it may well be possible to transform it into natural kaliophilite, perhaps by way of the anomalous natural kaliophilite. On this basis, the names natural kaliophilite, anomalous natural kaliophilite and synthetic kaliophilite have been provisionally assigned.

High- and Low-carnegieite.—Bowen (1912) and Bowen and Greig (1925) have shown that for the composition Ne_{100} nepheline is stable up to 1248°C where it inverts to high-carnegieite. The inversion is sluggish and carnegieite can be obtained at room temperature by quenching. At 680°C, high-carnegieite (cubic) undergoes an inversion of the displacive type to low-carnegieite which exists at room temperature as a metastable modification of $NaAlSiO_4$. The crystals were found to be intimately twinned, suggesting that the symmetry is low.

On a differential thermal analysis apparatus, they found that one of the preparations showed inversions at 226.5° and 658.3° on heating. On cooling, the upper inversion occurred at 653.7° and the lower was too weak to locate precisely. Other specimens gave inversions near 690°C with a temperature spread of about 6°.

High- and low-carnegieite were studied with the aid of a high-temperature x-ray camera. In conformity with the measurements of Barth and Posnjak (1932), high-carnegieite was found to be face-centered cubic with $a = 7.325 \pm 0.007$Å at 750°C. The stronger lines of low-carnegieite were almost identical in intensity and position (apart from the change caused by thermal contraction) with the lines of high-carnegieite. It was found that the intensity of the numerous weak lines, which reveal the difference between high- and low-carnegieite, varied with the rate of cooling through the inversion, suggesting that rapid cooling inhibits the inversion. A sample of high-carnegieite was slowly cooled to avoid metastable persistence of high-carnegieite and apart from the lattice shifts caused by thermal contraction there was no apparent change in the pattern on cooling from the inversion temperature of 690°C to room temperature. Table 11 contains the x-ray data for high- and low-carnegieite. An unsuccessful attempt to index the pattern of low-carnegieite was made by the method of Ito (1950). The lattice parameters and symmetry of carnegieite were not determined as crystals large enough for single-crystal investigations were not available.

TABLE 11
Powder Patterns of High- and Low-Carnegieite

High-carnegieite*			Low-carnegieite**		
I	d	Indices	I	d obs.	2θ obs.
			1	4.6131	19.24
100	4.229	111	150	4.1694	21.31
			7	3.7612	23.655
2	3.662	200	22	3.6115	24.65
			6	3.3083	26.95
			25	3.0338	29.44
			10	2.9034	30.795
				2.564	35.0
60	2.590	220	60d	2.5556	35.115
				2.536	35.4
			8	2.5041	35.86
			α_1 —		
			7	2.3100	38.955
			5	2.2607	39.84
3	2.209	311	20	2.1751	41.48
			3	2.1547	41.89
10	2.114	222	8	2.0825	43.415
			3	1.9532	46.45
			6	1.8834	48.28
			1	1.8219	50.02
5	1.831	400	2	1.8047	50.53
			1	1.6828	54.48
10	1.680	331	9	1.6536	55.525
1	1.638	420	3	1.6141	57.005
			7	1.5513	59.54
22	1.495	422			
5	1.410	511			
		333			
4	1.295	440			
4	1.238	531			
3	1.158	620			

* From heating camera, 750°C, CuKα. Calibrated with quartz. Cubic, $a = 7.325 \pm 0.007$ Å.

** Smear mount containing internal silicon standard. Cu-Kα. 25°C.

COMPARISON OF THE PHASES

The structure of high-carnegieite is based on the cristobalite framework (Barth and Posnjak, 1932) and the presence of the high-low inversion suggests that the structure of low-carnegieite is formed by a collapse of the cristobalite-type framework. Structure determinations of nepheline (Buerger, Klein and Hamburger, 1947; Buerger, Klein and Donnay, 1954; Hahn and Buerger, 1955) and kalsilite (Claringbull and Bannister, 1948) have shown that both have structures containing a tridymite-type framework. Half of the silicon atoms are replaced by aluminum and the charge is balanced by the entrance of sodium or potassium atoms into the cavities of the tridymite framework. All the other phases are hexagonal or pseudo-hexagonal with a true or

pseudo-cell of repeat distances $a \sim 5$Å, and $c \sim 8.5$Å in harmony with the tridymite parameters $a \sim 5.0$Å, and $c \sim 8.2$Å and it is virtually certain that these phases also have a tridymite-type framework. Buerger (1954) has characterized these structures as "stuffed derivatives of the silica structures".

Some light may be thrown on the relations between the phases by comparing the lattice parameters of the tridymite-type true or pseudo-cells. All the phases have $c = 8.5$Å but the a-axes are different: kalsilite and synthetic kaliophilite, 5Å; nepheline, 2 x 5Å; H4, 4 x 5Å, natural and anomalous natural kaliophilite, $3\sqrt{3}$ x 5Å; 01, orthorhombic pseudo-hexagonal, $a = 5\sqrt{3}$, $b = 3$ x 5Å; 02, orthorhombic pseudo-hexagonal, $a = 5\sqrt{3}$, $b = 2$ x 5Å; high-nepheline, orthorhombic pseudo-hexagonal, $a = 2$ x 5, $b = 2\sqrt{3}$ x 5Å. In order to compare the a lattice parameters, they have been transformed by the appropriate factor to a 10Å cell ($\sqrt{3}$ corresponds to a re-orientation of the cell with new axes at 30° to the old ones). Table 12 contains the values of a, c, and a^2c ($= 2/\sqrt{3}$ x cell volume) which are plotted in figure 3 against atomic composition (all other values of the paper are given in weight per cent).

The contraction of the lattice parameters with increase of the soda content is clearly shown because sodium has a smaller ionic radius than potassium. The contraction varies with direction and is different for the various structures; however, the volume change is approximately equal for all the structures and amounts to a change of about 11Å^3 for the replacement of a potassium atom by a sodium atom. The contraction in the alkali feldspars (12Å^3—deduced from the data of Donnay and Donnay (1952)) is of comparable size.

The c-parameter of synthetic nephelines is a linear function of the atomic composition except for the anomalous Na_{100} (atomic per cent of sodium). The measurements of the a-parameter, however, fall on two straight lines which meet near 75 atomic per cent of Na. The measurements of Na_{100} are again anomalous.

TABLE 12

Data for Figure 3

Material	Composition	True a	Converted a	c	a^2c
Ks	0	5.159_7	10.319	8.703_3	926.8
Ks	10	5.148_5	10.297	8.642_8	916.4
H4	27 ± 3	20.46_8	10.231	8.534	893.4
O1	0	18.12_4*	10.462	8.562	937.1
O1	10	18.07_4*	10.434	8.528	928.4
Synthetic kaliophilite	0	5.180	10.360	8.559	918.7
O2	~15	8.892** / 10.468**	10.267 / 10.468	8.547	918.6
	$NaAlSiO_4$ Weight per cent	Å	Å	Å	Å

* pseudo-hexagonal cell

** orthorhombic; $a = 8.892$, $b = 10.468$ Å.

There are three possible explanations of the break in lattice parameters as a function of composition:

1. Buerger, Klein and Hamburger (1947); Buerger, Klein and Donnay (1954); and Hahn and Buerger (1955) have shown that the cavities in the structure of a natural nepheline have two sizes, three-quarters are small and the others are large. Ideally the small holes are filled by sodium ions and the large ones by potassium ions. As the lattice spacings of natural nephelines are closely similar to those of synthetic nephelines (Smith and Sahama, 1954) it is likely that the structures are very similar and that in both natural and synthetic nephelines more soda-rich than Na_{75} small sodium ions are occupying large holes, whereas for nephelines more potash-rich than Na_{75} large potassium ions are occupying small holes. In the latter case the tridymite-type framework is forced to expand whereas in the first case the framework might tend to resist the collapse around the small ions in the large holes. The position of the break in slope observed in a plot of lattice parameters as a function of composition falls at the composition expected from theoretical considerations and moreover the observed rate of contraction is less for the soda-rich composition range. This suggests that the composition $Na_3KAl_4Si_4O_{16}$ may be a compound and not merely a single composition in a solid solution series. In this event we may, then, actually be dealing with two binary systems, $KAlSiO_4$-$Na_3KAl_4Si_4O_{16}$ and $Na_3KAl_4Si_4O_{16}$-$NaAlSiO_4$.

2. There may be a symmetry change at Na_{75} as a result of an inversion (as in an orthoclase (MacKenzie, 1952; Laves, 1952)) in compositions richer (or poorer) in Na than Na_{75}. Nephelines of compositions Na_{62}, Na_{82}, and Na_{91} were heated in an x-ray camera from 25°C to 1100°C, in an attempt to locate such an inversion but for all three materials the changes in the powder patterns, although non-linear, were continuous and were probably a result of thermal expansion of the lattice. These observations suggest that if an anorthoclase-type inversion is present the changes in the x-ray powder pattern were below the limits of detection.

3. Under equilibrium conditions nepheline solid solution having the composition Na_{75} and kalsilite (Na_0) are the stable phases at low temperatures and nepheline solid solutions in this compositional range (Na_0-Na_{75}) are metastable at room temperature. It is perhaps possible that the break in slope of the curve of lattice parameters vs. composition is related to this non-equilibrium in the materials x-rayed at room temperature. Measurements of the lattice parameters of synthetic nephelines lying in the composition range Na_{62} to Na_{91} were made at 325°C and 800°C by comparing the reflection angles of quartz and nepheline. If the discontinuity is related to lack of equilibrium the break should migrate to the composition Na_{59} at 800°C—the composition of nepheline solid solution in equilibrium with kalsilite at this temperature. Unfortunately the measurements were inconclusive for the magnitude of the change of gradient between the two sides of the discontinuity became smaller as the temperature increased and its position could not be located with sufficient accuracy to establish a difference.

The lattice parameters of the low-temperature form of $NaAlSiO_4$ vary slightly from specimen to specimen, and to some extent these variations are

related to the thermal history of the samples. For example, nepheline (Na_{100}) prepared hydrothermally is slightly different from nepheline prepared dry at high temperatures. However, in either case the lattice parameter *a* is larger and *c* is smaller than the values obtained by extrapolation from compositions carrying potash in solid solution (fig. 3). The cell volumes are approximately equal to the value obtained by extrapolation from solid solutions containing potash ($KAlSiO_4$). At the end-member composition ($NaAlSiO_4$) all of the large sites mentioned above are occupied by the small sodium atoms. It is suggested that the break in the plot of composition vs. *a* parameter near Na_{95} may be the result of a slight collapse of the tridymite-type framework which in turn is brought about by the large number of Na atoms in the large holes of the structure. The critical value lies between Na_{91} and Na_{100}.

The cause of the variation of the lattice parameters of nepheline (Na_{100}) with the thermal history is unknown. Similar variations were found for synthetic albites by MacKenzie (1952). Two possibilities readily come to mind; first, order-disorder between the silicon and aluminum ions and secondly the presence of H^+ ions in the lattice perhaps as OH^- replacing O^{2-}.

The *c* parameters of the 01 and the synthetic kaliophilite are approximately the same and fall on the line extrapolated from the synthetic nephelines. The *c* parameter of kalsilite is considerably larger. As kalsilite (Claringbull and Bannister, 1948) has straight Si-O-Si linkages parallel to the *c*-axis and nepheline has bent Si-O-Si linkages this suggests that the 01 and synthetic kaliophilite have bent linkages along the *c*-axis. The converted *a* parameter of synthetic kaliophilite also lies near the extrapolation line which represents the *a* parameter of the potash-rich nephelines, thus suggesting a close resemblance between the structures. The converted *a*-axis of the 01 phase is slightly greater than the *a*-axis of synthetic kaliophilite and the *a*-axis of kalsilite is somewhat less. The converted *a* parameter of H_4 lies near the extrapolated nepheline curve and the *c* parameter lies between the extrapolated nepheline and kalsilite curves, thus indicating that its structure lies intermediate between the structure of potash-rich nepheline and soda-bearing kalsilite.

The close similarity between the lattice parameters of the potash-rich phases indicates that the growth or persistence of metastable phases should be pronounced. This may be one reason why it has proved difficult to elucidate the phase relations in the potash-rich portion of the system. A small change of composition may change the phase relations to a marked degree.

The close relation between the lattice geometry of kalsilite and synthetic kaliophilite is intriguing for there are marked intensity differences between the two powder patterns which indicates that there is a considerable difference between the two structures. Unfortunately crystals of synthetic kaliophilite suitable for single-crystal study have not been available and an attempt to deduce the crystal structure from the powder pattern would be unwise for the determination of the space-group would be uncertain and it seems likely that disorder is present in many of the phases in this system. For example, Hahn and Buerger (1955) have shown that one of the oxygen atoms in nepheline is statistically distributed in three positions. A further complication is the possibility of order-disorder of the Si-Al atoms. Hahn and Buerger (1955) have

shown that the arrangement of Si and Al atoms in nepheline is complex with 12 tetrahedra occupied by disordered Si and Al atoms, two occupied by Si atoms, and two by Al atoms. It is possible that the differences between the potash-rich phases in the nepheline-kalsilite systems arise from the order-disorder of the Si and Al atoms. Thus synthetic kaliophilite might have disordered atoms and natural kaliophilite ordered atoms with an intermediate stage represented by the anomalous type of natural kaliophilite. Very detailed structure determinations would be required for the detection of such small structural variations.

ACKNOWLEDGMENTS

We are indebted to Drs. Bowen and Schairer for permission to use the mixtures which were prepared for their studies of this system. Discussions with Profs. Tilley and Sahama have been of considerable help to us. The kind assistance of Drs. Douglas and MacKenzie is gratefully acknowledged.

REFERENCES

Bannister, F. A., 1931, A chemical, optical and x-ray study of nepheline and kaliophilite: Mineralog. Mag., v. 22, p. 569-608.

Bannister, F. A., and Hey, M. H., 1942, Kalsilite, a polymorph of $KAlSiO_4$, from Uganda: Mineralog. Mag., v. 26, p. 218-224.

Bannister, F. A., Sahama, Th.G., and Wiik, H. B., 1952, Kalsilite in venanzite from San Venanzo, Umbria, Italy: Mineralog. Mag., v. 30, p. 46-48.

Barth, T. F. W., and Posnjak, E., 1932, Silicate structures of the cristobalite type. I. The crystal structure of carnegieite ($NaAlSiO_4$): Zeit. Krist., v. 81, p. 135-141.

Bowen, N. L., 1912, The binary system: $Na_2Al_2Si_2O_8$ (nephelite, carnegieite)-$CaAl_2Si_2O_8$ (anorthite): Am. Jour. Sci., v. 33, p. 551-573.

———, 1917, The sodium-potassium nephelites: Am. Jour. Sci., 4th ser., v. 43, p. 115-132.

Bowen, N. L., and Greig, J. W., 1925, The crystalline modifications of $NaAlSiO_4$: Am. Jour. Sci., 5th ser., v. 10, p. 204-212.

Buerger, M. J., 1954, The stuffed derivatives of the silica structures: Am. Mineralogist, v. 39, p. 600-614.

Buerger, M. J., Klein, G. E., and Donnay, G., 1954, Determination of the crystal structure of nepheline: Am. Mineralogist, v. 39, p. 805-818.

Buerger, M. J., Klein, G. E., and Hamburger, G., 1947, The structure of nepheline: Am. Mineralogist, v. 32, p. 197.

Claringbull, G. F., and Bannister, F. A., 1948, The crystal structure of kalsilite: Acta Cryst., v. 1, p. 42-43.

Donnay, G., and Donnay, J. D. H., 1952, The symmetry change in the high-temperature alkali-feldspar series: Am. Jour. Sci., Bowen v., p. 115-132.

Duboin, A., 1892, Reproduction de la leucite, de la cryolithe potassique et de nepheline potassique: Bull. Soc. Min. France, v. 15, p. 191-195.

Hahn, T., and Buerger, M. J., 1955, The detailed structure of nepheline, $KNa_3N_4Si_4O_{16}$: Zeit. Krist., v. 106, p. 308-338.

Holmes, A., 1942, A suite of volcanic rocks from south-west Uganda containing kalsilite (a polymorph of $KAlSiO_4$): Mineralog. Mag., v. 26, p. 197-217.

Ito, T., 1950, X-ray studies on polymorphism: Tokyo, Maruzen Co., Ltd.

Jay, A. H., 1933, The thermal expansion of quartz by x-ray measurements: Proc. Roy. Soc. London, ser. A, v. 142, p. 237-247.

Jay, A. H., and Andrews, K. W., 1947, X-ray reflections of kalsilite ($K_2O.Al_2O_3.2SiO_2$): Mineralog. Mag., v. 28, p. 88-89.

Kunze, G., 1954, Uber die rhombische modifikation von $KAlSiO_4$ in Anlehnung an den Kalsilit: Heidelberger Beitr. zur Min. und Pet., v. 4, p. 99-129.

Laves, F., 1952, Phase relations of the alkali feldspars. II. The stable and pseudo-stable phase relations in the alkali feldspar system: Jour. Geology, v. 60, p. 549-574.

Lukesh, J. S., and Buerger, M. J., 1942, The unit cell and space-group of kaliophilite: Am. Mineralogist, v. 27, p. 226-227.

MacKenzie, W. S., 1952, The effect of temperature on the symmetry of high-temperature soda-rich feldspars: Am. Jour. Sci., Bowen v., p. 319-342.

Miyashiro, A., and Miyashiro, T., 1954, Unit cell dimensions of synthetic nepheline: Jour. Faculty Sci. Univ. Tokyo, sec. 2, v. 9, p. 267-270.

Rigby, G. R., and Richardson, H. M., 1947, The occurrence of artificial kalsilite and allied potassium aluminum silicates in blast-furnace linings: Mineralog. Mag., v. 28, p. 75-88.

Sahama, Th.G., 1953a, Mineralogy and petrology of a lava flow from Mt. Nyiragongo, Belgian Congo: Annales Acad. Sci. Fennia, ser. A III, no. 35, p. 1-25.

————, 1953b, Parallel growth of nepheline and microperthitic kalsilite from North Kivu, Belgian Congo: Annales Acad. Sci. Fennia, ser. A III, no. 36, p. 1-18.

Sahama, Th.G., Neuvonen, K. J., and Hytönen, K., 1956, Determination of the composition of kalsilites by an x-ray method: Mineralog. Mag., in press.

Schairer, J. F., 1950, The alkali-feldspar join in the system $NaAlSiO_4$-$KAlSiO_4$-SiO_2: Jour. Geology, v. 58, p. 512-517.

Schairer, J. F., and Bowen, N. L., 1935, Preliminary report on equilibrium-relations between feldspathoids, alkali-feldspars and silica: Am. Geophysical Union Trans., 16th Ann. Mtg., pt. 1, p. 325-328.

Smith, J. V., and Sahama, Th.G., 1954, Determination of the composition of natural nephelines by an x-ray method: Mineralog. Mag., v. 30, p. 439-449.

Smith, J. V., and Tuttle, O. F., 1954, The system $KAlSiO_4$-$NaAlSiO_4$: Carnegie Inst. of Washington Year Book No. 53, p. 118-119.

Thugutt, S. J., 1937, O syntety cznym kaliofilicie: Arch. Min. Tow. Nauk. Warszaw, v. 13, p. 109-111.

Tilley, C. E., 1954, Nepheline-alkali feldspar parageneses: Am. Jour. Sci., v. 252, p. 65-75.

Tilley, C. E., and Henry, N. F. M., 1953, Latiumite (sulphatic potassium-calcium-aluminum silicate), a new mineral from Albano, Latium, Italy: Mineralog. Mag., v. 30, p. 39-45.

Tuttle, O. F., and Smith, J. V., 1953, The system $KAlSiO_4$: Carnegie Inst. of Washington Year Book No. 52, p. 53-56.

Geophysical Laboratory
Carnegie Institution of Washington
Washington, D. C.

[American Journal of Science, Vol. 255, April 1957, P. 306-318]

THE TEMPERATURE IN THE NEIGHBORHOOD OF A COOLING INTRUSIVE SHEET

J. C. JAEGER

ABSTRACT. The cooling by conduction of an intrusive sheet in the neighborhood of a contact is discussed, taking into account the effect of heat of solidification. General formulae are given, and the important case in which the magma and country rock have the same thermal conductivity and density and the magma is intruded at its liquidus temperature is discussed in detail. Numerical values for the contact temperature are given for this case, calculated for various values of the range of solidification and latent heat of the magma. These values are more than 100°C higher than those calculated by previous workers who have not adequately allowed for the effect of heat of solidfication. Numerical values are also given for temperatures in and around cooling intrusive sheets of any thicknesses with typical thermal properties and ranges of solidification of 1100-800, 1000-800 and 700-500°C. The effect of the amount of cover over such a sheet is studied. Applications to metamorphism, rock magnetism, and to the variation of the grain size of an igneous body near a contact are discussed.

I. INTRODUCTION

In studying many geological problems it is desirable to have as accurate information as possible about the variation of temperature in and around an intrusive igneous body throughout its time of cooling. Examples of this arise in discussions of metamorphism and rock magnetism, as well as of differentiation, grain size and the process of solidification of the igneous body. The object of this paper is to give a theoretical study of the cooling of an intrusive sheet, such as a sill or dike, together with some applications to the problems mentioned above.

The cooling of a dike-like mass of igneous rock has been discussed by Lovering (1935) and Larsen (1945). These authors, however, avoid the main difficulty of the problem, namely, the evolution of latent heat of solidification. Larsen[1], in fact, indicates a perfectly adequate method of taking this into account which will be used here, but he makes no use of this and follows Lovering in using the simple solution [Carslaw and Jaeger, 1947, §20 (16)] for the cooling of a uniform infinite solid with an initial temperature which is constant over a region and zero outside it. If the evolution of latent heat is taken into account accurately, results very different from those of Lovering and Larsen are obtained, for example, their values of the time necessary for complete solidification have approximately to be doubled: this change may not be regarded as important since the time of solidification is not a quantity for which accurate values are needed, but a more serious discrepancy is that they give values for the temperatures in the neighborhood of the contacts which are too low by an amount of the order of 100°C; this can seriously affect studies of metamorphism and rock magnetism.

The mathematical discussion will be given in II-IV below, where the assumptions made will be stated precisely in mathematical terms; applications will be discussed in VI-VIII. Here, a general discussion of the assumptions

[1] It should be said that Larsen's discussion is mainly of the cooling of a large batholith. If the intrusion of this is not as a single whole but by stoping or by tongues of intrusive penetrating the country rock, much of the latent heat of the igneous rock will be quickly absorbed in heating the country rock and the present objections will not apply to the estimate for the time of cooling.

which must be made in any calculation of this type will be given briefly.

(i) The intrusive body is assumed to be in the form of a flat sheet of thickness d in one direction and extending indefinitely in the perpendicular directions. This is, in fact, a reasonable approximation to most dike- or sill-like bodies. The country rock is supposed to extend indefinitely on either side, but this assumption can be removed as in V.

(ii) The intrusion is assumed to take place rapidly, that is, in a time which is very short compared to the time of solidification given in IV. The country rock is assumed to be at constant temperature which will be taken to be zero; if it is not zero, the present results are to be added to the initial temperature. The magma is supposed to be intruded at a constant temperature, which, for simplicity, will be taken to be the liquidus temperature appropriate to its composition. There is good geological evidence that this is frequently the case, but calculations can also easily be made for superheated magma.

(iii) The thermal properties of the country rock and solidified magma are taken to be the same and to be independent of temperature. This assumption, again, is made for simplicity, but inspection of the values given in Birch, Schairer and Spicer (1942) shows that it is a reasonable one in view of the uncertainty of these quantities. The only exceptional case likely to affect the results is that in which the country rock is quartzite which may show rather high values of thermal conductivity.

(iv) Heat removed by escaping volatiles is not considered. If the amount of this could be estimated it should be subtracted from the latent heat and treated separately. Since the effects of volatiles are dispersed over a region whose thickness is many times that of the igneous sheet, it is reasonable to assume that the heat conveyed by them is also dispersed over a large region and so will make little contribution to the temperature in the narrow region which is heated by conduction from the cooling sheet.

(v) Effects of convection in the magma are neglected and cooling is assumed to be by conduction only. This question is discussed in IX.

(vi) Exceptional situations which may occur near the surface, such as intrusion into porous rock containing water, are not considered. It may be remarked that the cooling of an extrusive sheet may be treated accurately in the same way but will not be studied here.

II. SOLIDIFICATION OF MAGMA WITH A PLANE CONTACT WITH COUNTRY ROCK

It is supposed that the region $x<0$ to the left of an infinite plane consists of country rock at a constant temperature which may be taken to be zero, and that at time $t=0$ the region $x>0$ to the right of this plane is suddenly filled with magma at a constant temperature. Suppose that the range of solidification of the magma is from T_2 to T_1, where $T_2>T_1$, and that its latent heat is L calories per gram of liquid, then if it is assumed that this latent heat is liberated uniformly over the range from T_2 to T_1 and if c'_2 is the specific heat of liquid magma, an amount of heat c_2 defined by

$$c_2 = c'_2 + \frac{L}{T_2 - T_1} \qquad \ldots\ldots (1)$$

is given up by each gram of liquid when its temperature falls through 1°C in

the range of solidification. Thus, the effect of the latent heat of solidification may be taken into account to a good approximation by using c_2 defined by (1) in place of c'_2 in thermal calculations. This is the method suggested by Larsen (1945) and the one which will be used here. In fact, as pointed out by Weiner (1955), this assumption has been shown to be adequate for studying the solidification of metallic alloys for which a great deal of experimental information is available for comparison with the results of theoretical calculations. The liquid magma is assumed to have density ρ_2, total specific heat c_2 defined as in (1) to include the contribution from latent heat, thermal conductivity K_2, and diffusivity $\kappa_2 = K_2/\rho_2 c_2$. The corresponding quantities for the country rock and solidified magma (assumed to be the same) are ρ_1, c_1, K_1, κ_1. A solution of the case in which solidified magma and country rock have different thermal properties has been given by Schwarz (1933), but this has not been used here since it has been desired to keep the number of parameters to be considered as small as possible. For this reason, also, it is assumed that the magma is intruded at the temperature T_2, that is, exactly at the top of the solidification range; there is evidence that this is frequently very nearly the case (Walker, 1956) but superheating of the magma can be taken into account if desired as in Weiner (1955).

It can be shown by the type of analysis given in Carslaw and Jaeger (1947) §31 or Weiner (1955) that, at time t after intrusion, the position X of the plane at which solidification is just complete and so the temperature is T_1, is given by

$$X = 2\lambda(\kappa_1 t)^{1/2}, \qquad \ldots\ldots\ldots (2)$$

where λ is a numerical parameter which is the root of the equation

$$\frac{1-\mathrm{erf}\, b\lambda}{1+\mathrm{erf}\lambda}\exp[(b^2-1)\lambda^2] = \frac{a(T_2-T_1)}{T_1}, \qquad \ldots\ldots\ldots (3)$$

where

$$a = \frac{K_2\kappa_1^{1/2}}{K_1\kappa_2^{1/2}} = \left(\frac{K_2\rho_2 c_2}{K_1\rho_1 c_1}\right)^{1/2}, \qquad b = \left(\frac{\kappa_1}{\kappa_2}\right)^{1/2}, \qquad \ldots\ldots\ldots (4)$$

and

$$\mathrm{erf}\lambda = \frac{2}{\pi^{1/2}}\int_0^{\lambda} e^{-\xi^2}\, d\xi \qquad \ldots\ldots\ldots (5)$$

is the tabulated error function.

The temperature T_s in the solidified magma and country rock for which $x<X$ is then given by

$$T_s = \frac{T_1}{(1+\mathrm{erf}\lambda)}\left\{1+\mathrm{erf}\,\frac{x}{2(\kappa_1 t)^{1/2}}\right\}, \qquad \ldots\ldots\ldots (6)$$

and the temperature T_l in the liquid in the region $x>X$ is

$$T_l = \frac{T_1-T_2\mathrm{erf}\, b\lambda}{1-\mathrm{erf}\, b\lambda} + \frac{T_2-T_1}{1-\mathrm{erf}\, b\lambda}\,\mathrm{erf}\,\frac{x}{2(\kappa_2 t)^{1/2}}. \qquad \ldots\ldots\ldots (7)$$

By (6), the temperature T_c at the contact with the country rock, $x=0$, is given by

$$T_c = T_1/(1+\mathrm{erf}\lambda). \qquad \ldots\ldots\ldots (8)$$

The contact temperature rises suddenly to this value and remains there.

In table 1 values of λ and T_c are given for various values of T_1 and T_2. They have been calculated for the case $K_1 = K_2$, $\rho_1 = \rho_2$, so that by (4) the values of these quantities do not affect the results, $c_1 = 0.25$, $c'_2 = 0.3$, and the two values 100 and 80 of L. The units used will always be c.g.s., calorie and °C unless otherwise stated. The numerical values used are reasonable average values, (Birch, Schairer and Spicer, 1942). The wide range of values given for T_2 and T_1 has been intended to allow for most possible conditions: the especially low values may occur in connection with a second intrusion into partially cooled rock.

TABLE 1

Melting Range	L = 100		L = 80	
	λ	Tc	λ	Tc
1400-1300	0.546	833	0.595	812
1400-1200	0.414	832	0.451	812
1400-1100	0.298	829	0.327	811
1400-1000	0.191	824	0.214	808
1400-900	0.090	818	0.108	803
1200-1100	0.490	728	0.537	708
1200-1000	0.349	726	0.385	707
1200-900	0.224	720	0.252	704
1200-800	0.108	713	0.129	699
1200-700			0.012	691
1100-1000	0.457	675	0.504	656
1100-900	0.312	671	0.347	654
1100-800	0.182	665	0.208	650
1100-700	0.060	656	0.079	643
1000-900	0.421	621	0.468	603
1000-800	0.270	617	0.304	600
1000-700	0.134	609	0.158	595
1000-600	0.004	597	0.022	586
900-800	0.382	567	0.427	551
900-700	0.224	561	0.256	546
900-600	0.079	551	0.102	538
800-700	0.338	512	0.382	496
800-600	0.170	504	0.201	490
800-500	0.016	491	0.036	480
700-600	0.288	456	0.330	442
700-500	0.109	446	0.137	434
600-500	0.230	398	0.269	386
600-400	0.036	385	0.060	375
500-400	0.161	339	0.196	328
400-300	0.076	276	0.106	268

It appears from table 1 that the contact temperature is not greatly affected by the width of the range of solidification: for example, it only changes by 15°C for magma intruded at 1400°C if the range of solidification is extended from 100°C to 500°C. It may be inferred that the way in which latent heat is liberated within the range of solidification has no important effects on the

temperatures in the country rock, and that, from this point of view, the assumption of uniform liberation of latent heat is quite adequate. In the calculations of Lovering (1935) latent heat is not considered and the contact temperature is just $\frac{1}{2}T_1$. This is also the case if a modified value of the specific heat or diffusivity is used in the results of Lovering: this was done by Larsen (1945) who, while he indicated the method used here, did not use it in his numerical calculations. It appears from table 1 that values obtained in this way are always too low by a value of the order of 100°C.

The actual values of the heats of solidification of magmas are very uncertain, and to show the effects of variations in this quantity, calculations have been made for two commonly used values of $L = 100$ and $L = 80$ cal./gm. The way in which the contact temperature varies with L can be seen by comparing the results in table 1 with the value $\frac{1}{2}T_1$ for the case $L = 0$.

When λ is known, the position of the plane at which solidification is complete and the temperatures in the solid and liquid regions can be calculated. For example, with the typcial values $K_1 = 0.005$, $\rho_1 = 2.8$, $c_1 = 0.25$, $\kappa_1 = 0.0071$, the distance from the contact, X_m in metres, of the plane at which solidification is complete is given by

$$X_m = 9.5\lambda(t_y)^{\frac{1}{2}}, \qquad \ldots\ldots (9)$$

where t_y is the time in years after the intrusion.

III. MELTING OF SURROUNDING ROCK

If

$$a(T_2-T_1)/T_1 = 1 \qquad \ldots\ldots\ldots (10)$$

in (3), this equation is satisfied by $\lambda = 0$, that is, the contact is maintained at T_1 and the surface of solidification does not advance into the liquid. If $a(T_2-T_1)/T_1 < 1$, the root of (3) is negative, implying that a surface at temperature T_1 at which melting begins advances into the surrounding rock. Spaces where negative values of λ arise have been left blank in table 1. Using (1) and (4), (10) becomes

$$(T_2-T_1)\left\{\frac{K_2\rho_2}{K_1\rho_1 c_1}\left(c'_2 + \frac{L}{T_2-T_1}\right)\right\}^{\frac{1}{2}} = T_1. \qquad \ldots\ldots\ldots (11)$$

If T_1 is less than the value given by (11), melting in the surrounding rock will begin: it may be remarked that a low value of K_1 assists this.

The theory now involves the assumption that the surrounding rock and the solidified magma have the same range of solidification which is improbable *except* in the case of a second intrusion into solidified but not completely cooled magma. In this case T_2-T_1 is given, and (11) gives a value for T_1 which is now the excess of the solidification temperature over that of the solid magma into which it is injected. For example, suppose that magma with a freezing range of 1000-800°C and $L = 100$ is injected into a partially cooled dike of the same material. Then, assuming typical values of $K_1 = K_2$, $\rho_1 = \rho_2$, $c_1 = c'_2 = 0.25$, (11) gives $T_1 = 346$°C. Thus, if the temperature of the partially cooled dike is greater than 800-346 = 454°C, its temperature will be raised above the solidus near the contact and some of the lowest melting constituents (that is, in effect, the mesostasis) will be remelted.

IV. THE COOLING OF AN INTRUSIVE SHEET

The idealized problem solved in II is, in fact, one of the very few problems involving latent heat for which an exact mathematical solution is available. The simplest problem of geological importance is that in which a plane sheet of magma is intruded into the region $-\frac{1}{2}d<x<\frac{1}{2}d$ between country rock which occupies the regions $x>\frac{1}{2}d$ and $x<-\frac{1}{2}d$. This is the problem of the dike, or the sill with very thick cover. No exact solution of this problem is available and special cases must be treated numerically.

It was pointed out by Lovering (1935) that the same family of curves of temperature against time may be used for sheets of all thicknesses provided an appropriate change is made in the time-scale. This result still holds in the present case and is expressed by the factor D^2 in the time-scale, where D is the thickness of the sheet in meters.

Solutions for three typical cases are presented in figures 1, 2, 3. These have been obtained by using the solutions of II until such time as the fall in temperature at the center is appreciable and subsequently by numerical analysis (Price and Slack, 1954). In each case the temperatures are plotted as functions of the time in years for selected points of the body, distant O, 0.1D, 0.2D, 0.3D and 0.4D from the center (in the igneous material), 0.5D (the contact), and 0.6D, 0.7D, 0.8D, 0.9D and 1.0D (in the country rock), where D is the thickness of the sheet in meters. Figure 1 is the example calculated by Larsen (1945) for which $T_2 = 700$, $T_1 = 500$, $L = 80$, $K_1 = K_2 = 0.005$, $c_1 = c'_2 = 0.28$, $\rho_1 = \rho_2 = 2.7$ which may be taken as typical of a granite intrusion. Solidification is complete after $0.016D^2$ years instead of the $0.007D^2$ years found from Larsen's less accurate calculation.

Figure 2 corresponds to a dolerite intrusion with $\rho_1 = \rho_2 = 2.8$, $K_1 = K_2 = 0.005$, $c_1 = 0.25$, $c'_2 = 0.3$, $L = 100$, $T_2 = 1000°C$, $T_1 = 800°C$, and Fig. 3 to the same values except that T_2 has the higher value of 1100°C. Times for complete solidification are, respectively, $0.012D^2$ and $0.014D^2$ years.

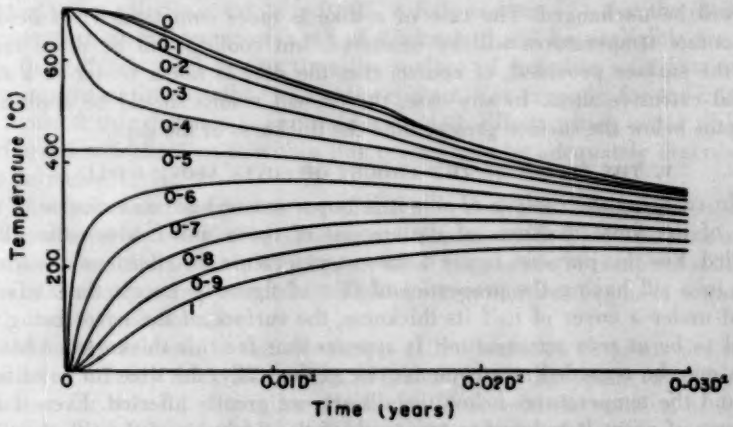

Fig. 1. Temperatures T at various points in an intrusive sheet of thickness D metres for which $T_2 = 700°C$, $T_1 = 500°C$, $L = 80$. The numbers on the curves are distances from the center measured as fractions of the thickness.

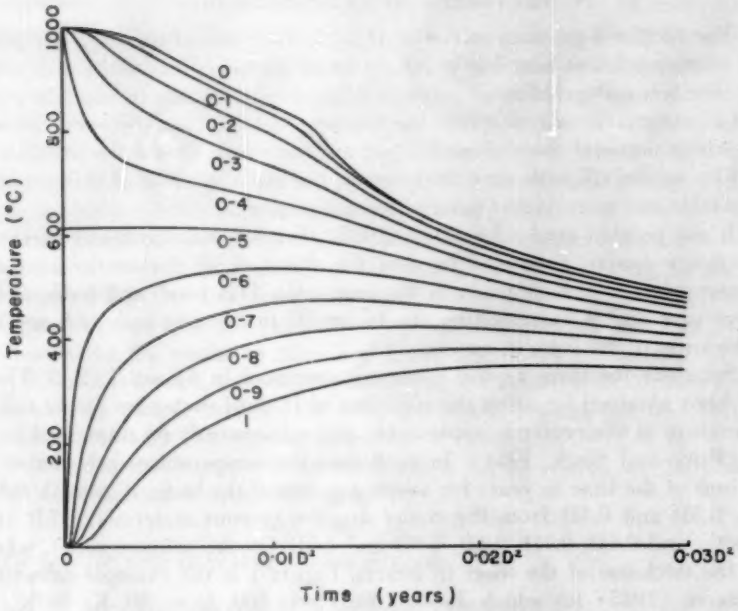

Fig. 2. Temperatures T at various points in an intrusive sheet of thickness D metres for which $T_2 = 1000°C$, $T_1 = 800°C$, $L = 100$. The numbers on the curves are distances from the center measured as fractions of the thickness.

The present results apply immediately to deeply buried sills and dikes. The effect of the amount of cover over a sill is discussed in V where it will be shown that this has little effect on conditions near the lower contact: at the upper contact cooling may be much more rapid though the initial temperature will be unchanged. The case of a dike is more complicated: as before, the contact temperatures will be unaltered, but cooling will be more rapid near the surface provided, of course, that the dike is not a feeder to a substantial extrusive sheet. In any case, the present results should be applicable at depths below the surface greater than the thickness of the dike.

V. THE EFFECT OF THE AMOUNT OF COVER ABOVE A SILL

In studying the cooling of sills it is important to have an estimate of the effect of the finite thickness of the amount of cover under which the sill is intruded. For this purpose, figure 4 shows temperature distributions at various times in a sill having the properties of that of figure 2, except that it is intruded under a cover of half its thickness, the surface of the cover being assumed to be at zero temperature. It appears that for this thickness of cover, which may be regarded as a common one geologically, the time for solidification and the temperatures below the sill are not greatly affected. Even if the thickness of cover is reduced to one tenth of the thickness of the sill, the temperatures attained near the lower contact are little changed, though the times involved are shortened.

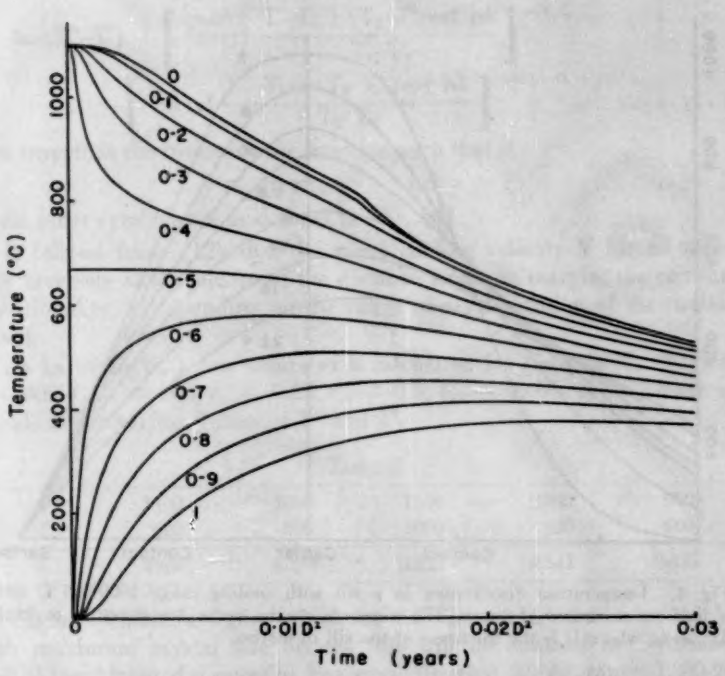

Fig. 3. Temperatures T at various points in an intrusive sheet of thickness D metres for which $T_2 = 1100°C$, $T_1 = 800°C$, $L = 100$. The numbers on the curves are distances from the center measured as fractions of the thickness.

VI. SOLIDIFICATION NEAR A CONTACT

As remarked in IV the formulae of II are applicable to effects near the contacts of a sill. Since erf 2 = 0.995, it follows from (7) that the change in temperature at the center of a sill of thickness d will be negligible for times less than $d^2/64\kappa_2$ and at this time the surface of complete solidification will have moved a distance $db\lambda/4$ from the contact. For example, for the intrusion of figure 2 this distance is approximately d/8. Effects which occur while the surface of solidification is within this region may be adequately described by the formulae of II.

As one example of such an effect, it is desirable in discussions of the mechanism of differentiation (Jaeger and Joplin, 1955, 1956) to have as precise an estimate as possible of the position of the surface of complete solidification in the early stages of cooling. This investigation was begun in connection with such calculations.

Another example is the calculation of the variation in grain size near a contact of a fairly thick sill or dike. Winkler (1949) has made calculations of this sort for thin dikes: similar effects should arise at the contacts of a thick sill and may be considered accurately using the results of II.

Winkler's procedure may be summarized as follows: he defines the mean cooling velocity V for a mineral crystallizing from a melt as the temperature

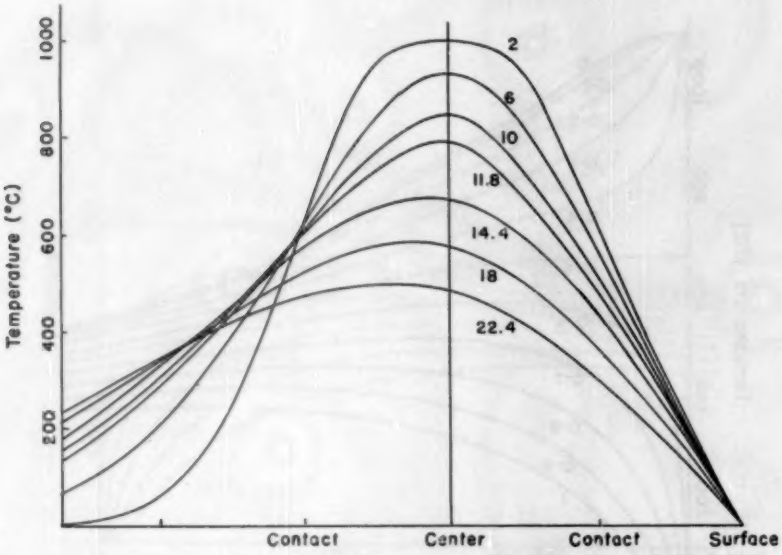

Fig. 4. Temperature distribution in a sill with cooling range 1000-800°C intruded under half its thickness of cover. The numbers on the curve are times in multiples of $10^{-5}D^2$ years, where D is the thickness of the sill in meters.

range within which that mineral crystallizes divided by the time taken to cool through this range. He then gives reasons to show that the grain size of a mineral is a function of V and has a maximum at a fairly low value of V (which for nepheline is found experimentally to be 0.2°C per hour). Winkler calculates V as a function of position in thin dikes by an analysis similar to Lovering's for various ranges of crystallization, and from these and his experimental results for nepheline he deduces typical curves of grain size against position. By comparing these with observed grain sizes, he attempts to determine the temperature range in which individual minerals crystallized. Clearly, if it can be put on a firm experimental basis, the method might prove to be a very useful one.

The complication of Winkler's curves is due to the fact that he has considered thin dikes a few meters in thickness and has therefore had to consider the cooling of the dike as a whole. It may be remarked that since he has neglected the effects of latent heat of solidification, his curves might be modified considerably by a more accurate calculation.

For the case of a relatively thick sill, in which the margins can be considered separately, the calculation of the mean cooling velocity V in Winkler's sense is extremely simple. If the temperature range in which the mineral concerned crystallizes is from T'' to T', where $T''>T'$ the value of V at distance x from the margin is by (7)

$$V = k/x^2, \qquad \ldots\ldots (12)$$

where k does not involve x and is given by

$$k = 4\kappa_2(T''-T')\left\{\left[\text{inverf}\,\frac{T'-T_1+(T_2-T')\,\text{erf}\,b\lambda}{T_2-T_1}\right]^{-2} - \left[\text{inverf}\,\frac{T''-T_1+(T_2-T'')\,\text{erf}\,b\lambda}{T_2-T_1}\right]^{-2}\right\}^{-1}, \quad \ldots\ldots\ldots (13)$$

where inverfξ is the inverse error function such that if

$$y = \text{inverf}\xi, \qquad \text{erf}\,y = \xi, \qquad \ldots\ldots\ldots (14)$$

and the other symbols are as defined in (3), (4).

It follows from (12) that the mean cooling velocity V for all minerals varies inversely as the square of the distance from the margin, the constant of proportionality, k, depending on the range of crystallization of the individual mineral.

As an example, a few values of k calculated for the case $T_2 = 1100°C$, $T_1 = 800°C$, $L = 100$, $c_1 = 0.25$, $c'_2 = 0.3$, $K_2 = 0.005$, $\rho_2 = 2.8$ are given in Table II for various values of T″ and T′.

TABLE 2

T″	1100	1000	1100	1000	900
T′	900	800	1000	900	800
k	0.630	0.213	0.822	0.511	0.135

Taking Winkler's figure of about 0.2°C/hour as the value of V for which maximum crystal size occurs, this will be attained at a distance of $60\sqrt{(5k)}$ cm. from the margin. For crystallization in the range 1100-900°C this is at a distance of 106 cm, and for the range 1000-800°C the distance is 62 cm. A few measurements made in this laboratory on a lower contact of a thick dolerite sill appear to indicate maxima of grain sizes at distances of this order from the contact, approximately 2 feet for plagioclase and 4 feet for augite, but the fairly rapid decrease in grain size at greater distances from the contact which is to be expected from Winkler's figure 2 does not occur.

VII. METAMORPHISM

Calculations of this sort allow a reasonably definite estimate to be made of the temperature history at any point in either the cooling magma or the country rock.

For example, consider a dolerite sill of thickness D meters. If the dolerite has a range of solidification of 1100-800°C and the properties of the material described in figure 3, the contacts are raised to a temperature of 665°C and remain at a temperature above 600°C for a time of the order of $0.017D^2$ years. A point in the country rock at a distance of D/10 from a contact has its temperature raised to a maximum of about 580°C and it remains at a temperature above 550°C for a time of $0.012D^2$ years. If the inversion or transformation temperatures of any indicator minerals are known it is possible to predict the region in which these have been exceeded and the time at which any point has been held above these temperatures. For example, the inversion temperature of low to high quartz is 573°C so it follows that for an intrusive with the properties of figure 3, any low quartz within a distance D/10 from a contact

will have been raised to a temperature above its inversion temperature and held at such a temperature for a time of up to $0.019D^2$ (at the contact). It appears from figure 4 that these values are not substantially altered for the region beneath the sill if it is intruded under a thickness of cover as low as $\frac{1}{2}D$.

This discussion, of course, neglects the effect of the heats of transformation of the metamorphosed minerals which would have to be taken into account in a more complete analysis.

VIII. ROCK MAGNETISM

Igneous rocks acquire a remanent magnetization on cooling through the Curie points of their ferrimagnetic mineral constituents. The most important of these is magnetite whose Curie point is 578°C. It is of some interest to know the way in which the Curie temperature moves through the rock.

For example, for the dolerite sill of figure 2, taking 500°C as a round figure for the Curie point, the contact takes $0.017\ D^2$ years to fall to this temperature, and the 500°C level takes another $0.006D^2$ years to progress to the center of the sill, D being the thickness of the sill in meters. For a thick sill for which D of the order of 1000 meters, this time, 6000 years, is sufficiently long to permit a study of the secular variation of the Earth's magnetic field at the time of the intrusion of the sill.

As a specific example, the dolerite sill described by Jaeger and Joplin (1955), which is believed to be about 2000 feet thick and to be a single and not a multiple intrusion, has its upper 650 feet magnetized normally while the available region below 750 feet is magnetized in the reverse direction. Reversed magnetization may be due either to a reversal in direction of the Earth's field or to a petrological mechanism of some sort. It follows from figure 2 that the Curie point takes about 150 years to move over the hundred feet between the normal region at 650 feet and the reversed region at 750 feet. Thus, if the Earth's field reversed during the cooling of the sill, it must have done so in the improbably short time of 150 years.

Sediments also acquire a remanent magnetization in the direction of the Earth's field at the time of their deposition or consolidation, the sources of this magnetization being detrital particles of iron minerals. If such sediments are heated by an intrusion above the Curie points of their magnetic minerals they will become remagnetized on cooling in the direction of the Earth's field at the time of cooling. For example, it appears from figure 2 that a dolerite intrusion of thickness D will heat the country rock within a distance 0.04D of its margin above the Curie point (578°C) of magnetite and that it will heat the rock within a distance greater than 0.5D of the margin above the Curie point (320°C) of pyrrhotite.

If the direction of the Earth's magnetic field at the time of the intrusion is significantly different from that at the time of deposition of the sediment, a change in the direction of magnetization of the sediment should be observed at the point of greatest penetration of the Curie point. Even if this is not observable, it is probable that in certain types of sediment a change in the dispersion of the directions of magnetization should be noticed, since Irving

(1954) has shown that coarse-grained, ill-sorted sediments may be expected to show a wide dispersion in directions, but if they have been remagnetized after heating above their Curie points they should show a narrow dispersion.

IX. THE EFFECTS OF CONVECTION

The problem of the cooling of an intrusive sheet in which convection may take place has not yet been solved. It is probable that convection in some form does take place in moderately thick sills but possible mechanisms are a matter for speculation. The question which has to be discussed here is that of how far convection might affect the numerical results given above which have been calculated on the assumption of pure conduction.

A gross overestimate of the effect of convection may be obtained by assuming the magma to be so well stirred by convection that it is kept at constant temperature. Then, if its thickness is d and its initial temperature is T_2, its temperature at time t is given by [Carslaw and Jaeger, 1947, §115 (11)]

$$T_2 e^{h^2\kappa_1 t}\left\{1-\text{erf } h(\kappa_1 t)^{\frac{1}{2}}\right\}, \qquad \ldots\ldots\ldots (15)$$

where

$$h = 2\rho_1 c_1/d\rho_2 c_2 \qquad \ldots\ldots\ldots (16)$$

and the other quantities are as defined in II.

Taking an example of the sill of figure 1, its temperature will have fallen to 500°C (the temperature of complete solidification) after a time of $0.008D^2$ years, where D is the thickness in meters. This, which must be a gross underestimate, may be compared with the value of $0.016D^2$ years calculated above and with Larsen's (1945) value of $0.007D^2$ years. It appears that the time of cooling is determined by conduction in the country rock rather than in the sill.

Further, since the cooling magma is stable in the lower part of the sill, it may be assumed that the contact effects and temperatures below the lower contact do not differ markedly from those described here. It is only towards the center of the sill that the process of solidification may be expected to be greatly affected. Even in this region, effects which take place after solidification, such as the movement of the Curie point, will be little affected.

X. ACKNOWLEDGMENTS

The writer is indebted to Dr. G. A. Joplin for discussion on metamorphism and on likely temperatures of intrusion, also to Mrs. A. Davidson for much of the numerical work.

REFERENCES

Birch, F., Schairer, J. F. and Spicer, H. C., 1942, Handbook of physical constants: Geol. Soc. America, Special Paper, no. 36.

Carslaw, H. S. and Jaeger, J. C., 1947, Conduction of heat in solids: Oxford University Press.

Irving, E., 1954, The palaeomagnetism of the Torridonian sandstone series: Thesis, Cambridge.

Jaeger, J. C. and Joplin, G. A., 1955, Rock magnetism and the differentiation of a dolerite sill: Geol. Soc. Australia, Jour., v. 2, p. 1-19.

Jaeger, J. C. and Joplin, G. A., 1956, Discussion of a paper by F. Walker: Am. Jour. Sci., v. 254, p. 443-446.

Larsen, E. S., 1945, Time required for the crystallization of the great batholith of southern and lower California: Am. Jour. Sci., v. 243A, p. 399-416.

Lovering, T. S., 1935, Theory of heat conduction applied to geological problems: Geol. Soc. America, Bull., v. 46, p. 69-93.

Price, P. H. and Slack, M. R., 1954, The effect of latent heat on numerical solutions of the heat flow equations: British Jour. Applied Physics, v. 5, p. 285-287.

Schwarz, C., 1933, Zur rechnerischen Behandlung der Erstarrungsvorgänge beim Giessen von Metallen: Zeitschr.f.angew.math.mech., v. 13, p. 202-223.

Walker, F., 1956, The magnetic properties and differentiation of dolerite sills—a critical discussion: Am. Jour. Sci., v. 254, p. 433-443.

Weiner, J. H., 1955, Transient heat conduction in multiphase media: Brit. Jour. Applied Physics, v. 6, p. 361-363.

Winkler, H. G. F., 1949, Crystallization of basaltic magma as recorded by variations of crystal size in dikes: Mineralog. Mag., v. 28, p. 557-574.

Australian National University
Canberra, Australia

REVIEW

Jurassic Geology of the World; by W. J. ARKELL, P. xv, 806, 102 figs., 46 pls, 28 tbls. London, 1956 (Oliver and Boyd Ltd., 5, 5s—approximately $15.00).—This volume is the first world-wide systematic treatment of the rocks of an entire geologic period. Fittingly, it is about the Jurassic system in whose abundantly fossiliferous terrains the science of historical geology originated. An appropriate dedication honors the outstanding pioneers of this science, and of Jurassic stratigraphy, William Smith and Albert Oppel.

Arkell's work is an impressive source book of facts about Jurassic rocks. A short but stimulating introductory chapter on stratigraphic classification and correlation establishes the framework for the following twenty-five chapters which describe Jurassic terrains throughout the world. Five short chapters at the end discuss Jurassic ocean basins, marine realms, climate, shields, mobile belts, geosynclines, volcanicity and diastrophism. Text illustrations are chiefly of three types. For each region outline maps show the Jurassic outcrop, stratigraphic tables give the essentials of the sequence with reference to both local and standard nomenclatures, and excellent photographic plates depict Jurassic outcrops. A supplement of 16 photographic plates illustrates the principal zonal ammonite guides of the Jurassic.

Arkell's short lead chapter on stratigraphic terminology will be of interest to all stratigraphers and paleontologists; it supplements the more comprehensive analyses of zones and stages in his earlier volume on Great Britain (Arkell, 1933). A comparison of the two volumes shows little change in philosophy but one marked change in the interpretation of the Jurassic system. The Rhaetian stage which Arkell formerly regarded as earliest Juarssic is regarded as latest Triassic in the present volume.

The regional descriptions which make up the bulk of the text are uniformly organized; they include geographic orientation, summary of geologic history, review of literature, and stage by stage description of Jurassic rocks. The five summary chapters at the end of the book are a conservative synthesis. Arkell concludes from the distribution of facies and faunas that the ocean basins were much as they are today; he argues, with particular emphasis, that the Pacific could not have been a land area as postulated by other paleogeographers of the Jurassic. On the subject of faunal provinces he chides paleontologists who " . . . insist on the universality of all ammonite assemblages and on unlimited incompleteness of the geological record . . . (p. 606)" and goes on to outline the gradual differentiation of Jurassic faunas from cosmopolitan distribution in the Lias to obvious Pacific, Boreal and Tethyan realms with fluctuating frontiers in the late Jurassic. Jurassic climate was warmer at higher latitudes than today and the temperate aspect of boreal faunas indicates a lack of arctic and antarctic ice. In discussing areas of sedimentation Arkell stresses the gradational nature of shelves, mobile belts, and geosynclines, relating those of the Jurassic to preceding areas of deposition and diastrophism. Of the Jurassic orogenic phases he deals at length with the Nevadan, the most intense of the period, emphasizing the remarkably short duration of this and other Jurassic orogenic phases. Reviewing Stille's conclusions on the nature of orogenic and epeirogenic movements, Arkell finds that they fit the observable facts of Jurassic stratigraphy with relatively slight modification.

Critics are likely to find themselves disarmed by Arkell's conservatism and his acute awareness of the equivocal and controversial parts of his subject matter. In his preface he explains the scope of the volume, accounting for the lack of paleogeographic maps and for the emphasis on ammonites to the exclusion of other groups of fossils. American stratigraphers, in particular, may find the omission of paleogeographic maps disappointing but it is obviously Arkell's intention that the reader assume responsibility for such generalization from the facts he presents. Throughout the book Arkell uses, and campaigns for, simplified nomenclature whether it be the nomenclature of stages, formations, or geosynclines. That he has achieved such a lucid presentation of so complex a subject is a compelling argument in favor of his position, although his ideas on the role of the formation as an historical unit protected by tradition are incompatible with the pragmatic interpretation of the formation prevalent in this country.

Jurassic Geology of the World is praiseworthy in many respects but its outstanding contribution is its able synthesis of the vast literature of the Jurassic. The bibliography occupies 115 pages of the volume and includes over 2800 references. Arkell not only has gleaned the pertinent factual matter from these references but has deciphered the complex tangle of conflicting stratigraphic nomenclatures by employing throughout a standard set of stages which he treats thoroughly in the first chapters. Moreover, his own firsthand knowledge of many of the individual regions, his grasp of the overall patterns of Jurassic history, and his acute assessment of the work of others combine to produce a critical review of much of the literature which is invaluable to students of the Jurassic. Although primarily a synthesis the volume is spared from being a dull recital of stratigraphic facts by Arkell's enthusiastic style and his emphasis on the problems yet to be solved. In addition it is spiced by his spirited comments and criticisms which, whether they generate ire or amusement, serve to liven the text. The avenues of adventure in Jurassic stratigraphy and paleontology opened by this masterful synthesis should attract students to the unsolved problems of the Jurassic for many years to come.

REFERENCE

Arkell, W. J., 1933, The Jurassic system in Great Britain: London, Oxford Univ. Press.

KARL M. WAAGE

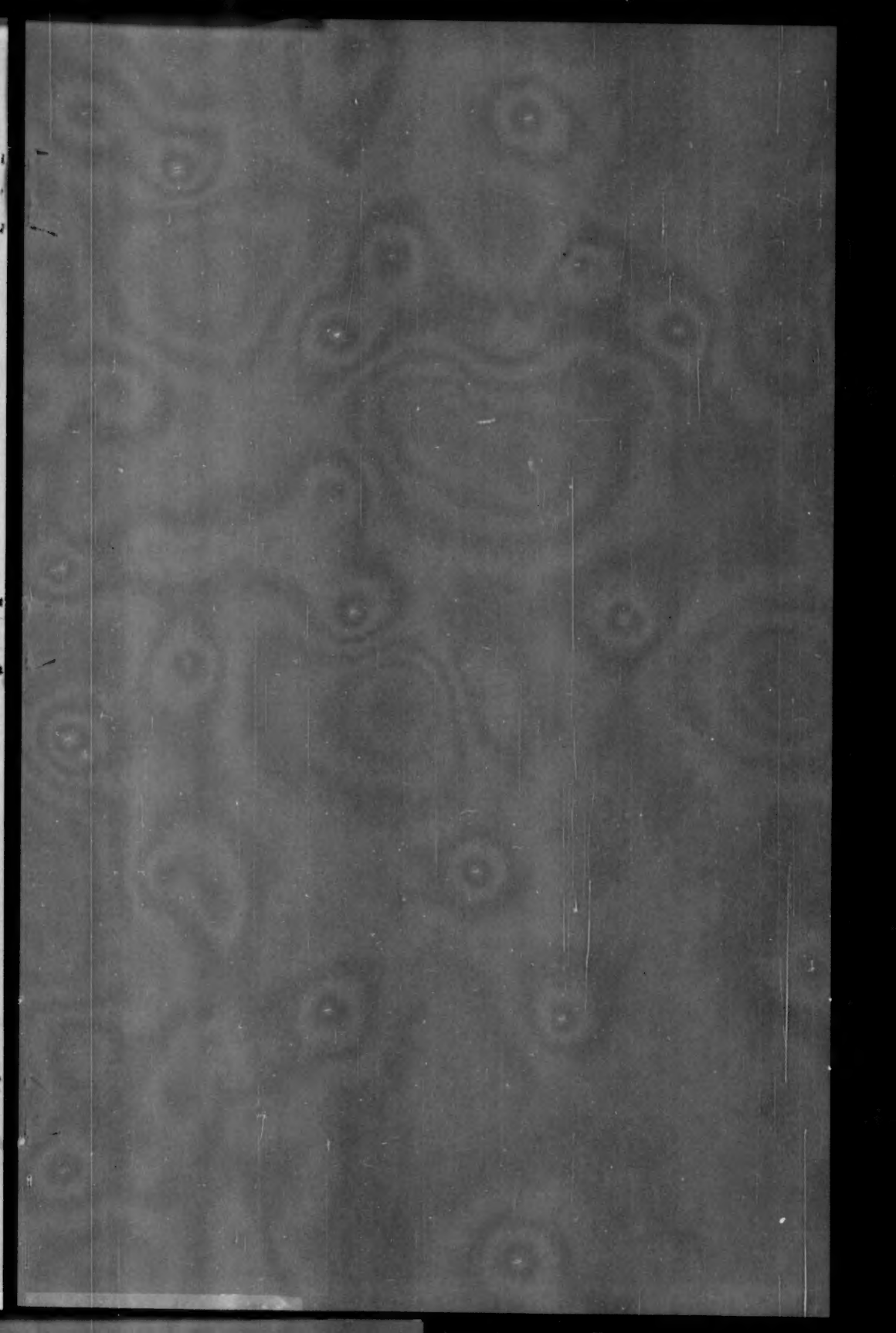

VOL. 255 No. 4, 1957

American Journal of Science

APRIL 1957

CONTENTS

Contributions to the Petrology of Hawaiian Basalts: I. The Picrite-Basalts of Kilauea ..... *J. D. Muir and C. E. Tilley* 241

Pollen Analysis of a Valley Fill Near Umiat, Alaska .... *D. A. Livingstone* 254

Evaluation of the Chemical Potential in Terms of Intensive Quantities *George Tunell* 261

Thermodynamics of Solids Under Non-hydrostatic Stress with Geologic Applications ..... *Gordon J. F. MacDonald* 266

The Nepheline-Kalsilite System: I. X-Ray Data for the Crystalline Phases *J. V. Smith and O. F. Tuttle* 282

The Temperature in the Neighborhood of a Cooling Intrusive Sheet *J. C. Jaeger* 306

REVIEW

Jurassic Geology of the World; by W. J. Arkell ..... *Karl M. Waagé* 319